Research Project Number SPR-3(017)

DEVELOPMENT OF TIE-DOWN AND TRANSITION SYSTEMS FOR TEMPORARY CONCRETE BARRIER ON ASPHALT ROAD SURFACES

Submitted by

Bob W. Bielenberg, M.S.M.E., E.I.T.
Research Associate Engineer

Ronald K. Faller, Ph.D., P.E.
Research Assistant Professor

John R. Rohde, Ph.D., P.E.
Associate Professor

John D. Reid, Ph. D.
Associate Professor

Dean L. Sicking, Ph.D., P.E.
Professor and MwRSF Director

James C. Holloway, M.S.C.E., E.I.T.
Research Associate Engineer

MIDWEST ROADSIDE SAFETY FACILITY
University of Nebraska-Lincoln
527 Nebraska Hall
Lincoln, Nebraska 68588-0529
(402) 472-0965

Submitted to

MIDWEST STATES REGIONAL POOLED FUND PROGRAM
Nebraska Department of Roads
1500 Nebraska Highway 2
Lincoln, Nebraska 68502

MwRSF Research Report No. TRP-03-180-06

February 23, 2007

TECHNICAL REPORT DOCUMENTATION PAGE

1. Report No. TRP-03-180-06	2.	3. Recipient's Accession No.	
4. Title and Subtitle DEVELOPMENT OF TIE-DOWN AND TRANSITION SYSTEMS FOR TEMPORARY CONCRETE BARRIER ON ASPHALT ROAD SURFACES		5. Report Date February 23, 2007 6.	
7. Author(s) Bielenberg, B.W., Faller, R.K., Rohde, J.R., Reid, J.D., Sicking, D.L., and Holloway, J.H.		8. Performing Organization Report No. TRP-03-180-06	
9. Performing Organization Name and Address Midwest Roadside Safety Facility (MwRSF) University of Nebraska-Lincoln 527 Nebraska Hall Lincoln, Nebraska 68588-0529		10. Project/Task/Work Unit No. 11. Contract © or Grant (G) No. SPR-3(017)	
12. Sponsoring Organization Name and Address Midwest States Regional Pooled Fund Program Nebraska Department of Roads 1500 Nebraska Highway 2 Lincoln, Nebraska 68502		13. Type of Report and Period Covered Final Report 2002-2007 14. Sponsoring Agency Code	
15. Supplementary Notes Prepared in cooperation with U.S. Department of Transportation, Federal Highway Administration.			

16. Abstract (Limit: 200 words)

The objective of this research was to design a tie-down system for temporary concrete barriers for use on asphalt road surfaces, and then apply that tie-down system to the design of an approach transition from free-standing to rigid barriers. The tie-down and transition systems were to be evaluated according to the Test Level 3 (TL-3) safety performance criteria set forth in NCHRP Report No. 350.

For the asphalt tie-down system, three steel pins were installed in holes on the front face of the barrier. The new tie-down design was crash tested according to NCHRP Report No. 350 test designation 3-11. The test was judged acceptable, barrier deflections were reduced, and all of the barriers in the system were safely restrained.

The approach transition to rigid barrier was developed through strategic application of the previously designed asphalt tie-downs. Computer simulation with LS-DYNA was used to locate the critical impact point for the full-scale crash test. The system was tested according to NCHRP Report No. 350 test designation 3-21. The results showed that the vehicle was safely redirected, and the test was judged acceptable.

Recommendations regarding the application of both the tie-down and transition designs were given.

17. Document Analysis/Descriptors Highway Safety, Temporary Barriers, Work Zones, Longitudinal Barriers, Concrete Barriers		18. Availability Statement No restrictions. Document available from: National Technical Information Services, Springfield, Virginia 22161	
19. Security Class (this report) Unclassified	20. Security Class (this page) Unclassified	21. No. of Pages 152	22. Price

DISCLAIMER STATEMENT

The contents of this report reflect the views of the authors who are responsible for the facts and the accuracy of the data presented herein. The contents do not necessarily reflect the official views nor policies of the Midwest States Regional Pooled Fund Program, State Highway Departments participating in the Midwest States' Regional Pooled Fund Research Program, nor the Federal Highway Administration. This report does not constitute a standard, specification, or regulation.

ACKNOWLEDGEMENTS

The authors wish to acknowledge several sources that made a contribution to this project: (1) the Midwest States' Regional Pooled Fund Program funded by the California Department of Transportation, Connecticut Department of Transportation, Illinois Department of Transportation, Iowa Department of Transportation, Kansas Department of Transportation, Minnesota Department of Transportation, Missouri Department of Transportation, Nebraska Department of Roads, New Jersey Department of Transportation, Ohio Department of Transportation, South Dakota Department of Transportation, Wisconsin Department of Transportation, and Wyoming Department of Transportation for sponsoring this project; (2) the Florida Department of Transportation for sponsoring this project; and (3) MwRSF personnel for constructing the barriers and conducting the crash tests.

Acknowledgment is also given to the following individuals who made a contribution to the completion of this research project.

Midwest Roadside Safety Facility

K.A. Polivka, M.S.M.E., E.I.T., Research Associate Engineer
C.L. Meyer, B.S.M.E., E.I.T., Research Engineer II
A.T. Russell, B.S.B.A., Laboratory Mechanic II
K.L. Krenk, B.S.M.A, Field Operations Manager
Tom McMaster, Laboratory Mechanic I
Undergraduate and Graduate Assistants

California Department of Transportation

Gary Gauthier, Roadside Safety Research Specialist
Wes Lum, P.E., Office Chief National Liaison

Connecticut Department of Transportation

Dionysia Oliveira, Transportation Engineer 3

Illinois Department of Transportation

David Piper, P.E., Highway Policy Engineer

Iowa Department of Transportation

David Little, P.E., Assistant District Engineer
Deanna Maifield, Methods Engineer

Florida Department of Transportation

Charles E. Boyd, P.E., Senior Structures Design Engineer

Kansas Department of Transportation

Ron Seitz, P.E., Assistant Bureau Chief
Rod Lacy, P.E., Road Design Leader

Minnesota Department of Transportation

Jim Klessig, Implementation Liaison
Mohammad Dehdashti, P.E., Design Standard Engineer
Michael Elle

Missouri Department of Transportation

Joseph G. Jones, P.E., Technical Support Engineer

Montana Department of Transportation

Susan Sillick, Research Bureau Chief

Nebraska Department of Roads

Amy Starr, Research Engineer
Phil Tenhulzen, P.E., Design Standards Engineer
Jodi Gibson, Research Coordinator

New Jersey Department of Transportation

Kiran Patel, P.E., P.M.P., C.P.M., Deputy State Transportation Engineer

Ohio Department of Transportation

Dean Focke, P.E., Standards Engineer

South Dakota Department of Transportation

David Huft, Research Engineer
Bernie Clocksin, Lead Project Engineer

Texas Department of Transportation

Mark Bloschock, P.E., Supervising Design Engineer
Mark Marek, P.E., Design Engineer

Wisconsin Department of Transportation

John Bridwell, Standards Development Engineer
Patrick Fleming, Standards Development Engineer

Wyoming Department of Transportation

William Wilson, P.E., Standards Engineer

Federal Highway Administration

John Perry, P.E. Nebraska Division Office
Danny Briggs, Nebraska Division Office

Dunlap Photography

James Dunlap, President and Owner

TABLE OF CONTENTS

Page
DISCLAIMER STATEMENT iii
ACKNOWLEDGEMENTS iv
TABLE OF CONTENTS vii
LIST OF FIGURES ix
LIST OF TABLES xii
1 INTRODUCTION 1
1.1 Problem Statement 1
1.2 Research Objective 3
1.3 Scope 3
2 DESIGN OF THE ASHPALT TIE-DOWN TEMPORARY CONCRETE BARRIER 5
2.1 Initial Design Concept 5
2.2 Component Testing Of Asphalt Pins 7
3 ASPHALT PIN TIE-DOWN DESIGN DETAILS 11
4 TEST REQUIREMENTS AND EVALUATION CRITERIA 22
4.2 Evaluation Criteria 23
5 TEST CONDITIONS 25
5.1 Test Facility 25
5.2 Vehicle Tow and Guidance System 25
5.3 Test Vehicles 25
5.4 Data Acquisition Systems 27
5.4.1 Accelerometers 27
5.4.2 Rate Transducers 31
5.4.3 High-Speed Photography 31
5.4.4 Pressure Tape Switches 32
6 FULL-SCALE TEST NO. FTB-1 35
6.2 Test Description 35
6.3 System Damage 35
6.4 Vehicle Damage 36
6.5 Occupant Risk Values 37
6.6 Discussion 37
7 DEVELOPMENT OF A TEMPORARY CONCRETE BARRIER TRANSITION 50
7.1 Introduction 50
7.2 Transition Design Details 50
7.3 LS-DYNA Simulation of the Critical Impact Point 54
8 TRANSITION DESIGN DETAILS 61
9 FULL-SCALE TEST NO. FTB-2 72
9.2 Test Description 72
9.3 System Damage 72
9.4 Vehicle Damage 73
9.5 Occupant Risk Values 73
9.6 Discussion 74
10 SUMMARY AND CONCLUSIONS 87
11 RECOMMENDATIONS 89

12 REFERENCES 93
13 APPENDICES 95
APPENDIX A - Asphalt Pin Tie-Down, English Units 96
APPENDIX B - Test Summary Sheet in English Units, Test No. FTB-1 104
APPENDIX C - Occupant Compartment Deformation, Test No. FTB-1..... 106
APPENDIX D - Accelerometer and Rate Gyro Analysis Test, No. FTB-1 109
APPENDIX E - Free-Standing to Rigid Barrier Transition Details, English Units 117
APPENDIX F - Test Summary Sheet in English Units, Test No. FTB-2 126
APPENDIX G - Occupant Compartment Deformation, Test No. FTB-2 128
APPENDIX H - Accelerometer and Rate Gyro Analysis, Test No. FTB-2 131
APPENDIX I - Florida Department of Transportation – F-shape PCB Standards..... 138

LIST OF FIGURES

Page
Figure 1. Temporary Concrete Barrier Installations on Asphalt: a) Near Drop-Off and b) Transition to Rigid Barrier 4
Figure 2. F-shape Temporary Concrete Barrier 6
Figure 3. Asphalt Pin Component Testing 8
Figure 4. Effect of Pin Diameter on Tie-Down Performance 10
Figure 5. Asphalt Pin Tie-Down Design Details 13
Figure 6. Asphalt Pin Tie-Down Design Details 14
Figure 7. Asphalt Pin Tie-Down Design Details 15
Figure 8. Asphalt Pin Tie-Down Design Details 16
Figure 9. Asphalt Pin Tie-Down Design Details 17
Figure 10. Asphalt Pin Tie-Down Design Details 18
Figure 11. Asphalt Pin Tie-Down Design Details 19
Figure 12. Asphalt Pin Tie-Down Design Photographs 20
Figure 13. Asphalt Pin Tie-Down Design Photographs 21
Figure 14. Vehicle Dimensions, Test No. FTB-1 26
Figure 15. Vehicle Dimensions, Test No. FTB-2 28
Figure 16. Vehicle Target Locations, Test No. FTB-1 29
Figure 17. Vehicle Target Locations, Test No. FTB-2 30
Figure 18. Location of High-Speed Cameras, Test No. FTB-1 33
Figure 19. Location of High-Speed Cameras, Test No. FTB-2 34
Figure 20. Summary of Test Results and Sequential Photographs, Test FTB-1 38
Figure 21. Additional Sequential Photographs, Test FTB-1 39
Figure 22. Documentary Photographs, Test FTB-1 40
Figure 23. Documentary Photographs, Test FTB-1 41
Figure 24. Documentary Photographs, Test FTB-1 42
Figure 25. Documentary Photographs, Test FTB-1 43
Figure 26. Impact Location, Test No. FTB-1 44
Figure 27. System Damage, Test FTB-1 45
Figure 28. System Damage, Test FTB-1 46
Figure 29. System Damage, Test FTB-1 47
Figure 30. Vehicle Damage, Test FTB-1 48
Figure 31. Vehicle Damage, Test FTB-1 49
Figure 32. Free-Standing to Rigid Barrier Transition Schematic 51
Figure 33. Comparison of F-Shape Barrier Deflections 53
Figure 34. LS-DYNA Asphalt Pin Model 55
Figure 35. LS-DYNA Asphalt Pin Simulation 56
Figure 36. LS-DYNA F-Shape Barrier Model 58
Figure 37. Typical LS-DYNA Results for Critical Impact Point Simulations 59
Figure 38. Free-Standing to Rigid Concrete Barrier Transition Details 63
Figure 39. Free-Standing to Rigid Concrete Barrier Transition Details 64
Figure 40. Free-Standing to Rigid Concrete Barrier Transition Details 65
Figure 41. Free-Standing to Rigid Concrete Barrier Transition Details 66
Figure 42. Free-Standing to Rigid Concrete Barrier Transition Details 67

Figure 43. Free-Standing to Rigid Concrete Barrier Transition Details 68
Figure 44. Free-Standing to Rigid Concrete Barrier Transition Details 69
Figure 45. Free-Standing to Rigid Concrete Barrier Transition Details 70
Figure 46. Free-Standing to Rigid Concrete Barrier Transition Photographs 71
Figure 47. Summary of Test Results and Sequential Photographs, Test FTB-2 75
Figure 48. Additional Sequential Photographs, Test FTB-2 76
Figure 49. Documentary Photographs, Test FTB-2 77
Figure 50. Documentary Photographs, Test FTB-2 78
Figure 51. Documentary Photographs, Test FTB-2 79
Figure 52. Documentary Photographs, Test FTB-2 80
Figure 53. Impact Location, Test No. FTB-2 81
Figure 54. System Damage, Test FTB-2 82
Figure 55. System Damage, Test FTB-2 83
Figure 56. System Damage, Test FTB-2 84
Figure 57. Vehicle Damage, Test FTB-2 85
Figure 58. Vehicle Damage, Test FTB-2 86
Figure A-1. Asphalt Pin Tie-Down Design Details 97
Figure A-2. Asphalt Pin Tie-Down Design Details 98
Figure A-3. Asphalt Pin Tie-Down Design Details 99
Figure A-4. Asphalt Pin Tie-Down Design Details 100
Figure A-5. Asphalt Pin Tie-Down Design Details 101
Figure A-6. Asphalt Pin Tie-Down Design Details 102
Figure A-7. Asphalt Pin Tie-Down Design Details 103
Figure B-1. Summary of Test Results and Sequential Photographs, Test FTB-1 105
Figure C-1. Occupant Compartment Deformation, Test No. FTB-1 107
Figure C-2. OCDI, Test No. FTB-1 108
Figure D-1. Graph of Longitudinal Acceleration, Test No. FTB-1 110
Figure D-2. Graph of Longitudinal Occupant Impact Velocity, Test No. FTB-1 111
Figure D-3. Graph of Longitudinal Occupant Displacement, Test No. FTB-1 112
Figure D-4. Graph of Lateral Acceleration, Test No. FTB-1 113
Figure D-5. Graph of Lateral Occupant Impact Velocity, Test No. FTB-1 114
Figure D-6. Graph of Lateral Occupant Displacement, Test No. FTB-1 115
Figure D-7. Angular Displacements, Test No. FTB-1 116
Figure E-1. Free Standing to Rigid Barrier Transition Design Details 118
Figure E-2. Free Standing to Rigid Barrier Transition Design Details 119
Figure E-3. Free Standing to Rigid Barrier Transition Design Details 120
Figure E-4. Free Standing to Rigid Barrier Transition Design Details 121
Figure E-5. Free Standing to Rigid Barrier Transition Design Details 122
Figure E-6. Free Standing to Rigid Barrier Transition Design Details 123
Figure E-7. Free Standing to Rigid Barrier Transition Design Details 124
Figure E-8. Free Standing to Rigid Barrier Transition Design Details 125
Figure F-1. Summary of Test Results and Sequential Photographs, Test FTB-2 127
Figure G-1. Occupant Compartment Deformation, Test No. FTB-2 129
Figure G-2. OCDI, Test No. FTB-2 130
Figure H-1. Graph Longitudinal Acceleration, Test No. FTB-2 132
Figure H-2. Graph of Longitudinal Occupant Impact Velocity, Test No. FTB-2 133

Figure H-3. Graph of Longitudinal Occupant Displacement, Test No. FTB-2 134
Figure H-4. Graph of Lateral Acceleration, Test No. FTB-2 135
Figure H-5. Graph of Lateral Occupant Impact Velocity, Test No. FTB-2..... 136
Figure H-6. Graph of Lateral Occupant Displacement, Test No. FTB-2 137
Figure I-1. Florida Department of Transportation – F-shape PCB Standards 139
Figure I-2. Florida Department of Transportation – F-shape PCB Standards 140
Figure I-3. Florida Department of Transportation – F-shape PCB Standards 141
Figure I-4. Florida Department of Transportation – F-shape PCB Standards 142
Figure I-5. Florida Department of Transportation – F-shape PCB Standards 143
Figure I-6. Florida Department of Transportation – F-shape PCB Standards 144
Figure I-7. Florida Department of Transportation – F-shape PCB Standards 145
Figure I-8. Florida Department of Transportation – F-shape PCB Standards 146
Figure I-9. Florida Department of Transportation – F-shape PCB Standards 147
Figure I-10. Florida Department of Transportation – F-shape PCB Standards 148
Figure I-11. Florida Department of Transportation – F-shape PCB Standards 149
Figure I-12. Florida Department of Transportation – F-shape PCB Standards 150
Figure I-13. Florida Department of Transportation – F-shape PCB Standards 151
Figure I-14. Florida Department of Transportation – F-shape PCB Standards 152

LIST OF TABLES

Page
Table 1. Test Requirements 24
Table 2. Evaluation Criteria 24
Table 3. Test Summary 88

1 INTRODUCTION

1.1 Problem Statement

Temporary concrete barriers are one of the most common types of roadside hardware found on the nation's highways. These types of barriers are used primarily in work zones due to their portability and versatility. Typically, temporary barriers are segmented units which are attached end-to-end by a load bearing connection. The segmentation of the barriers allows them to be easily installed, repositioned, and removed from the work-zone area.

Recently, a significant amount of highway safety research has been focused on methods for constraining or limiting the deflection of free-standing, temporary concrete barriers. These designs are generally referred to as tie-down temporary concrete barriers. The Midwest Roadside Safety Facility (MwRSF) has developed two tie-down systems for use with a 3.81-m (150-in.) long, F-shape temporary concrete barrier design currently used by the Florida Department of Transportation and several other state departments of transportation. The new tied-down systems are:

1. A steel strap tie-down system designed for use on concrete roadways and bridge decks [1-2].
2. A bolt-through tie-down system designed for use on concrete roadways and bridge decks that passed three threaded rods through holes on the lower portion of the front face of the barrier to constrain deflection [2-3].

Deflection levels for both of these tie-down designs are reduced over the deflection of the free-standing, F-shape, temporary concrete barrier. These options provide designers more flexibility in using the barriers for installations with space limitations. However, there remain some unresolved issues with the use of tie-down temporary concrete barrier designs.

The previous tie-down systems were developed for use on concrete surfaces, and thus are not appropriate for use on asphalt roadway surfaces. A design for constraining temporary concrete barrier deflections on asphalt roadways was previously developed and successfully tested to the National Cooperative Highway Research Program (NCHRP) Report No. 350 criteria [4] by the California Department of Transportation (CALTRANS) [5]. The K-rail system consisted of 6.1-m (240-in.) long segments of New Jersey safety shape barrier connected by a pin and loop connection. Each barrier was constrained by a set of four 25-mm (1-in.) diameter by 610-mm (24-in.) long steel stakes that were driven into the ground through cast holes near the corners of the barrier. These stakes penetrated to a depth of 420 mm (16.5 in.) into the road surface. The system limited the dynamic and permanent set deflections to 254 mm (10 in.) and 70 mm (2.75 in.), respectively. While the system adequately constrained the barriers, the K-rail system was not believed to be appropriate for the F-shape barrier used in this research due to the differences in the size, reinforcement, and connections of the two barriers. In addition, it was desired that the performance of the tie-down system be evaluated when the barriers are installed adjacent to a vertical drop-off, which had not been considered in the CALTRANS design.

The second unresolved issue pertained to the transition between barrier systems. When a free-standing temporary concrete barrier system is connected to a rigid barrier, such as a concrete bridge rail, there exists a need for a transition in the relative stiffness and deflection of the systems. While the issue of approach transitions has been addressed many times with regards to metal beam guardrail, there has been little or no research addressing these transitions when using temporary barriers. Without an effective transition design, there exists a serious potential for pocketing of the barrier, snag of the wheels or other vehicle components on the rigid barrier, as well as problems with vehicle stability. Thus, a need exists for the design of a safe approach

transition between free-standing temporary concrete barrier and rigid barriers. Figure 1 shows examples of installations requiring both an asphalt tie-down adjacent to a vertical cutout and an approach transition from free-standing to rigid barrier.

1.2 Research Objective

The objective of the research described herein was to design a tie-down temporary concrete barrier for use on asphalt road surfaces, and then apply that tie-down system to the design of an approach transition from free-standing barriers to a rigid concrete barrier. The tie-down temporary barrier and the transition were to be evaluated according to the Test Level 3 (TL-3) safety performance criteria set forth in the NCHRP Report No. 350, *Recommended Procedures for the Safety Performance Evaluation of Highway Features*.

1.3 Scope

The research objective was achieved by performing several tasks. First, design concepts for the asphalt tie-down were developed and component tested in order to determine this desired design. Next, full-scale crash testing of the asphalt tie-down design was conducted according to NCHRP Report 350 test designation no. 3-11. After the asphalt tie-down was developed and tested, it was applied to create an approach transition from free-standing temporary concrete barrier to rigid barrier. The new transition design was analyzed in order to determine the proper Critical Impact Point (CIP), and a full-scale crash test of the transition was conducted according to NCHRP Report 350 test designation no. 3-21. After data from the development and testing of the asphalt tie-down and transition was collected, documented, and analyzed, conclusions and recommendations were developed that pertain to the safety performance of theses systems.

Figure 1. Temporary Concrete Barrier Installations on Asphalt: a) Near Drop-Off and b) Transition to Rigid Barrier

2 DESIGN OF THE ASHPALT TIE-DOWN TEMPORARY CONCRETE BARRIER

2.1 Initial Design Concept

The temporary concrete barrier used for this research was the Kansas F-shape temporary concrete barrier, as shown in Figure 2. This barrier had been previously developed during the research for the bolt-through tie-down system for use on concrete roadways. The barrier segments were 3.81-m (150-in.) long and 813-mm (32-in.) tall, and six 51-mm (2-in.) diameter, vertical holes, three holes per side, were cast into the toe of the barrier. Additional steel reinforcement was required around the holes to provide sufficient resistance and containment for the retainer bolts. Adjacent barriers were joined using a pin and loop type connection comprised of three sets of rebar loops on each barrier interconnection. The three loop connection detail provided double shear at two locations on each pin and consequently allowed for the elimination of the retainer bolt at the bottom of the vertical pin.

The design goal for the asphalt tie-down was to limit the deflection and rotation of the temporary barrier segments during a vehicular impact when installed on an asphalt roadway with only a 152-mm (6-in.) gap between the back side of the barrier and a 914-mm (36-in.) deep vertical drop-off behind the barrier. With such a small area for barrier translation, it was imperative that the design be capable of developing large lateral loads in order to limit deflection. In addition, it was important that the tie-down design provide a measure of vertical restraint in order to prevent barrier rotation. Previous research has demonstrated that safety shape barriers have a higher potential for vehicle instability due to their shape [6]. The potential for the barrier to rotate increases when the translation of the barrier is constrained by a tie-down, thus further increasing the potential for vehicle instability.

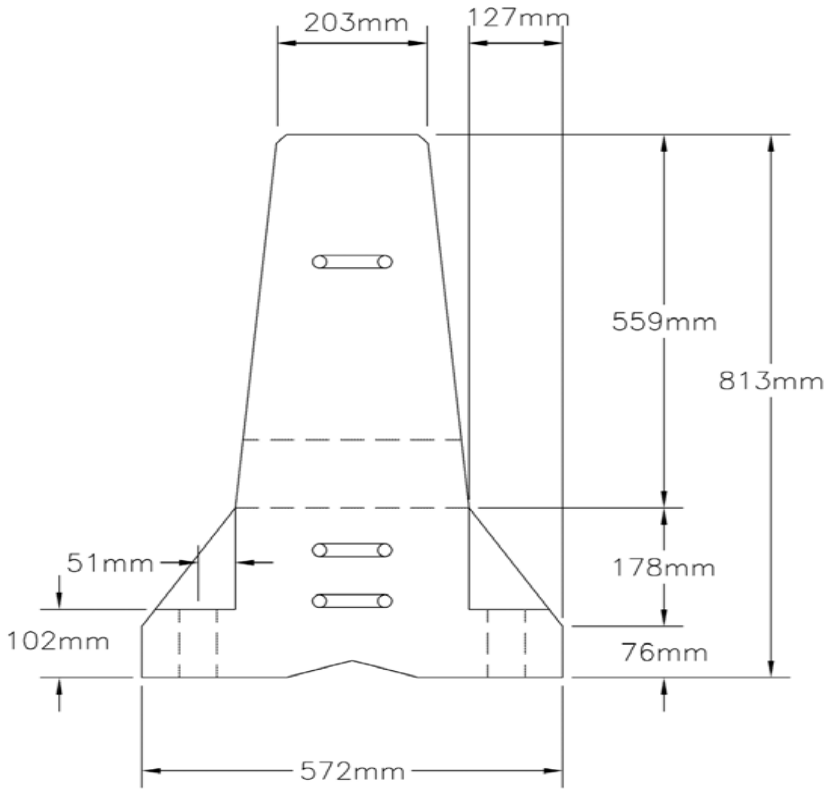

Figure 2. F-shape Temporary Concrete Barrier

With these concepts in mind, the researchers developed an initial design concept for the asphalt tie-down. The concept consisted of simple steel pins that could be easily installed by passing them through the existing vertical holes on the toe of the barrier. These pins could be sized based on diameter and embedment depth to provide adequate load capacity to restrain the barrier motion. Caps made from steel plate would be welded to the tops of the pins to provide vertical restraint. Pins would be installed on only the front face of the barrier because it was believed that pins on the backside of the barrier would create a pivot point and induce rotation of the barrier segments. This action could increase the propensity for impacting vehicles to climb the barrier face and vault over the top.

2.2 Component Testing Of Asphalt Pins

Component testing of prototype steel pin tie-downs was conducted to determine the proper size of the pin as well as to investigate the effects of varying asphalt depth. The basic test setup and schematics of the prototype pins are shown in Figure 3. The test matrix for the asphalt pin testing consisted of 914-mm (36-in.) long, A36 steel pins with both 28.575-mm (1.125-in.) and 38.1-mm (1.5-in.) diameters. A 76-mm x 76-mm x 13-mm (3-in. x 3-in. x 0.5-in.) A36 steel cap was welded to the top of each pin in order to provide vertical restraint. The pins were tested with 51-mm (2-in.), 102-mm (4-in.), and 152-mm (6-in.) asphalt cover depths. The initial pin diameters and lengths were based on hand calculations, and the asphalt depths were selected to represent a range of minimum and maximum cover on the roadway. The component test consisted of installing the steel pins in a steel sleeve sized to match the vertical holes in the F-shape barrier. The pin was loaded laterally through the soil and asphalt by pulling on the sleeve with a cable attached to a 2,160-kg (4,762-lbs) bogie sled moving away from the pins at approximately 6.71 m/s (15 mph). Force and deflection of the pin were measured during the pull

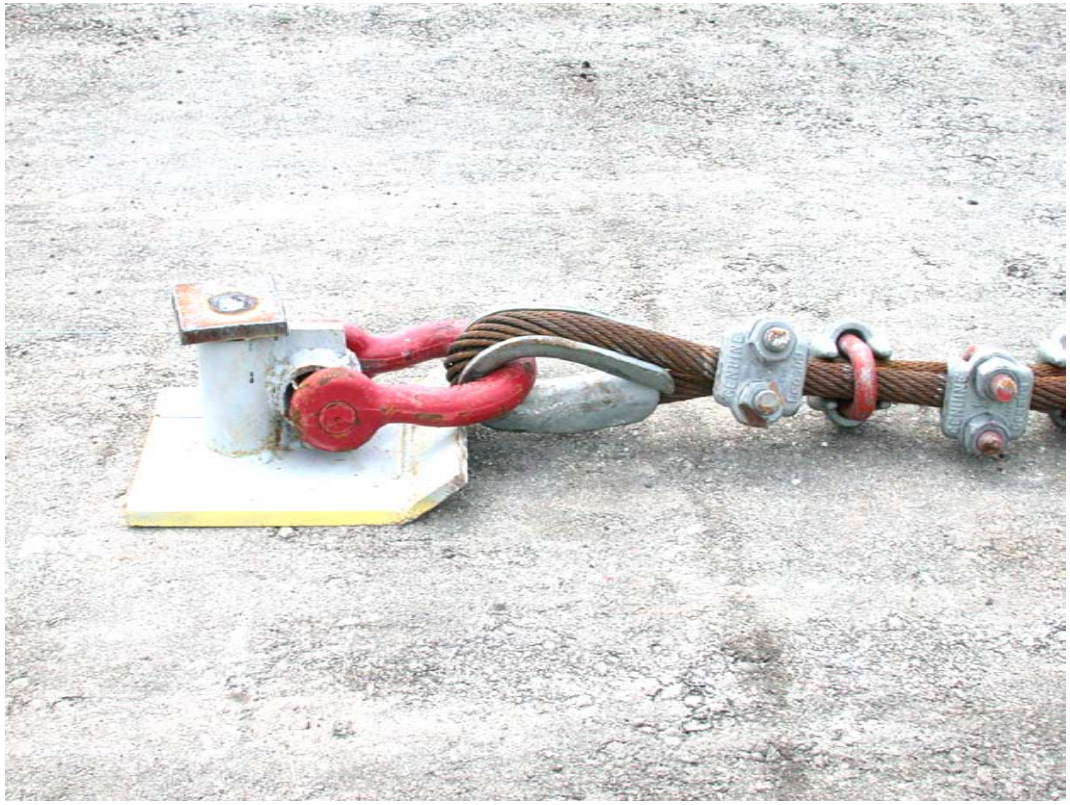

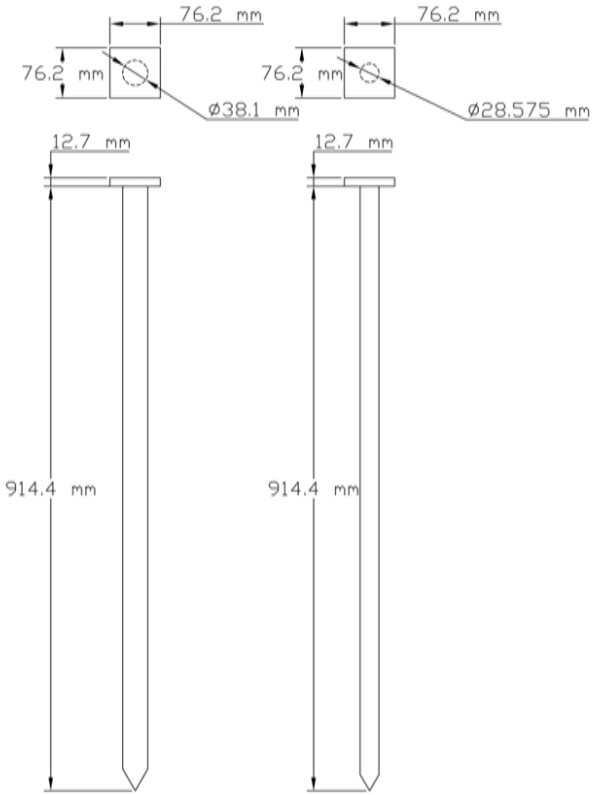

Figure 3. Asphalt Pin Component Testing

test using a load cell and a string potentiometer, respectively.

Results from the asphalt pin component testing were reviewed to determine the effect of pin diameter and asphalt depth on the tie-down behavior. Review of the test data from the component tests with the various asphalt depth found that the amount of asphalt cover had little or no effect on the steel pins performance. Peak loads were almost identical for the various levels of cover, and the pins exhibited very similar levels of deflection. A slight decrease in deflection of the pins was observed as the depth of the asphalt cover increased.

Comparison of the two pin diameters demonstrated a significant difference in behavior, as shown in Figure 4. The 38.1-mm (1.5-in.) diameter pin developed a 91.4 kN (20.54 kip) peak load, which was an 8 percent increase over the 84.6 kN (19.02 kip) peak load of the 28.575-mm (1.125-in.) diameter pin. Previous experience has shown that typical impact loading for rigid, concrete barriers, when impacted with a 2,000-kg (4,409-lbs) pickup truck at 100 km/h (62.14 mph) and 25 degrees, to be in the range of 267 kN (60 kip) to 311 kN (70 kip). If the tie-down system placed three pins on the face of the temporary concrete barrier, then the lateral constraint would be in the range of 254 kN (57.1 kip) to 274 kN (61.6 kip). Thus, it was believed that either pin diameter would possess sufficient capacity to restrain barrier motion. However, it was also noted that the larger 38.1-mm (1.5-in.) diameter pin behavior was more desirable as it provided lower deflection, reduced pin deformation, and less pullout of the pin from the asphalt and soil.

Based on the force versus deflection behavior observed during component testing, the 38.1-mm (1.5-in.) diameter x 914-mm (36-in.) long A36 steel pin with a 76-mm x 76-mm x 13-mm (3-in. x 3-in. x 0.5-in.) A36 steel cap was chosen for the asphalt temporary concrete barrier tie-down design.

a) 28.575 mm Diameter Pin
Peak Load = 84.6 kN

b) 38.1 mm Diameter Pin
Peak Load = 91.4 kN

Figure 4. Effect of Pin Diameter on Tie-Down Performance

3 ASPHALT PIN TIE-DOWN DESIGN DETAILS

3.1 Design Details, Test No. FTB-1

Design details for the asphalt pin tie-down evaluated in full-scale crash test no. FTB-1 are shown in Figure 5 through Figure 11. The design layout consisted of sixteen F-shape temporary concrete barriers placed on a 51-mm (2-in.) thick asphalt pad. The 51-mm (2-in.) asphalt depth was chosen because it was the minimum asphalt cover to provide a reasonable bearing surface for field installations of the system. In addition, component testing had shown that thicker asphalt cover would only decrease tie-down deflection. The back edge of the barrier was installed 152 mm (6-in.) from the edge of a 914-mm wide x 914-mm (36-in. x 36-in.) deep trench. Three 38.1-mm (1.5-in.) diameter x 914-mm (36-in.) long A36 steel pins with 76-mm x 76-mm x 13-mm (3-in. x 3-in. x 0.5-in.) A36 steel caps were installed in the holes on the front face of ten barriers in the mid-section of the installation. The corresponding English-unit drawings are shown in Appendix A. Photographs of the test installation are shown in Figure 12 through Figure 13.

The concrete used for the barriers consisted of Iowa's Concrete Barrier Mix, with a minimum 28-day concrete compressive strength of 34.5 MPa (5,000 psi). A minimum concrete cover varied at different rebar positions within the barrier. A minimum concrete cover of 51 mm (2 in.) was used along the top of the vertical stirrup rebar and the bottom longitudinal rebar. Minimum concrete cover of 44 mm (1.75 in.) and 25 mm (1 in.) were used along the sides of the vertical stirrup rebar and at the rebar around the anchor bolt block, respectively. All of the steel reinforcement in the barrier was ASTM A615 Grade 60 rebar, except for the loop bars which were ASTM A706 Grade 60 rebar. The barrier reinforcement details are shown in Figure 1 through Figure 11.

Barrier reinforcement consisted of three No. 5 and two No. 4 longitudinal bars, twelve No. 4 bars for the vertical stirrups, and six No. 6 bars for the anchor bolt block reinforcement loops. Each of the five longitudinal rebar was 3.71-m (12-ft 2-in.) long. The vertical spacing of the lower, middle, and upper longitudinal bars were 165 mm (6.5 in.), 368 mm (14.5 in.), and 780 mm (29.125 in.) from the ground to their centers, respectively. The vertical stirrups were 1,829-mm (72-in.) long and were bent into the shape of the barrier. Their spacing varied longitudinally, as shown in Figure 7. The anchor bolt block loops were 889-mm (35-in.) long, were bent into a U-shape, and were used to reinforce the anchor bolt area, as shown in Figure 7 through Figure 9.

The barriers used a pin and loop type connection comprised of two sets of three rebar loops on each barrier interconnection. Each loop assembly was configured with three ASTM A706 Grade 60 No. 6 bars that were bent into a loop shape, as shown in Figure 9. The vertical pin used in the connection consisted of a 32-mm (1.25 in.) diameter x 711-mm (28-in.) long round bar composed of ASTM, A36 steel, as shown in Figure 10. The pin was held in place using one 64-mm wide x 102-mm long x 13-mm thick (2.5-in. x 4-in. x 0.5-in.) ASTM A36 steel plate with a 35-mm (1.375-in.) diameter hole centered on it. The plate was welded 64mm (2.5 in.) below the top of the pin. A gap of 92 mm (3.625 in.) between the ends of two consecutive barriers was formed from the result of pulling the connection taut.

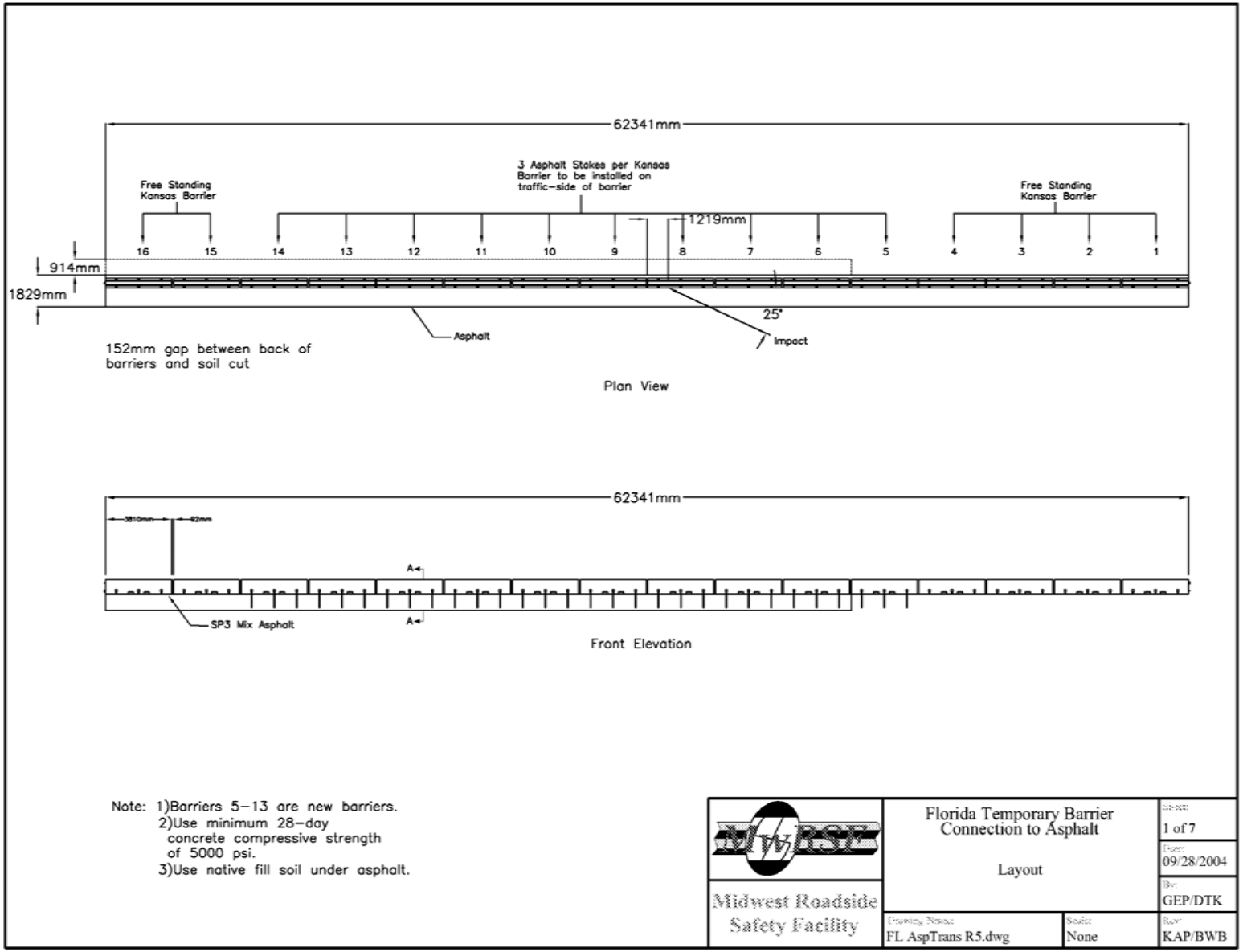

Figure 5. Asphalt Pin Tie-Down Design Details

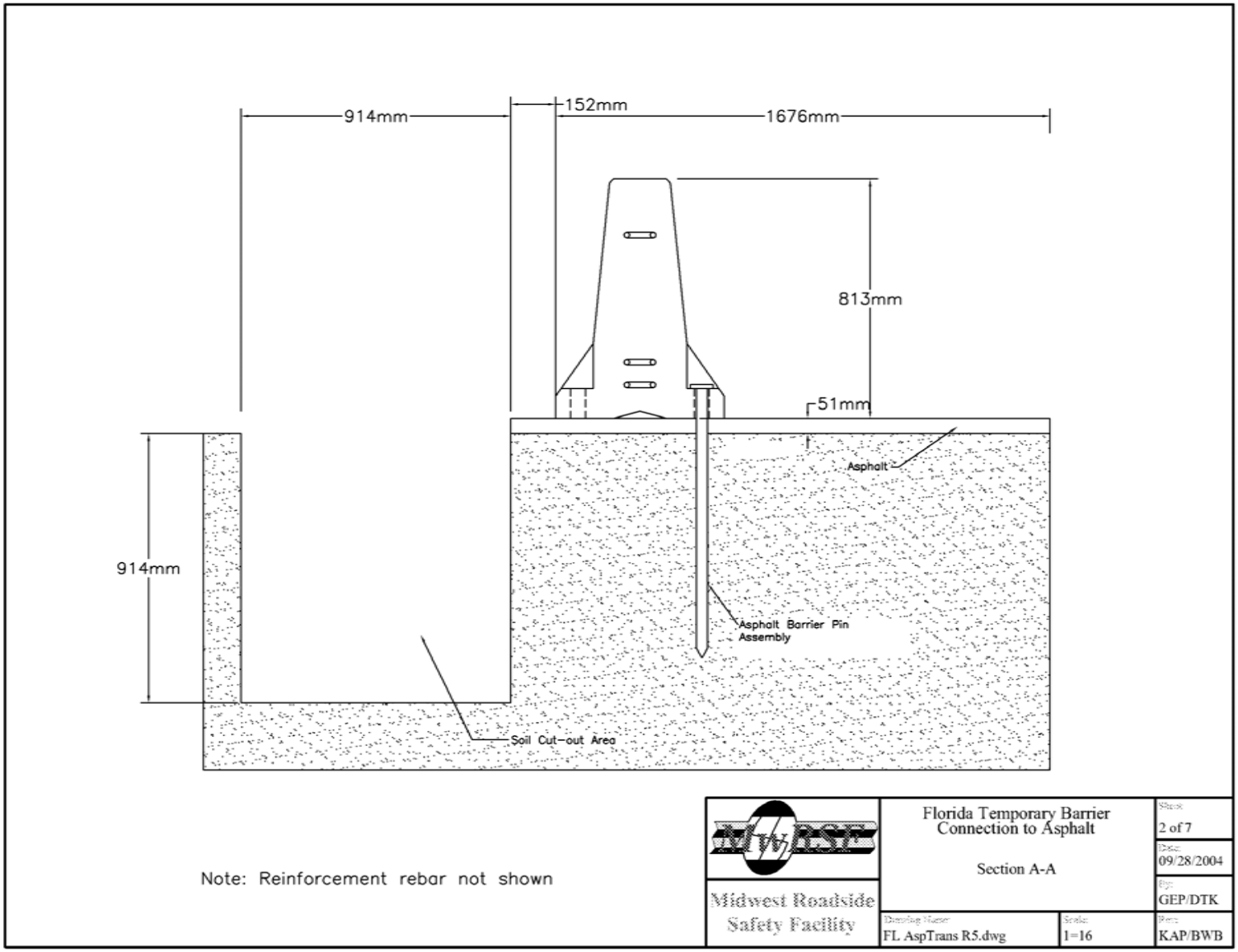

Figure 6. Asphalt Pin Tie-Down Design Details

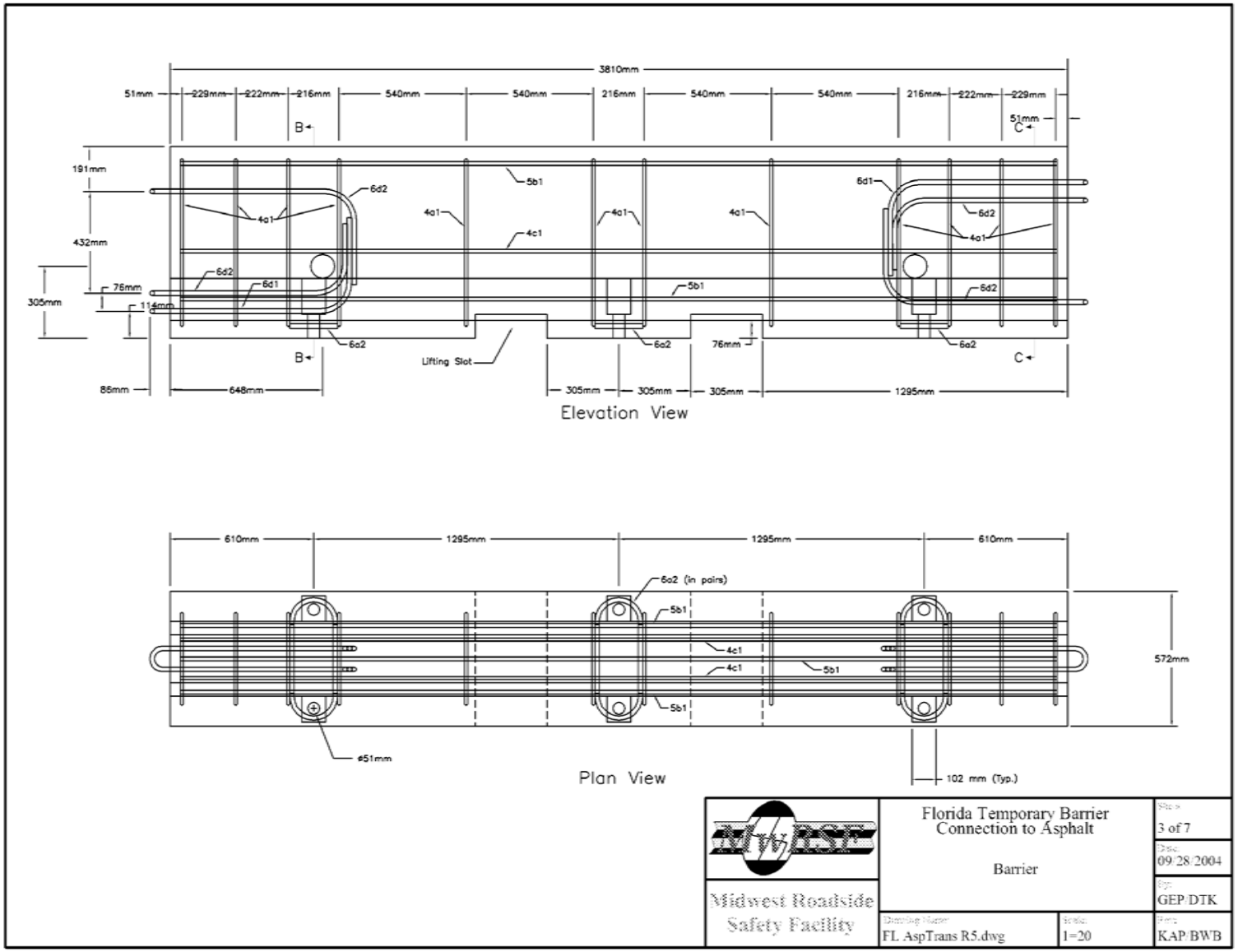

Figure 7. Asphalt Pin Tie-Down Design Details

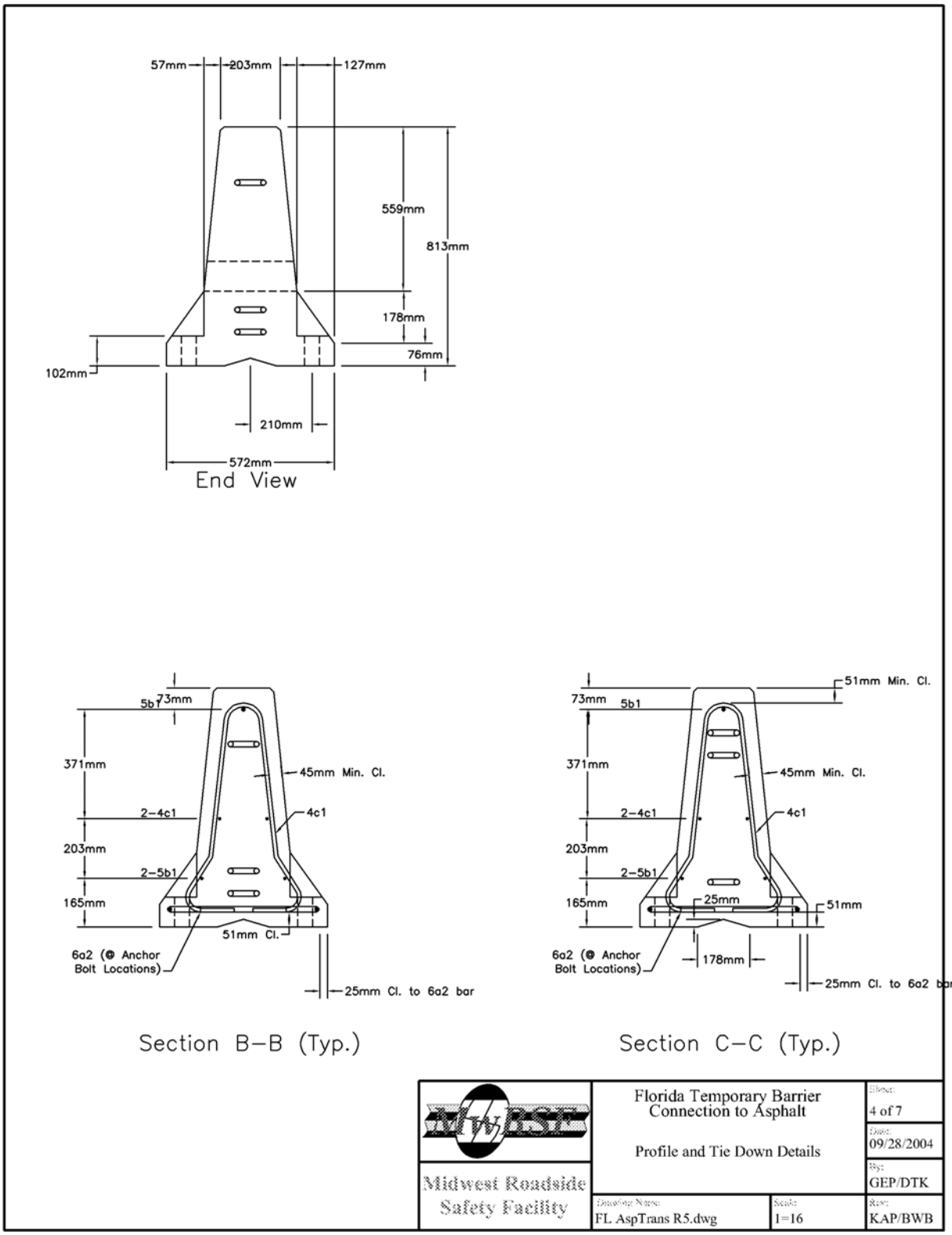

Figure 8. Asphalt Pin Tie-Down Design Details

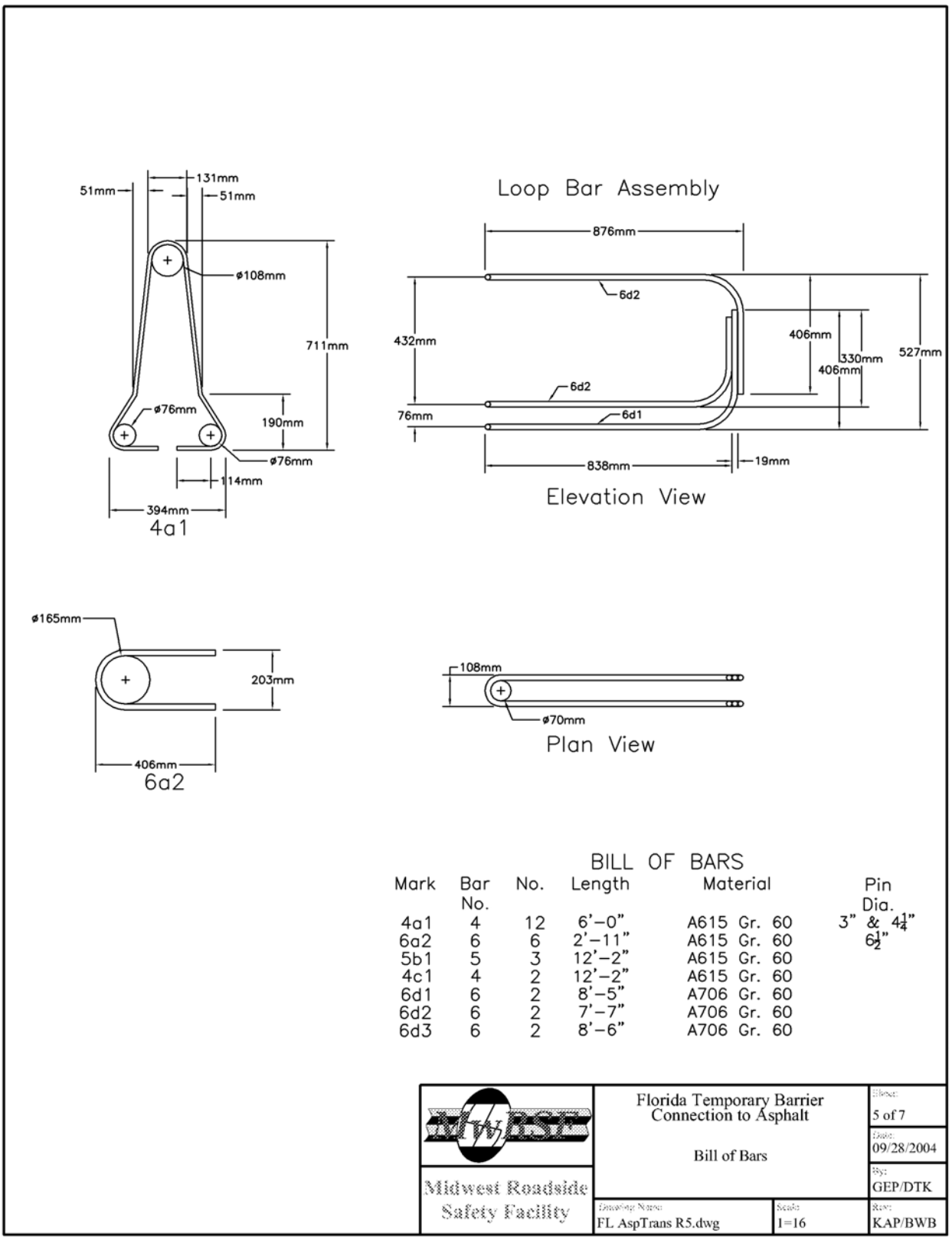

Figure 9. Asphalt Pin Tie-Down Design Details

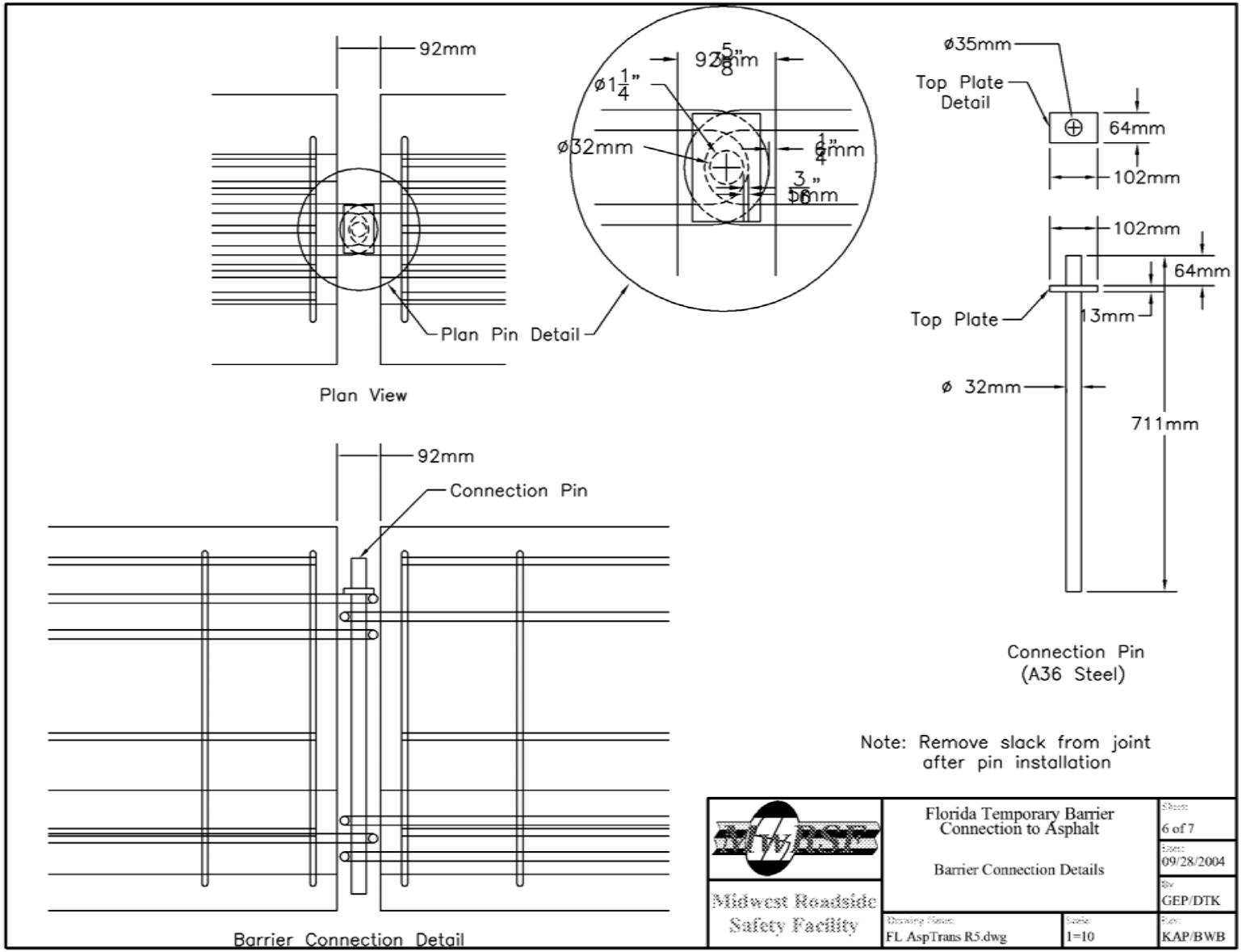

Figure 10. Asphalt Pin Tie-Down Design Details

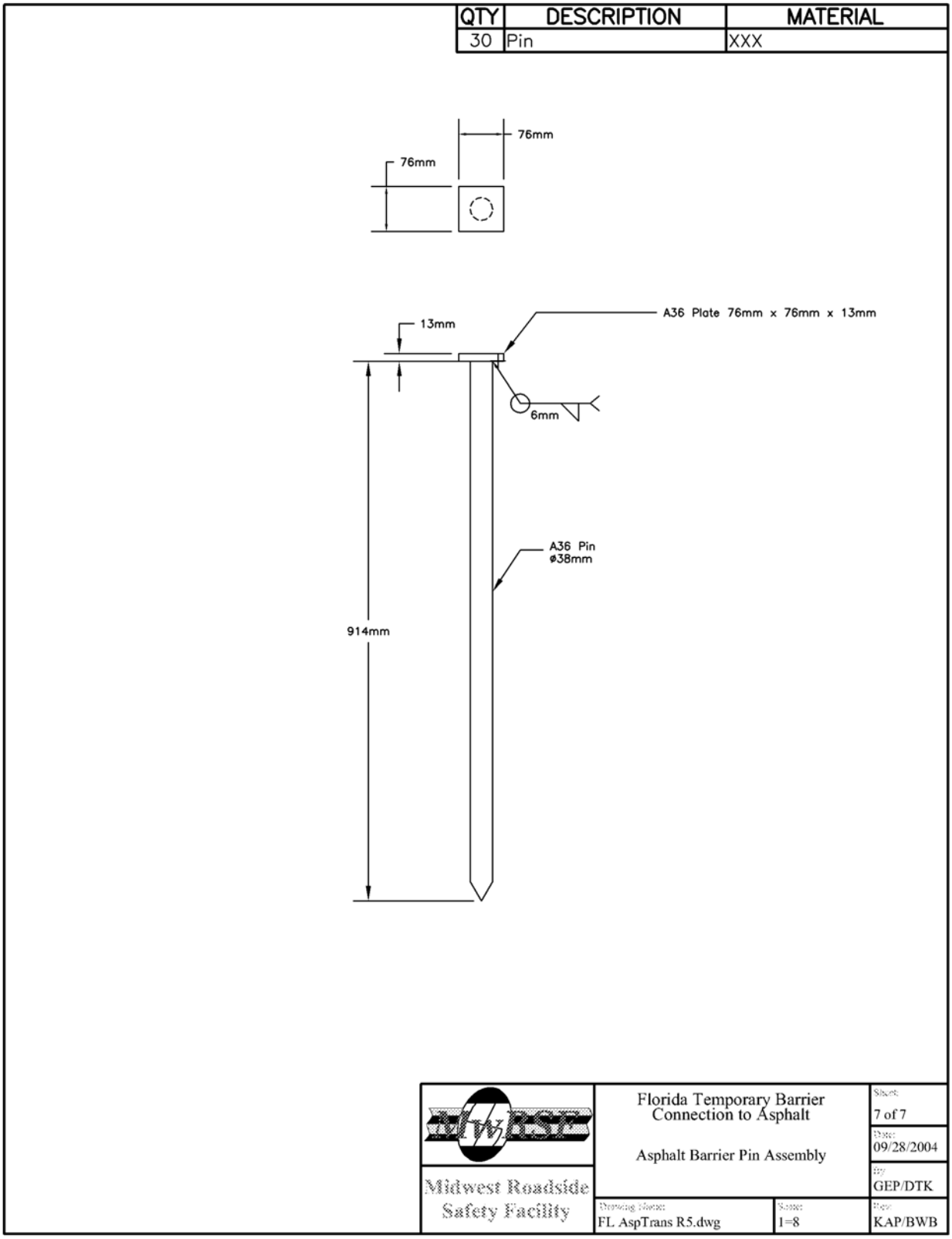

Figure 11. Asphalt Pin Tie-Down Design Details

Figure 12. Asphalt Pin Tie-Down Design Photographs

Figure 13. Asphalt Pin Tie-Down Design Photographs

4 TEST REQUIREMENTS AND EVALUATION CRITERIA

4.1 Test Requirements

Longitudinal barriers, such as temporary concrete barriers, must satisfy the requirements provided in NCHRP Report No. 350 to be accepted for use on National Highway System (NHS) construction projects or as a replacement for existing systems not meeting current safety criteria. According to TL-3 of NCHRP Report No. 350, the longitudinal barriers must be subjected to two full-scale vehicle crash tests. The two crash tests are as follows:

1. Test Designation 3-10, consisting of an 820-kg (1,808-lb) small car impacting the longitudinal barrier system at a nominal speed and angle of 100.0 km/hr (62.1 mph) and 20 degrees, respectively.
2. Test Designation 3-11, consisting of a 2,000-kg (4,409-lb) pickup truck impacting the longitudinal barrier system at a nominal speed and angle of 100.0 km/hr (62.1 mph) and 25 degrees, respectively.

In addition, guardrail transitions must be subjected to two full-scale vehicle crash tests. The two crash tests are as follows:

1. Test Designation 3-20, consisting of an 820-kg (1,808-lb) small car impacting the approach transition at a nominal speed and angle of 100.0 km/hr (62.1 mph) and 20 degrees, respectively.
2. Test Designation 3-21, consisting of a 2,000-kg (4,409-lb) pickup truck impacting the approach transition at a nominal speed and angle of 100.0 km/hr (62.1 mph) and 25 degrees, respectively.

The 820-kg small car tests were omitted based on previous research that demonstrated the performance of small cars on safety shape barriers. First, rigid New Jersey safety shape barriers

have been shown to meet safety performance standards when impacted by small cars [7-8]. Second, small car crash tests conducted on temporary New Jersey safety shape concrete median barriers resulted in little barrier movement [9]. Third, computer simulation modeling of safety shape barriers has revealed that the F-shape concrete median barrier offers a slight improvement in safety performance over the New Jersey safety shape [6]. Finally, a small car crash test was successfully conducted on a rigid, F-shape bridge rail; and therefore, it was reasoned to be a valid indicator of the safety performance of F-shape tie-down temporary barrier system [10]. As a result, only test nos. 3-11 and 3-21 were conducted as compliance tests for the systems described herein. These tests are summarized in Table 1.

4.2 Evaluation Criteria

Evaluation criteria for full-scale vehicle crash testing are based on three appraisal areas: (1) structural adequacy; (2) occupant risk; and (3) vehicle trajectory after collision. Criteria for structural adequacy are intended to evaluate the ability of the barrier to contain, redirect, or allow controlled vehicle penetration in a predictable manner. Occupant risk evaluates the degree of hazard to occupants in the impacting vehicle. Vehicle trajectory after collision is a measure of the potential for the post-impact trajectory of the vehicle to cause subsequent multi-vehicle accidents. This criterion also indicates the potential safety hazard for the occupants of other vehicles or the occupants of the impacting vehicle when subjected to secondary collisions with other fixed objects. These three evaluation criteria are defined in Table 1. The full-scale vehicle crash test was conducted and reported in accordance with the procedures provided in NCHRP Report No. 350.

Table 1. Test Requirements

Test Article	Test Level	Barrier Section	Test Designation	Impact Conditions				Evaluation Criteria*
				Test Vehicle	Speed		Angle	
					km/h	mph	degrees	
Longitudinal Barrier	3	Length of Need	3-10	820C	100	62.1	20	A,D,F,H,I,K,M
			S3-10[a]	700C	100	62.1	20	A,D,F,H,I,K,M
			3-11	2000P	100	62.1	25	A,D,F,K,L,M
		Transition	3-20[d]	820C	100	62.1	20	A,D,F,H,I,K,M
			S3-20[a]	700C	100	62.1	20	A,D,F,H,I,K,M
			3-21	2000P	100	62.1	25	A,D,F,K,L,M

Table 2. Evaluation Criteria

Structural Adequacy	A.	Test article should contain and redirect the vehicle; the vehicle should not penetrate, underride, or override the installation although controlled lateral deflection of the test article is acceptable.
	B.	The test article should readily activate in a predictable manner by breaking away, fracturaing, or yielding.
	C.	Acceptable test article performance may be by redirection, controlled penetration, or controlled stopping of the vehicle.
Occupant Risk	D.	Detached elements, fragments or other debris from the test article should not penetrate or show potential for penetrating the occupant compartment, or present an undue hazard to other traffic, pedestrians, or personnel in a work zone. Deformations of, or intrusions into, the occupant compartment that could cause serious injuries
	E.	Detached elements, fragments or other debris from the test article, or vehicular damage should not block the driver's vision or otherwise cause the driver to lose control of the vehicle.
	F.	The vehicle should remain upright during and after collision although moderate roll, pitching, and yawing are acceptable.
	G.	It is preferable, although not essential, that the vehicle remain upright during and after collision.
	H.	Longitudinal and lateral occupant impact velocities should fall below the preferred value of 9 m/s (29.53 ft/s), or at least below the maximum allowable value of 12 m/s (39.37 ft/s).
	I.	Longitudinal and lateral occupant ridedown accelerations should fall below the preferred value of 15 g's, or at least below the maximum allowable value of 20 g's.
	J.	(Optional) Hybrid III dummy. Response should conform to evaluation criteria of Part 571.208, Title 49 of Code of Federal Regulation, Chapter V (10-1-88 Edition). See Section 5.3 for limitations of Hybrid III dummy.
Vehicle Trajectory	K.	After collision it is preferable that the vehicle's trajectory not intrude into adjacent traffic lanes.
	L.	The occupant impact velocity in the longitudinal direction should not exceed 12 m/xec (39.37 ft/s), and the occupant ridedown acceleration in the longitudinal direction should not exceed 20 G's.
	M.	The exit angle from the test article preferably should be less than 60 percent of the test impact angle measured at the time of vehicle loss of contact with the test device.
	N.	Vehicle trajectory behind the test article is acceptable.

5 TEST CONDITIONS

5.1 Test Facility

The testing facility is located at the Lincoln Air Park on the northwest (NW) side of the Lincoln Municipal Airport and is approximately 8.0 km (5 mi.) NW of the University of Nebraska-Lincoln.

5.2 Vehicle Tow and Guidance System

A reverse cable tow system with a 1:2 mechanical advantage was used to propel the test vehicle. The distance traveled and the speed of the tow vehicle were one-half that of the test vehicle. The test vehicle was released from the tow cable before impact with the barrier system. A digital speedometer was located on the tow vehicle to increase the accuracy of the test vehicle impact speed.

A vehicle guidance system developed by Hinch [11] was used to steer the test vehicle. A guide-flag, attached to the front-right wheel and the guide cable, was sheared off before impact with the barrier system. The 9.5-mm (0.375-in.) diameter guide cable was tensioned to approximately 15.6 kN (3,500 lbs), and supported laterally and vertically every 30.48 m (100 ft) by hinged stanchions. The hinged stanchions stood upright while holding up the guide cable, but as the vehicle was towed down the line, the guide-flag struck and knocked each stanchion to the ground. For tests FTB-1 and FTB-2, the vehicle guidance systems were 305 m (1,000 ft) long.

5.3 Test Vehicles

For test no. FTB-1, a 1998 GMC C2500 pickup truck was used as the test vehicle. The test inertial and gross static weights were 2,011 kg (4,433 lbs). The test vehicle dimensions are shown in Figure 14.

Date: 9/27/2004 Test Number: FTB-1 Model: 2000P

Make: GMC Vehicle I.D.#: 1GDBC24R6WZ542276

Tire Size: 245/75 R16 Year: 1998 Odometer: 239992

*(All Measurements Refer to Impacting Side)

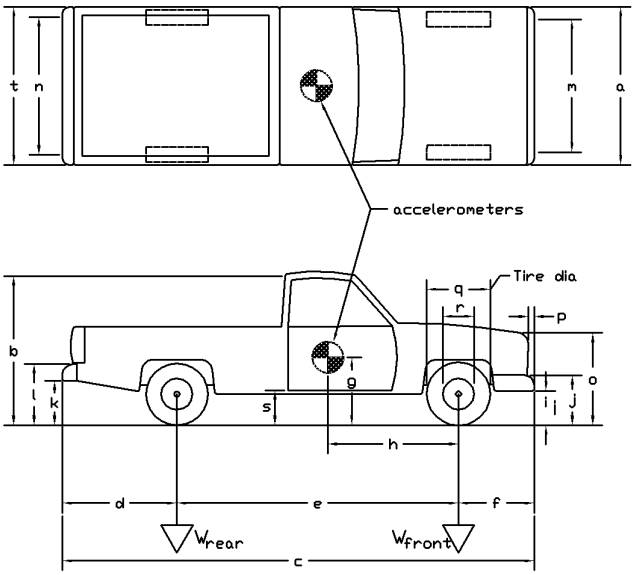

Vehicle Geometry – mm (in.)

a	1873 (73.75)	b	1854 (73)
c	5537 (218.0)	d	1311 (51.625)
e	3334 (131.25)	f	892 (35.125)
g	667 (26.25)	h	1391 (54.75)
i	457 (18)	j	667 (26.25)
k	591 (23.25)	l	781 (30.75)
m	1591 (62.625)	n	1626 (64.0)
o	1035 (40.75)	p	76 (3.0)
q	775 (30.5)	r	445 (17.5)
s	483 (19.0)	t	1854 (73.0)

Wheel Center Height Front 368 (14.5)

Wheel Center Height Rear 362 (14.25)

Wheel Well Clearance (FR) 413 (16.25)

Wheel Well Clearance (RR) 686 (27.0)

Engine Type 8 CYL. GAS

Engine Size 5.7 L 350 CID

Transmission Type:

Automatic or Manual

FWD or RWD or 4WD

Weights kg (lbs)	Curb	Test Inertial	Gross Static
W_{front}	1135(2503)	1172 (2583)	1172 (2583)
W_{rear}	819 (1805)	839 (1850)	839 (1850)
W_{total}	1954 (4308)	2011 (4433)	2011 (4433)

Note any damage prior to test: Minor cosmetic box damage

Figure 14. Vehicle Dimensions, Test No. FTB-1

For test no. FTB-2, a 2000 GMC C2500 pickup truck was used as the test vehicle. The test inertial and gross static weights were 2,030 kg (4,475 lbs). The test vehicle dimensions are shown in Figure 15.

Black and white, checkered targets were placed on the vehicles, as shown in Figure 16 and Figure 17, to aid in the analysis of the high-speed digital video. One target was placed directly above each of the wheels, and another was placed at the vehicle's center of gravity on both the driver and passenger sides. In addition, targets were placed on the top of the vehicle. One was placed at the vehicle's center of gravity, two were placed on the windshield, one was placed on the hood of the vehicle, two were placed in the pickup box, and four targets were placed on the side walls of the box, aligned with those placed in the box.

The front wheels of the test vehicle were aligned for camber, caster, and toe-in values of zero so the vehicle would track properly along the guide cable. A 5B flash bulb was mounted on the left quarter point of the vehicle's roof to pinpoint the time of impact with the test article on the high-speed video footage. The flash bulb was fired by a pressure tape switch mounted at the center point on the front face of the bumper. A remote-controlled brake system was installed in the test vehicle so the vehicle could be brought safely to a stop after the test.

5.4 Data Acquisition Systems

Three data acquisition systems, two accelerometers and one rate transducer, were used to measure the motion of the vehicle. The results of all three were analyzed and plotted using "DynaMax 1 (DM-1)" and "DADiSP" computer software programs.

5.4.1 Accelerometers

Two triaxial piezoresistive accelerometer systems, described below, were used to measure the acceleration in the longitudinal, lateral, and vertical directions.

Date: 04/20/2005 Test Number: FTB–2 Model: 2000P

Make: GMC Vehicle I.D.#: 1GDGC24R7YF476051

Tire Size: LT 245/75 R16 Year: 2000 Odometer: 248979

*(All Measurements Refer to Impacting Side)

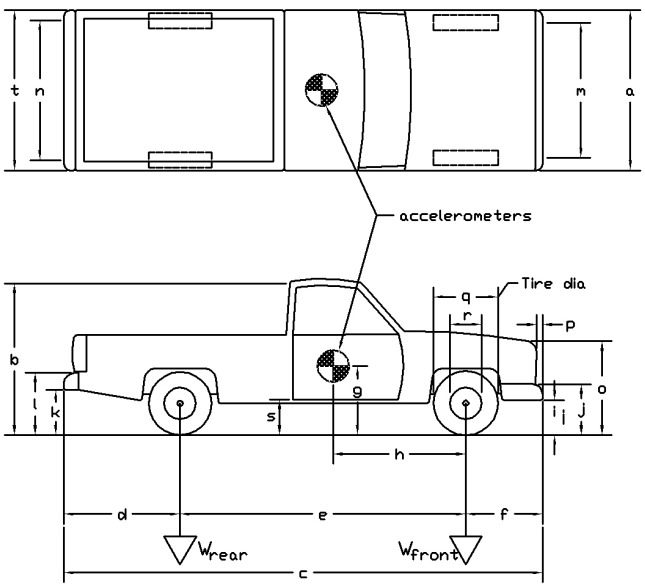

Vehicle Geometry – mm (in.)

a	1892 (74.5)	b	1857 (73.125)
c	5537 (218)	d	1321 (52.0)
e	3334 (131.25)	f	918 (36.125)
g	667 (26.25)	h	1400 (55.125)
i	464 (18.25)	j	664 (26.125)
k	603 (23.75)	l	794 (31.25)
m	1708 (67.25)	n	1626 (64)
o	1197 (47.125)	p	83 (3.25)
q	756 (29.75)	r	445 (17.5)
s	502 (19.75)	t	1867 (73.5)

Wheel Center Height Front 368 (14.5)

Wheel Center Height Rear 371 (14.625)

Wheel Well Clearance (FR) 981 (38.625)

Wheel Well Clearance (RR) 981 (38.625)

Frame Height (FR) 400 (15.75)

Frame Height (RR) 695 (37.375)

Weights kg (lbs)	Curb	Test Inertial	Gross Static
W_{front}	1144 (2521)	1177 (2596)	1177 (2596)
W_{rear}	850 (1874)	853 (1880)	853 (1880)
W_{total}	1971 (4395)	2030 (4476)	2030 (4476)

Engine Type 8 CYL. GAS

Engine Size 5.7 L 350c.i.

Transmission Type:

(Automatic) or Manual

FWD or (RWD) or 4WD

GVWR Ratings Front 1860 (4100)

Rear 2722 (6000)

Total 3901 (8600)

Note any damage prior to test: None

Figure 15. Vehicle Dimensions, Test No. FTB-2

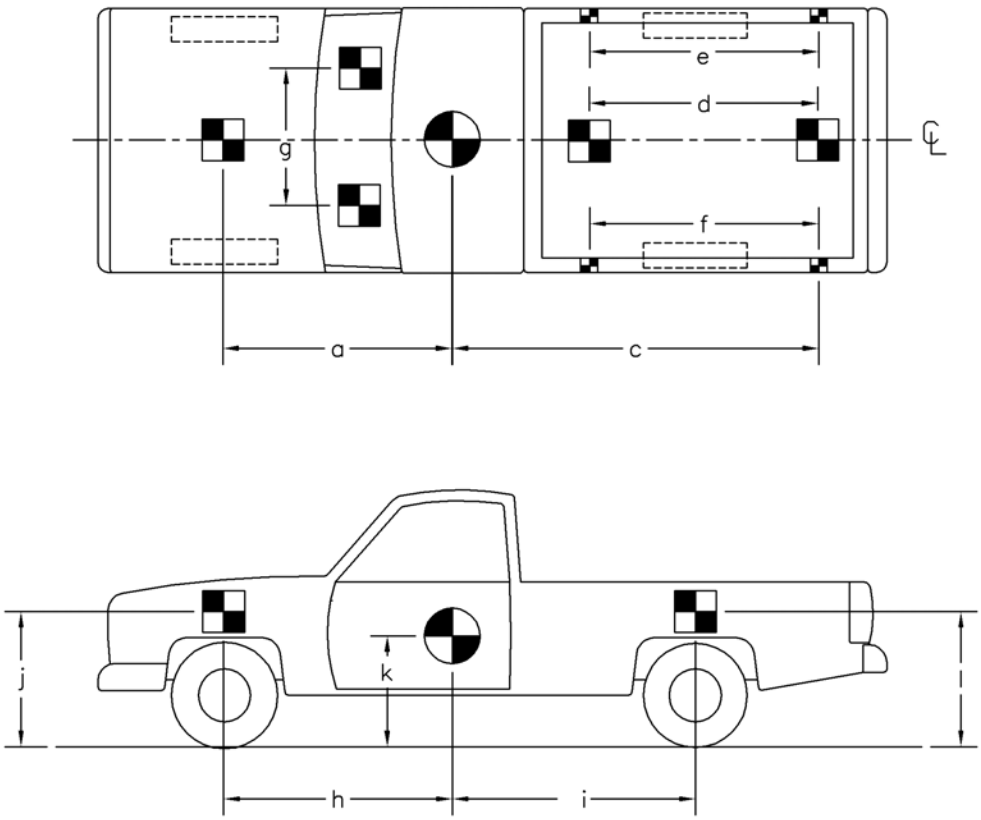

TEST #: FTB–1

TARGET GEOMETRY -- mm (in.)

a	1584 (62.375)	d	1886 (74.25)	g	911 (35.875)	j	1006 (39.625)
b	–	e	2153 (84.75)	h	1391 (54.75)	k	667 (26.25)
c	2750 (108.25)	f	2153 (84.75)	i	1943 (76.5)	l	1181 (46.5)

Figure 16. Vehicle Target Locations, Test No. FTB-1

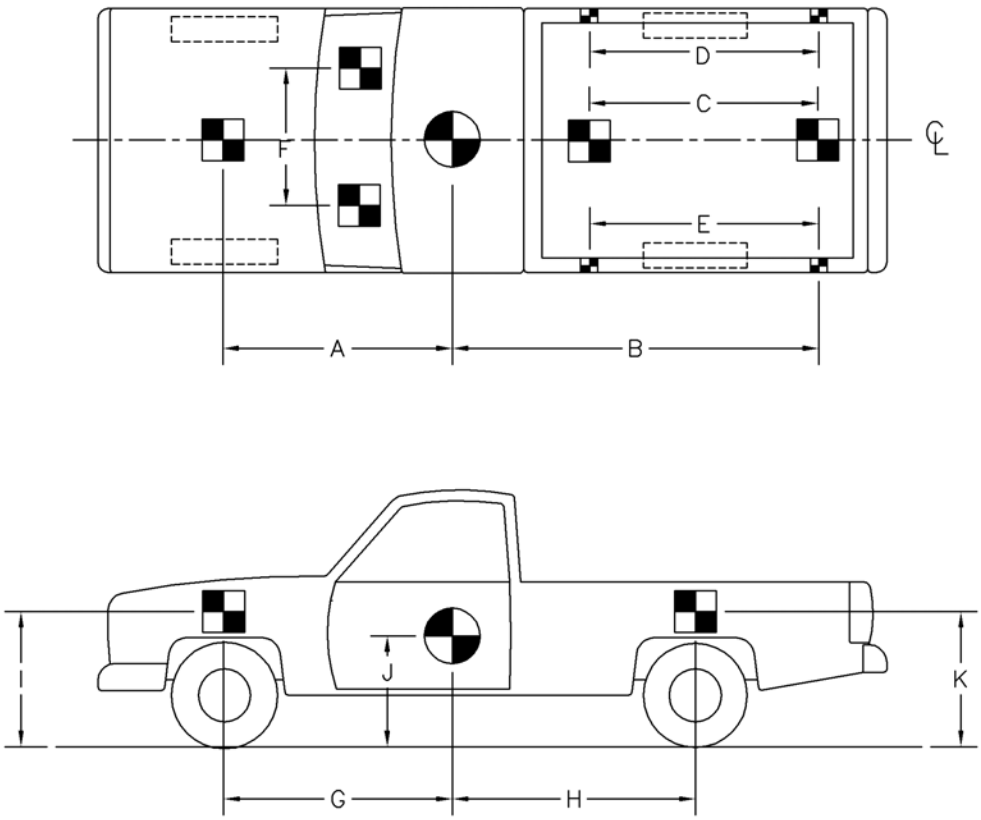

TEST #: FTB-2

TARGET GEOMETRY -- mm (in.)

A 1626 (64.0)	D 2121 (83.5)	G 1410 (55.5)	J 667 (26.25)
B 2635 (103.75)	E 2121 (83.5)	H 1969 (77.5)	K 1080 (42.5)
C 1683 (66.25)	F 1143 (45.0)	I 1022 (40.25)	

Figure 17. Vehicle Target Locations, Test No. FTB-2

Principle EDR:

- Model EDR-4M6 – Instrumented Sensor Technology (IST) of Okemos, MI
- ± 200 G's
- 10,000 Hz Sample Rate
- 3 Differential Channels, 3 Single-Ended Channels
- 6 Mb RAM Memory
- 1,500 Hz lowpass filter

Secondary EDR:

- Model EDR-3 – Instrumented Sensor Technology (IST) of Okemos, MI
- ± 200 G's
- 3,200 Hz Sample Rate
- 256 Kb RAM Memory
- 1,120 Hz lowpass filter

Computer software "DynaMax 1 (DM-1)" and "DADiSP," was used to analyze and plot the accelerometer data.

5.4.2 Rate Transducers

An Analog Systems 3-axis rate transducer with a range of 1,200 degrees/sec in each of the three directions (pitch, roll, and yaw) was used to measure the rates of motion of the test vehicle. The rate transducer was mounted inside the body of the EDR-4M6 and recorded data at 10,000 Hz to a second data acquisition board inside the EDR-4M6 housing. The raw data measurements were then downloaded, converted to the appropriate Euler angles for analysis, and plotted. Computer software, "DynaMax 1" and "DADiSP," was used to analyze and plot the rate transducer data.

5.4.3 High-Speed Photography

For test no. FTB-1, two high-speed Photron digital video cameras operating at 500 frames per second, three high-speed 16-mm Red Lake E/cam video cameras operating at 500 frames per second, one Locam high speed film camera operating at 500 frames per second, and

six digital video cameras were used. Camera layout details for test no. FTB-1 are detailed in Figure 18.

For test no. FTB-2, two high-speed Photron digital video cameras operating at 500 frames per second, two AOS high-speed digital video cameras operating at 500 frames per second, one high-speed 16-mm Red Lake E/cam video camera operating at 500 frames per second, and seven digital video cameras were used. Camera layout details for test no. FTB-2 are detailed in Figure 19.

The Photron and E/cam videos were analyzed using Image Express MotionPlus and Redlake Motion Scope software, respectively. Camera speed and camera divergence factors were considered in the analysis of the high-speed videos.

5.4.4 Pressure Tape Switches

For both tests, five pressure-activated tape switches, spaced at 2-m (6.56-ft) intervals, were used to determine the speed of the vehicle before impact. Each tape switch fired a strobe light which sent an electronic timing signal to the data acquisition system as the left-front tire of the test vehicle passed over it. The test vehicle speed was then determined from the electronic timing mark data recorded using the “DADiSP” software. Strobe lights and high-speed film analysis are used only as a backup in the event that vehicle speed cannot be determined from the electronic data.

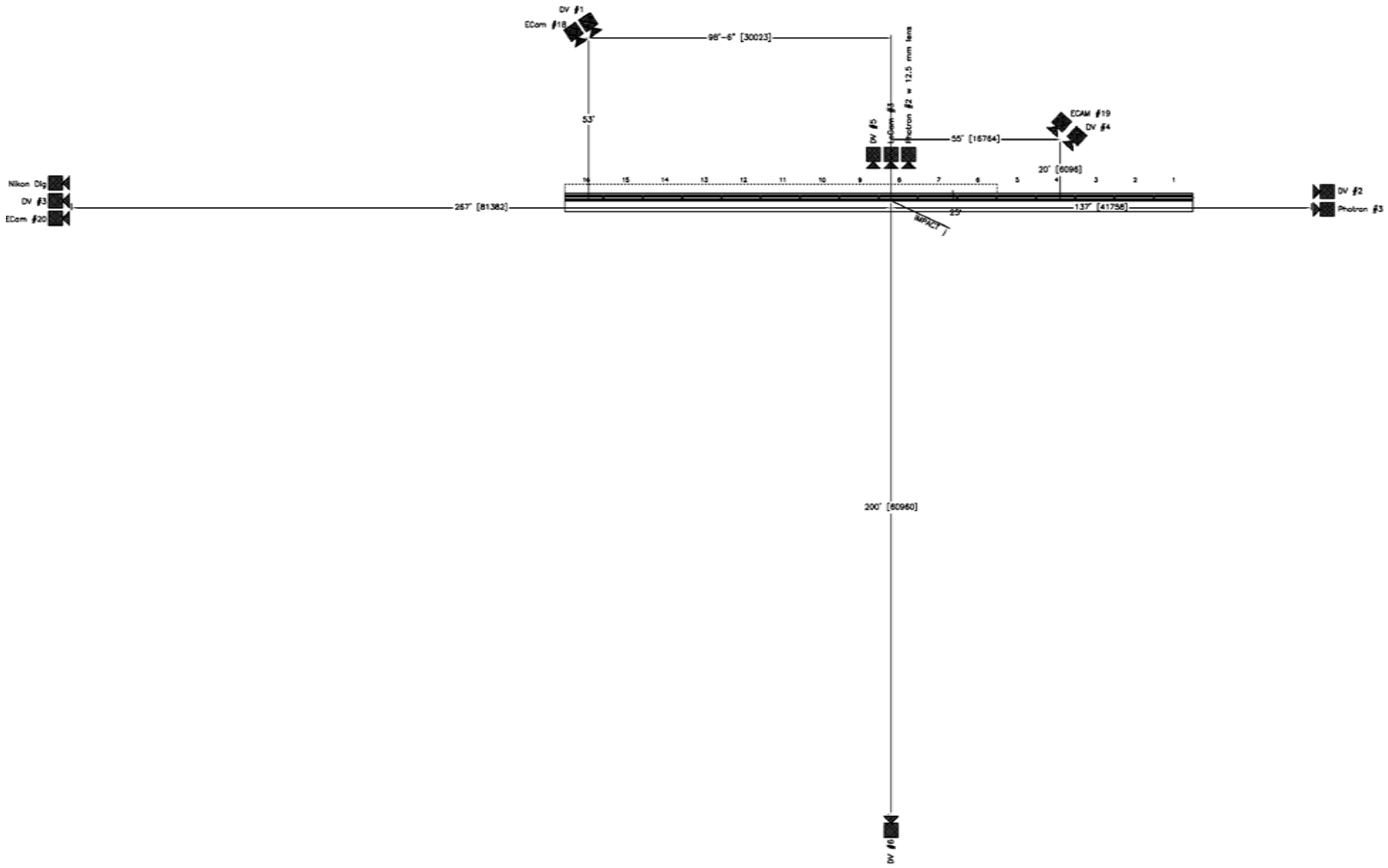

Figure 18. Location of High-Speed Cameras, Test No. FTB-1

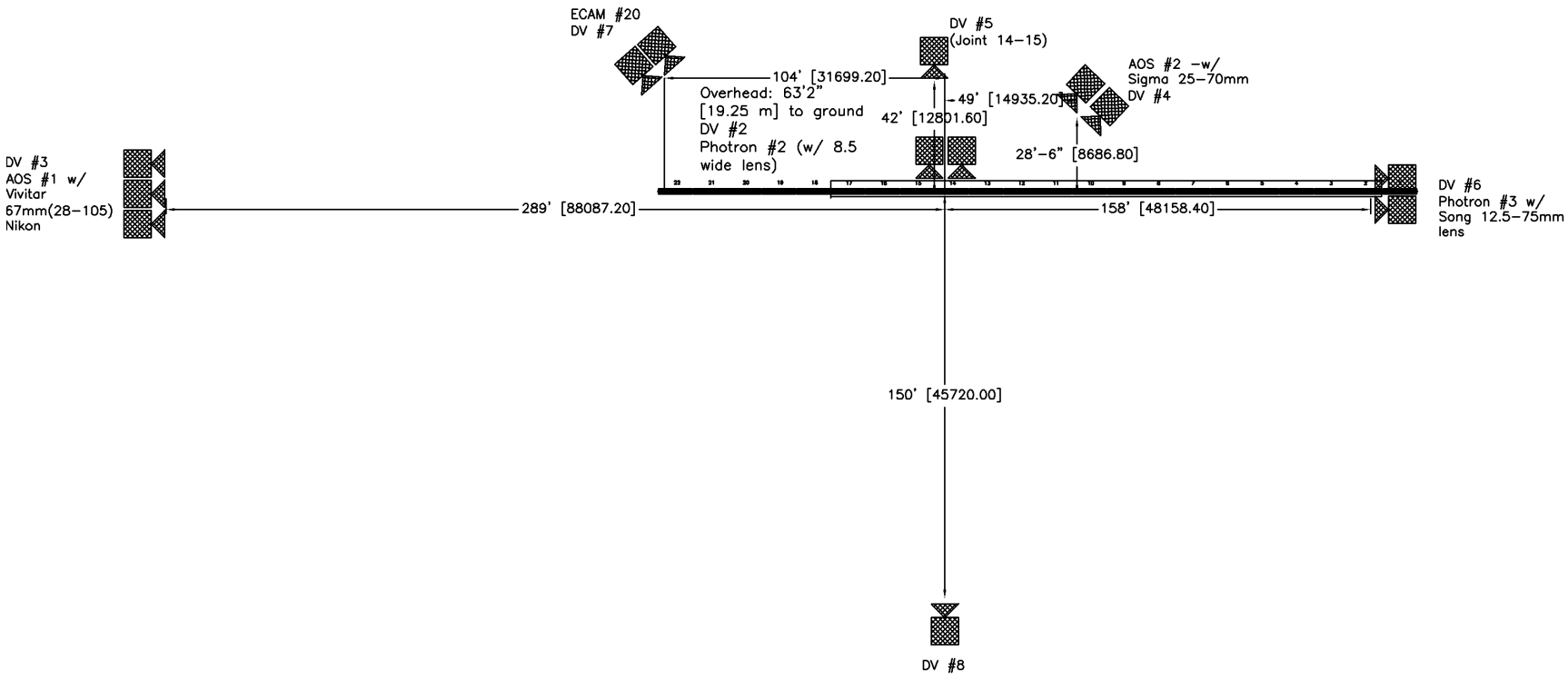

Figure 19. Location of High-Speed Cameras, Test No. FTB-2

6 FULL-SCALE TEST NO. FTB-1

6.1 Test No. FTB-1

For test no. FTB-1, a 2,011-kg (4,434 lbs) pickup truck impacted the asphalt tie-down temporary concrete barrier system at a speed of 98.7 km/hr (61.3 mph) and at an angle of 25.4 degrees. A summary of the test results and the sequential photographs are shown in Figure 20. The summary of the test results and sequential photographs in English units is shown in Appendix B. Additional sequential photographs are shown in Figure 21. Documentary photographs of the crash test are shown in Figure 22 through Figure 25.

6.2 Test Description

The impact point for this test was 1,219-mm upstream of the joint between barrier nos. 8 and 9, as shown in Figure 26. Immediately after impact, the impacted barrier segments began to deflect backwards, and the right-front corner of the pickup truck was deformed inward. At 0.105 sec, the leading edge of the right-front door panel snagged on the joint between barrier nos. 8 and 9. As the vehicle continued to redirect, the asphalt and soil in the impact region fractured and separated from the foundation. However, the separation was not complete, and the barrier segments remained upright and stable on the separated section of roadway. By 0.236 sec, the pickup truck had redirected parallel to the barriers with a speed of 64.9 km/h (40.3 mph). After exiting the barrier at 0.380 sec, the pickup truck continued to move downstream and to the left until coming to rest 69.7-m (228.7-ft) downstream and 6.9 m (22.6-ft) to the left of the original impact point. A summary of the test results and sequential photographs is shown in Figure 20.

6.3 System Damage

Damage to the tie-down temporary barrier system was moderate, as shown in Figure 27 through Figure 29. Tire marks, scrapes, and cracking of the concrete were visible on barrier

segment nos. 8 through 10. Barrier section nos. 8 through 10 were deflected laterally. A region of soil and asphalt was observed to fracture and separate from the main road surface beneath the barrier due to loading of the tie-down pins. The separation area was approximately 7.16-m (23.5-ft) long with an average separation of 178 mm (7 in.). Deformation to several of the barrier joints and the tie-down pins was noted in the impact region. Several of the tie-down pins were pulled up between 13 to 51 mm (0.5 to 2 in.) due to barrier rotation. The steel caps on three of the pins in the impact region were disengaged from the top of the pin due to fracture of the welds. No movement of the tie-down pins was noted on the non-impacted barrier segments. Damaged concrete was observed near several of the vertical holes on the front face of the barriers in the impact region, but the reinforcing steel surrounding the holes remained intact and safely around the pins. The maximum permanent set and dynamic barrier deflections were measured to be 283 mm (11.1-in.) and 554 mm (21.8-in.), respectively.

6.4 Vehicle Damage

Vehicle damage was moderate, as shown in Figure 30 and Figure 31. The majority of the damage to the pickup truck was focused on the right-front corner and right side where the impact occurred, including the right-front bumper, fender, and suspension components. Scrapes and dents from vehicle contact with the barriers were observed on the bottom of the truck bed and the right-side door of the vehicle. A section of the sheet metal on the front edge of the right-side door was torn away due to snagging on a barrier joint. The right-front tire and the outside of the steel rim were disengaged from the main body of the wheel assembly during impact. Minimal damage was observed in the interior occupant compartment of the vehicle, and the maximum deformation of the passenger-side floor pan was 38 mm (1.5 in.). Details from the occupant compartment deformation measurements are located in Appendix C.

6.5 Occupant Risk Values

The longitudinal and lateral occupant impact velocities (OIV) were determined to be 3.93 m/s (12.9 ft/s) and 5.73 m/s (18.8 ft/s), respectively. The maximum 0.010-sec average occupant ridedown decelerations (ORD) in the longitudinal and lateral directions were 18.89 g's and 14.00 g's, respectively. It is noted that the occupant impact velocities and the occupant ridedown decelerations were within the suggested limits provided in NCHRP Report No. 350. The results of the occupant risk, determined from the accelerometer data, are summarized in Figure 20. Results are shown graphically in Appendix D. Roll, pitch, and yaw data were collected from the rate gyroscope and are shown graphically in Appendix D.

6.6 Discussion

Following test no. FTB-1, a safety performance evaluation was conducted, and the asphalt tie-down system for temporary concrete barriers was determined to be acceptable according to the NCHRP Report No. 350 criteria for test designation no. 3-11. The deflection of the barriers was reduced from those observed in the free-standing barrier tests, and the barriers were safely constrained on the road surface. It should be noted that the separation of the road surface in the impact region allowed more deflection of the barrier system than was expected. However, even with the separation, the system reduced deflection and performed safely. It was expected that less severe installations with more foundation behind the installation would reduce deflections significantly.

0.000 sec | 0.152 sec | 0.350 sec | 0.500 sec | 0.768 sec

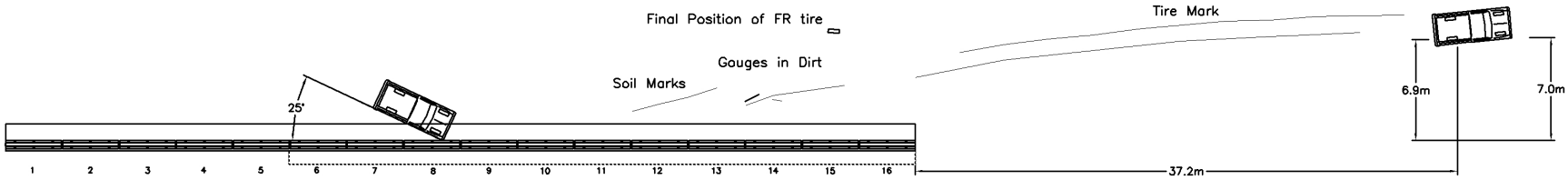

- Test Number FTB-1 (3-11)
- Date 9/27/04
- Test Article ..... F-shape PCB Asphalt Pin Tie-Down
- Total Length..... 62.34 m
- Overall Height..... 813 mm
- Placement..... 152 mm from the edge of a 914 mm vertical drop
- Barrier Elements ..... 16 Kansas F-shape PCB's
- Joint Connections..... 32-mm diameter by 712-mm long A36 steel pin with a 64x102x13-mm plate
- Tie-Down Anchors..... Three 38.1-mm dia. x 914-mm long A36 steel pins per barrier on the traffic side face only
- Soil Type..... Grading B - AASHTO M 147-65
- Vehicle Model..... 1998 GMC C2500
  - Curb..... 1,954 kg
  - Test Inertial ..... 2,011 kg
  - Gross Static ..... 2,011 kg
- Vehicle Speed
  - Impact..... 98.7 km/h
  - Exit ..... NA
- Vehicle Angle
  - Impact (trajectory)..... 25.4 deg
  - Exit (trajectory) ..... NA
- Vehicle Stability ..... Satisfactory
- Vehicle Snagging..... Minor
- Occupant Ridedown Deceleration (10 msec avg.)
  - Longitudinal..... 18.89 g's < 20 g's
  - Lateral (not req.)..... 14.00 g's < 20 g's
- Occupant Impact Velocity
  - Longitudinal..... 3.93 m/s < 12 m/s
  - Lateral (not req.)..... 5.73 m/s < 12 m/s
- THIV (not req.)..... 7.60 m/s < 12 m/s
- PHD (not req.) ..... 23.57 g's < 20 g's
- Vehicle Damage ..... Moderate
  - TAD 1-RFQ-3
  - SAE 1RFAW3
  - OCDI..... RF001100000
- Vehicle Stopping Distance..... 69.7 m downstream of impact 6.9 m from traffic side face
- Test Article Damage..... Moderate
- Maximum Deflection
  - Permanent Set ..... 283 mm
  - Dynamic..... 554 mm (top of barrier)
- Working Width..... 1,125 mm

Figure 20. Summary of Test Results and Sequential Photographs, Test FTB-1

0.000 sec

0.112 sec

0.268 sec

0.590 sec

1.030 sec

0.000 sec

0.090 sec

0.220 sec

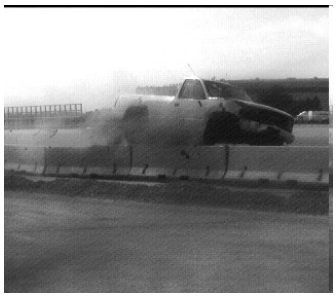

0.376 sec

0.552 sec

Figure 21. Additional Sequential Photographs, Test FTB-1

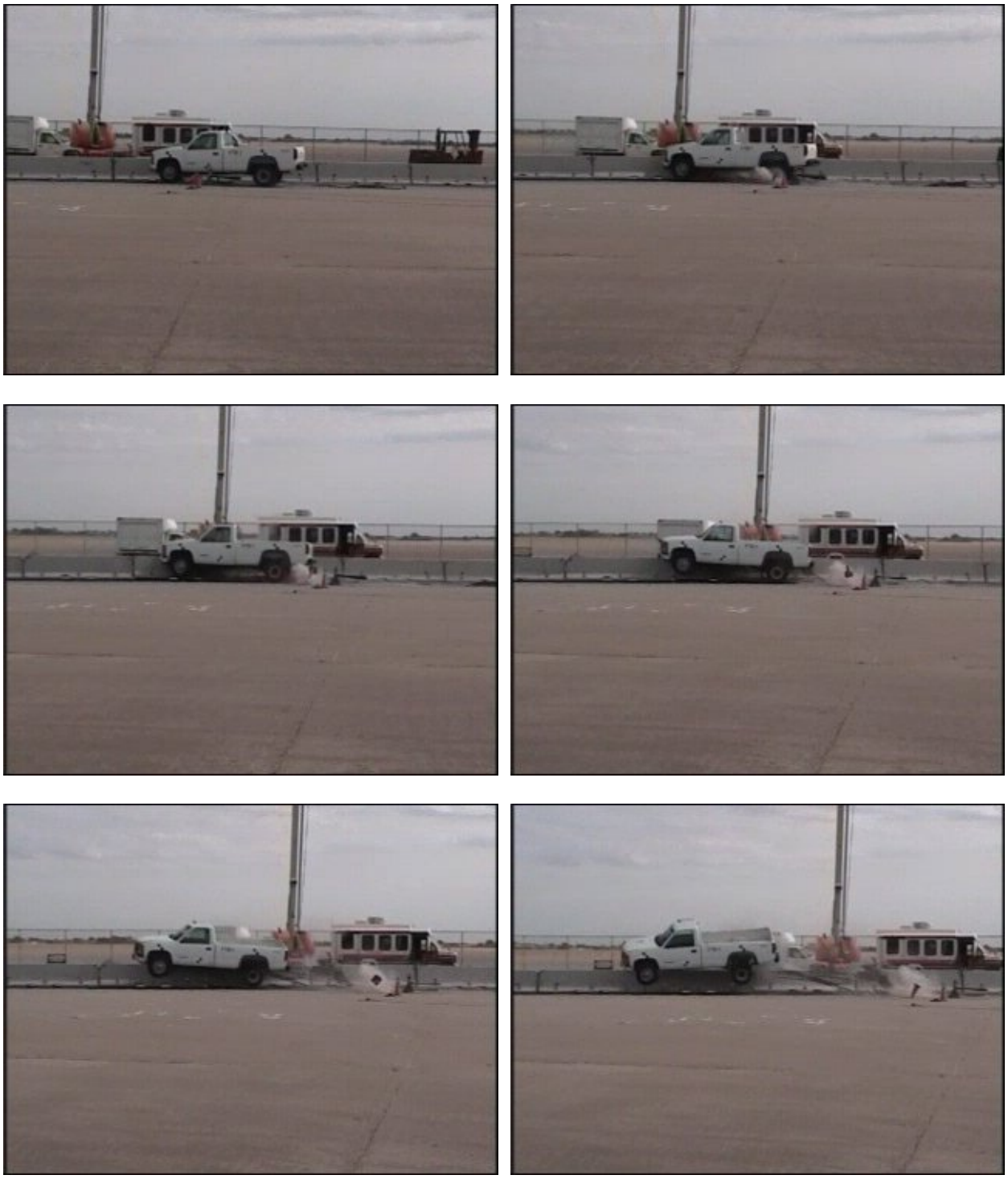

Figure 22. Documentary Photographs, Test FTB-1

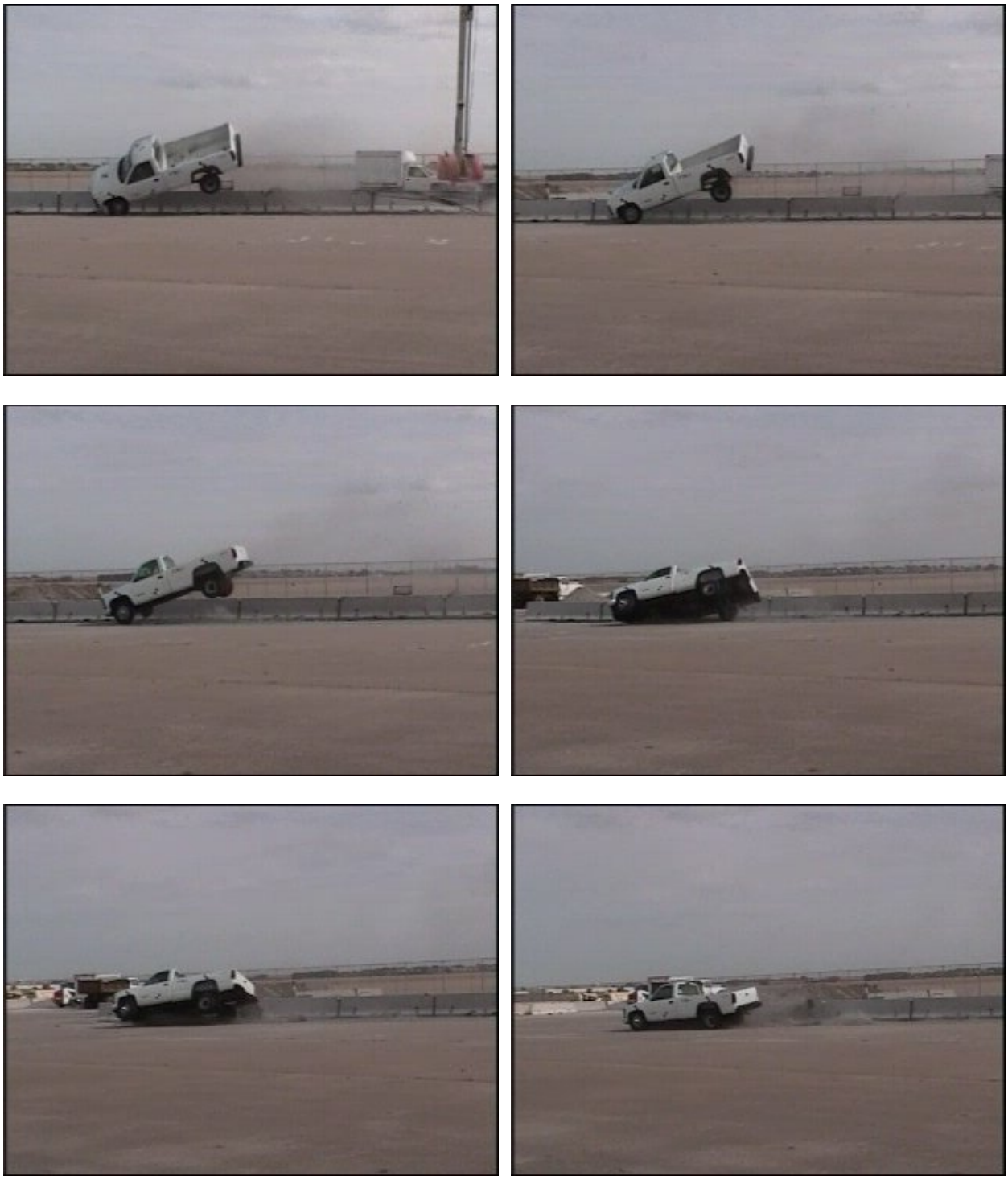

Figure 23. Documentary Photographs, Test FTB-1

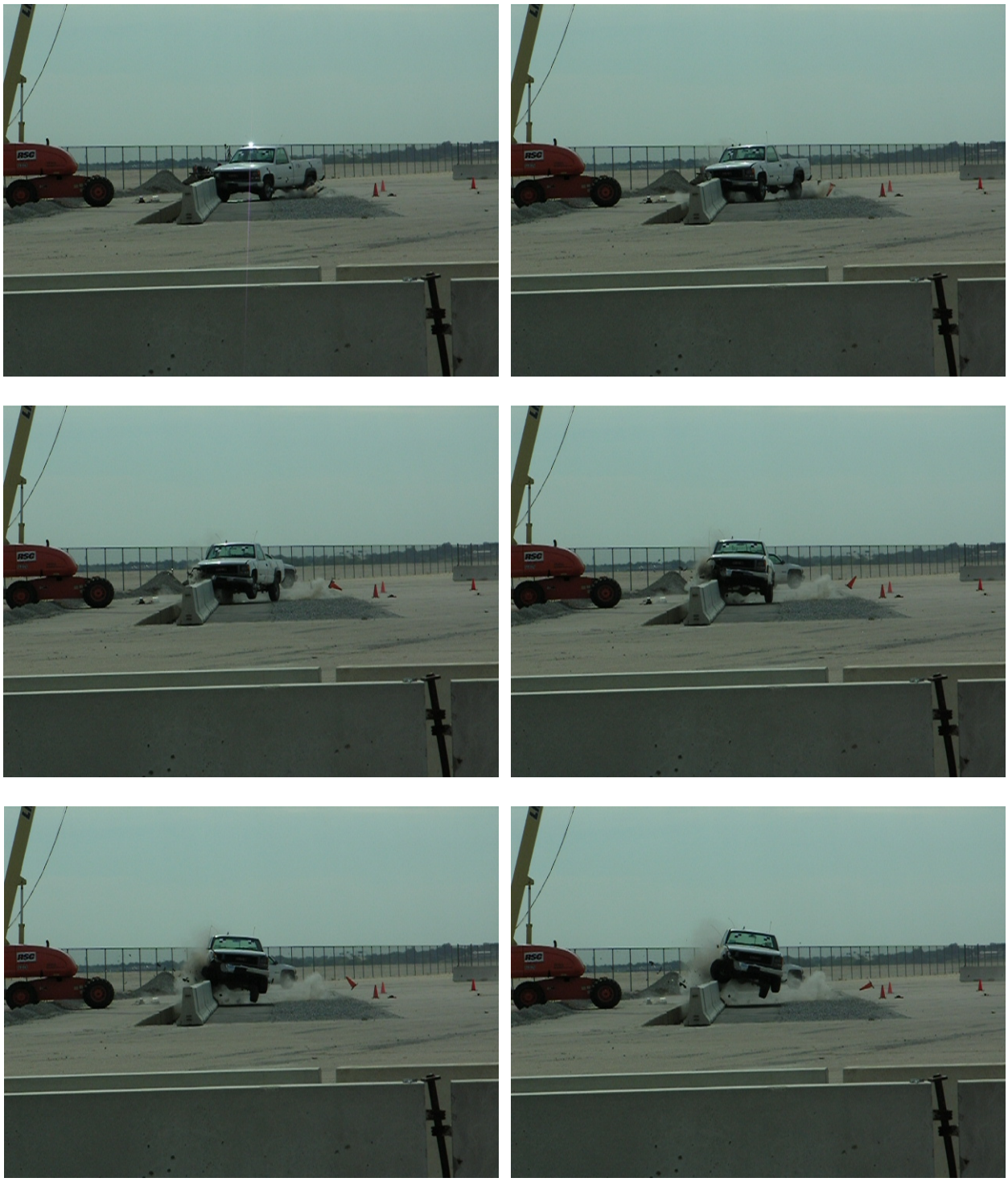

Figure 24. Documentary Photographs, Test FTB-1

Figure 25. Documentary Photographs, Test FTB-1

Figure 26. Impact Location, Test No. FTB-1

Figure 27. System Damage, Test FTB-1

Figure 28. System Damage, Test FTB-1

Figure 29. System Damage, Test FTB-1

Figure 30. Vehicle Damage, Test FTB-1

Figure 31. Vehicle Damage, Test FTB-1

7 DEVELOPMENT OF A TEMPORARY CONCRETE BARRIER TRANSITION

7.1 Introduction

With the asphalt tie-down temporary concrete barrier successfully designed and tested, the researchers proceeded to the second phase of the project. The objective of this phase was to apply the new tie-down design towards the creation of a transition from free-standing temporary concrete barrier to rigid concrete barrier. The researchers believed that the transition could be developed by varying the number of asphalt tie-down pins used on the barrier segments in the transition section.

7.2 Transition Design Details

After examining various design alternatives, the researchers agreed on a final design for the transition from a free-standing temporary concrete barrier installation to a rigid barrier, as shown in Figure 32. The transition utilized a varied spacing of the asphalt pin tie-down system to create a transition in stiffness over a series of four barrier segments. The first barrier in the transition had a single pin on the downstream end. The second barrier had pins installed at the two outside hole locations. The final two barriers had all three pins installed. In addition, either 10-gauge or nested 12 gauge thrie beam was bolted across both sides of the joint between the pinned barriers and the rigid barrier system in order to reduce the potential for vehicle snag at the joint.

Review of the transition design suggested that there were two possible Critical Impact Point (CIP) locations. The first was located at the transition between the free-standing and pinned barriers, and the second was located at the transition from the pinned to the rigid barriers. The researchers believed that the transition from free-standing barrier to pinned barrier was more critical than the transition from pinned barrier to rigid barrier. It was also believed that the

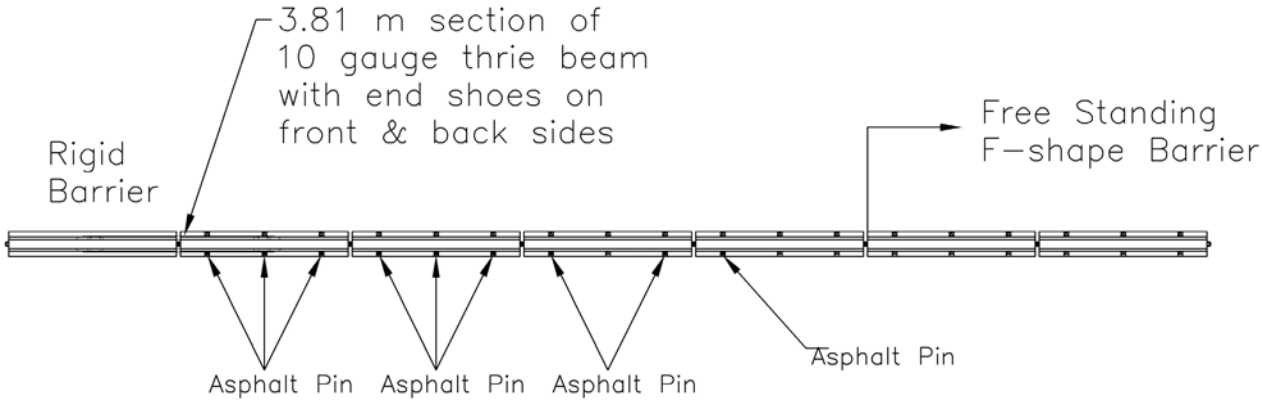

Figure 32. Free-Standing to Rigid Barrier Transition Schematic

transition from the pinned barrier to the rigid barrier posed little risk of failure and could be waived. The justification for these beliefs was based on the relative deflection of the barriers and the potential for pocketing and snagging at each of the transitions.

Figure 33 shows the maximum deflection and deflected shape of the free-standing F-shape barrier, the asphalt pin tie-down system, the bolt-through tie-down system, and a rigid barrier. Review of these deflections and deflected shapes illustrated the critical nature of the transition from free-standing barrier to pinned barrier. First, the difference in the static and dynamic displacements between the free-standing and pinned barriers was much higher than the difference between the pinned and the bolt-through or rigid barriers. The difference in deflection is more pronounced when one considered that the deflection recorded for the asphalt pin tie-down was inflated due to failure of the soil foundation constraining the pins, as discussed previously. Because the difference in the deflection was much higher for the free-standing to pinned barrier transition, there was more potential for pocketing, relative rotation of the barrier joint causing vehicle snag at the joint, and the possibility of the vehicle vaulting the system.

The second transition in the system, or the asphalt pin tie-down barrier transitioned to a bolt-through tie-down or rigid barrier, had very little potential for pocketing or snag. The difference in the deflections at the base of the barrier was low, which would represent a reduced potential for pocketing. The difference in these deflections is even lower if the soil failure experienced in the asphalt pin tie-down test is not present. In addition, the 10-gauge thrie beam pieces placed across the joint between the asphalt pin tie-down barrier and the rigid barrier would further reduce the potential for pocketing and relative rotation of the barriers at the joint which could lead to vehicle snag. Because the deflection level of the transition barriers and the rigid barrier were relatively close and the addition of the thrie beam across the

Free-Standing

Steel Pin in Asphalt Tie-Down

Bolt-Through Tie-Down

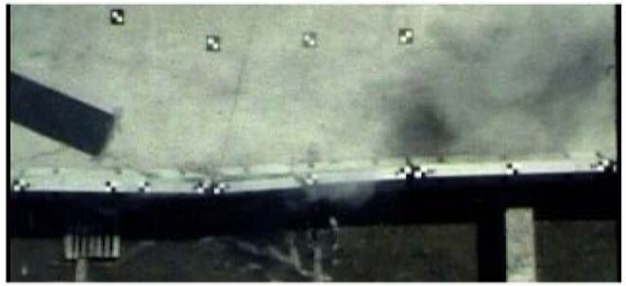

Figure 33. Comparison of F-Shape Barrier Deflections

Barrier Type	Maximum Static Deflection at Base of Barrier (mm)	Maximum Dynamic Deflection at Top of Barrier (mm)
Free-standing F-shape	1,140	1,149
Steel pin in asphalt tie-down	283	554
Bolt-through tie-down	89	287
Rigid Barrier	0	0

joint reduced the potential for snag, it was believed that the transition between the asphalt pin tie-down barrier and the bolt-through tie-down or rigid barrier was not critical and did not require further testing.

MwRSF researchers presented these arguments to the Federal Highway Administration (FHWA) and received approval to conduct only the more critical free-standing to pinned barrier transition test for compliance. However, it was still necessary to determine the critical impact point for this test.

7.3 LS-DYNA Simulation of the Critical Impact Point

Determination of the CIP for the full-scale test of the transition was a task best suited to computer simulation using LS-DYNA [12]. LS-DYNA simulation had been used throughout the design of the asphalt tie-down temporary concrete barrier. This previous simulation work consisted of developing validated models for the asphalt pins as well as full system models of the tie-down temporary concrete barrier. The model of the asphalt pin, as shown in Figure 34, consisted of a pin modeled with solid elements inserted into a rigid sleeve that was connected to two pairs of nonlinear springs. The rigid sleeve and nonlinear springs were used to develop the proper force deflection response of the pins when moving through soil and asphalt. The load curves for the springs were developed directly from the previously described asphalt pin component testing, and the force-deflection and pullout behaviors of the pins were compared in order to validate the model, as shown in Figure 35. The pin was modeled with the MAT_PIECEWISE_LINEAR_PLASTICITY material in LS-DYNA with the appropriate properties for A36 steel.

The model of the F-shape portable concrete barrier was based on a model developed previously at MwRSF for determining the deflection of F-shape barriers at various impact

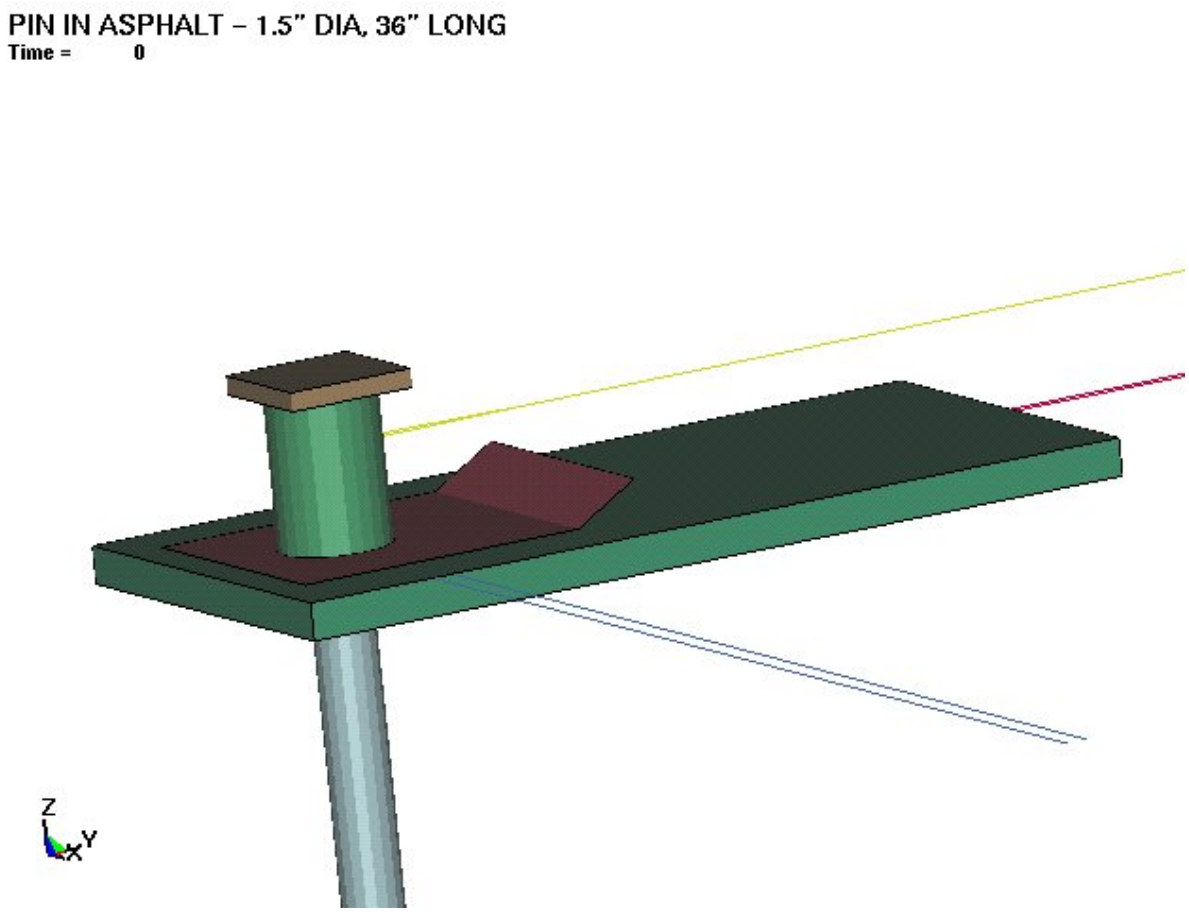

Figure 34. LS-DYNA Asphalt Pin Model

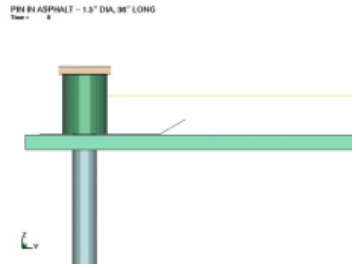

0.000 sec

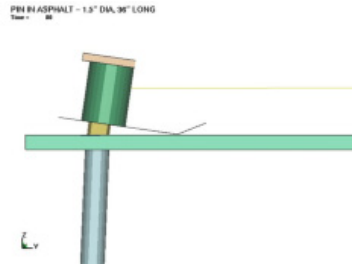

0.080 sec

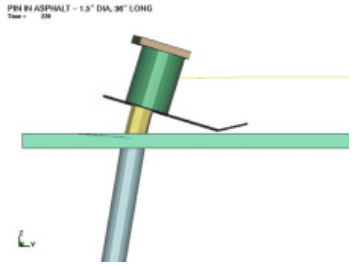

0.220 sec

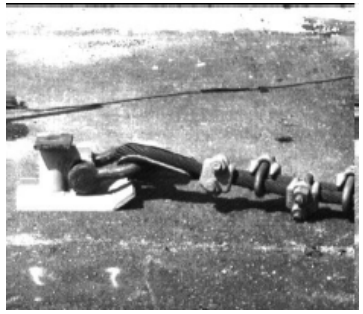

0.000 sec

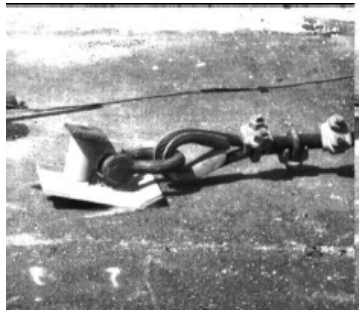

0.080 sec

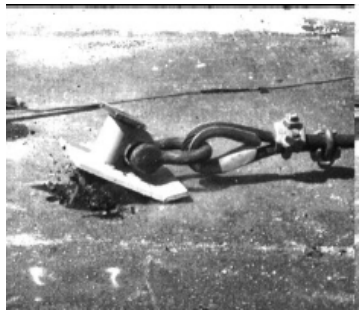

0.220 sec

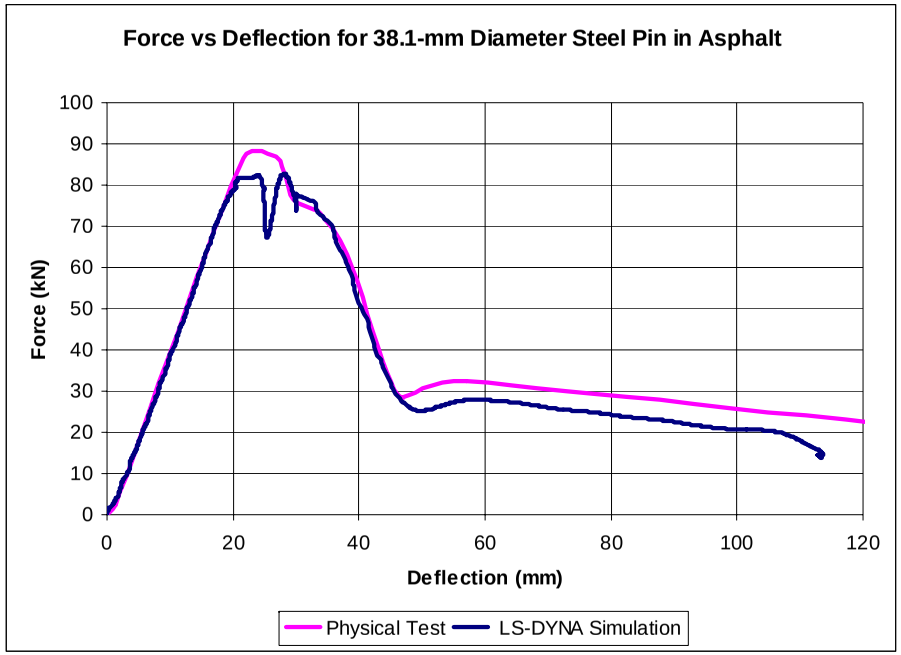

Figure 35. LS-DYNA Asphalt Pin Simulation

conditions [13]. The model consisted of the F-shape barrier, the end connection loops, and the connection pins, as shown in Figure 36. The model had some modifications from the previously developed model. First, the original model used solid elements with a rigid material definition to model the F-shape barrier. This approach was originally taken because the proper mass properties and geometry of the barrier are captured. However, the use of solid elements does not provide for a robust contact surface when used with the shell elements of the existing UNL 2000P model. Therefore, the F-shape barrier model developed for this work was created using shell elements with a rigid material definition. The rigid material definition allowed the proper mass and rotational inertias to be defined for the barrier even though it was essentially hollow. The use of the shell elements improved the overall contact of the barrier and the vehicle. In addition, the use of shell elements made it easier to fillet the corners and edges of the barrier. By rounding off the barrier edges, the edge contacts and penetrations were reduced, thus further improving the contact interface. The geometry of the barrier was also modified to include the holes in the face of the barrier used for the asphalt pins. The loops in the barrier model were also modified to match the current configuration which consisted of two sets of three rebar loops. The connection loops were modeled with a rigid material. The connection pin was modeled with the MAT_PIECEWISE_LINEAR_PLASTICITY material in LS-DYNA with the appropriate properties for A36 steel. The F-shape barrier model was validated with previous free-standing F-shape barrier testing [14]. The F-shape barrier model was combined with the asphalt pin model to create a model of the transition.

Using the previously developed simulation models for the tie-down pins and the barriers, LS-DYNA simulations of four CIP locations were conducted, as shown in Figure 37. These initial CIP locations were chosen using engineering judgment based on concerns for vehicle snag

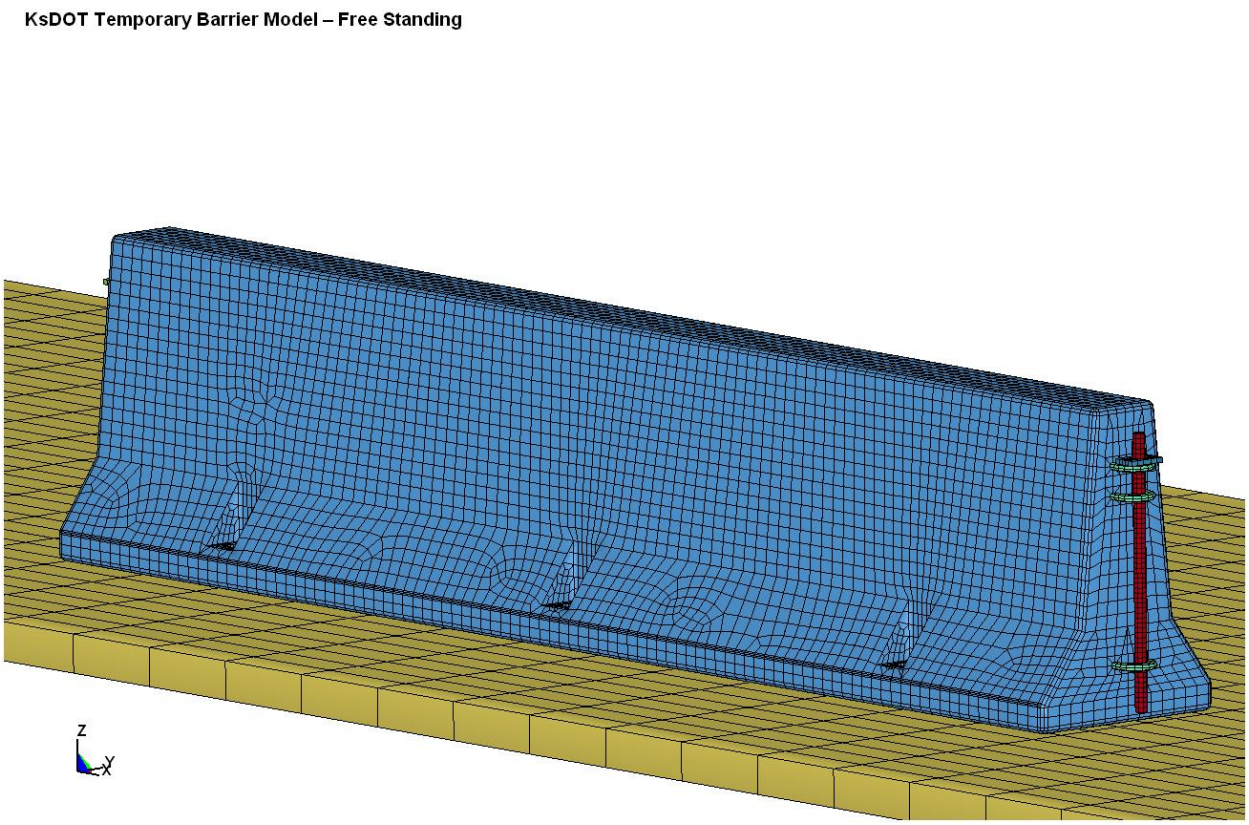

Figure 36. LS-DYNA F-Shape Barrier Model

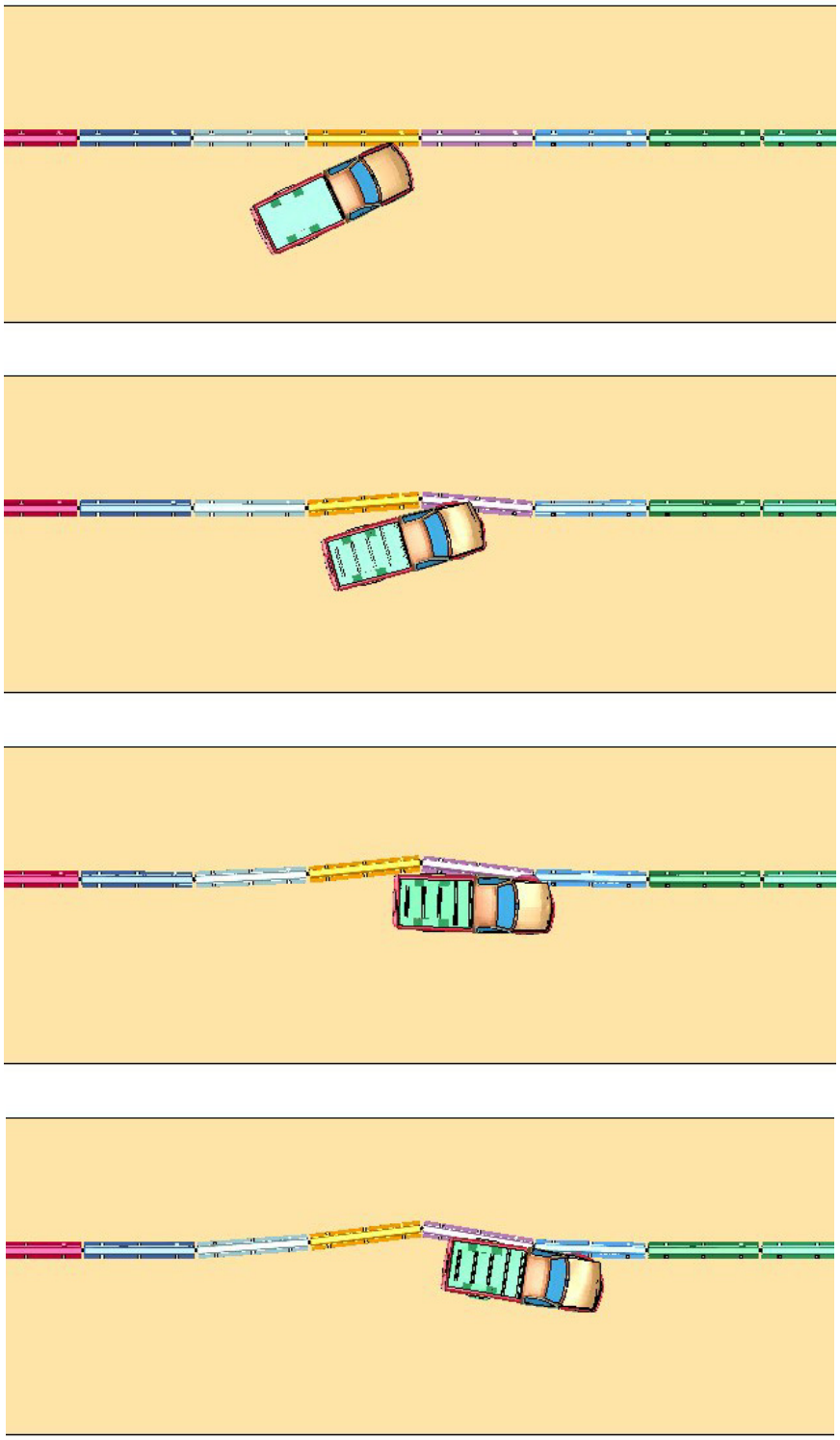

Figure 37. Typical LS-DYNA Results for Critical Impact Point Simulations

at joints and pocketing. The four CIP locations were as follows:

1. 1.2 m upstream of the joint between the last two free-standing barriers
2. 1.2 m upstream of the joint between last free-standing and first pinned barrier in the transition
3. 1.2 m upstream of the joint between the first and second pinned barrier in the transition
4. An impact point midway between impact point nos. 2 and 3

The simulation models of each impact point were reviewed to determine the worst CIP location. Because the vehicle model for the C2500 pickup truck used is not currently capable of accurately modeling behaviors such as the wheel, tire, and suspension failure modes typically observed in these types of physical tests, the vehicle behavior was not one of the main criteria for determining the CIP location. Instead, the researchers focused on critical barrier behaviors that would suggest a worst-case impact scenario. These behaviors included vertical rotation of the barrier segments which could lead to vehicle instability, separation of the barrier joints which could indicate potential vehicle snagging, and pocketing of the barrier segments.

Results from the simulation models revealed that an impact point 1.2 m upstream of joint between the first and second pinned barrier in the transition was the CIP of the system. This impact point generated the largest barrier rotations and joint separations, which would indicate a potential for vehicle snag and instability. Pocketing of the transition was not evident in any of the CIP models. This point was used as the CIP for the full-scale test of the transition.

8 TRANSITION DESIGN DETAILS

8.1 Design Details, Test no. FTB-2

Design details for the transition from free-standing temporary concrete barrier to rigid concrete barrier evaluated in full-scale crash test no. FTB-2 are shown in Figure 38 through Figure 45. The corresponding English-unit drawings are shown in Appendix E. Photographs of the test installation are shown in Figure 46.

The test installation used five rigidly constrained barriers on the downstream end, four transition barriers, and thirteen free-standing barriers on the upstream end. Sixteen of the F-shape temporary concrete barriers, including the four transition barriers and twelve of the free-standing barriers, were installed on a 51-mm (2-in.) thick asphalt pad. The five rigidly constrained barriers and one free-standing barrier were installed on concrete. The 51-mm (2-in.) asphalt depth was chosen because it was the minimum asphalt cover o provide a reasonable bearing surface for field installations of the system. In addition, component testing had shown that thicker asphalt cover would only decrease tie-down deflection. The F-shape concrete barriers used in test no. FTB-2 were identical to those used in test no. FTB-1. The only change to the system was to increase the number of barriers in order to account for the free-standing end, the transition section, and the rigid barrier end. The rigid barrier end was simulated by bolting down the final five F-shape barriers with epoxied anchors. The anchors consisted of 28.6-mm (1.125-in.) diameter B7 threaded rod embedded 304-mm (12-in.) into the concrete and epoxied.

The transition utilized a varied spacing of the asphalt pin tie-down system to create a transition in stiffness over a series of four barrier segments. The asphalt pins used in the design were 38.1-mm (1.5-in.) diameter x 978-mm (38.5-in.) long A36 steel pins with 76-mm x 76-mm x 13-mm (3-in. x 3-in. x 0.5-in.) A36 steel plates with a 38.1-mm (1.5-in.) diameter hole were

installed in the holes on the front face of the four barriers in the transition section of the installation. It should be noted that the tie-down pins were modified slightly prior to the transition test to prevent the disengagement of the top caps observed in test no. FTB-1. The modified design lengthened the pin 63.5 mm (2.5-in.) and a 38.1-mm (1.5-in.) diameter hole was cut in the steel cap. The cap was then slid onto the pin and welded on both the top and bottom surfaces of the plate 914 mm (36 in.) from the bottom of the pin. This modification strengthened the connection of the cap to the pin but did not change the pin embedment. The modified tie-down pin is shown in Figure 44. The first barrier in the transition had a single pin on the downstream end. The second barrier had pins installed at the two outside hole locations. The final two barriers had all three pins installed. In addition, nested 12-gauge thrie beam was bolted across both sides of the barrier at the joint between the pinned barriers and the rigid barrier system in order to reduce the potential for vehicle snag at the joint. It should be noted that 10-gauge thrie beam could be substituted for the nested 12 gauge in actual installations if desired. The thrie beam was bolted to the barriers using five 19.05-mm (0.75-in.) diameter x 152-mm (6-in.) long, Powers Fasteners Wedge Bolt anchors at each end of the beam.

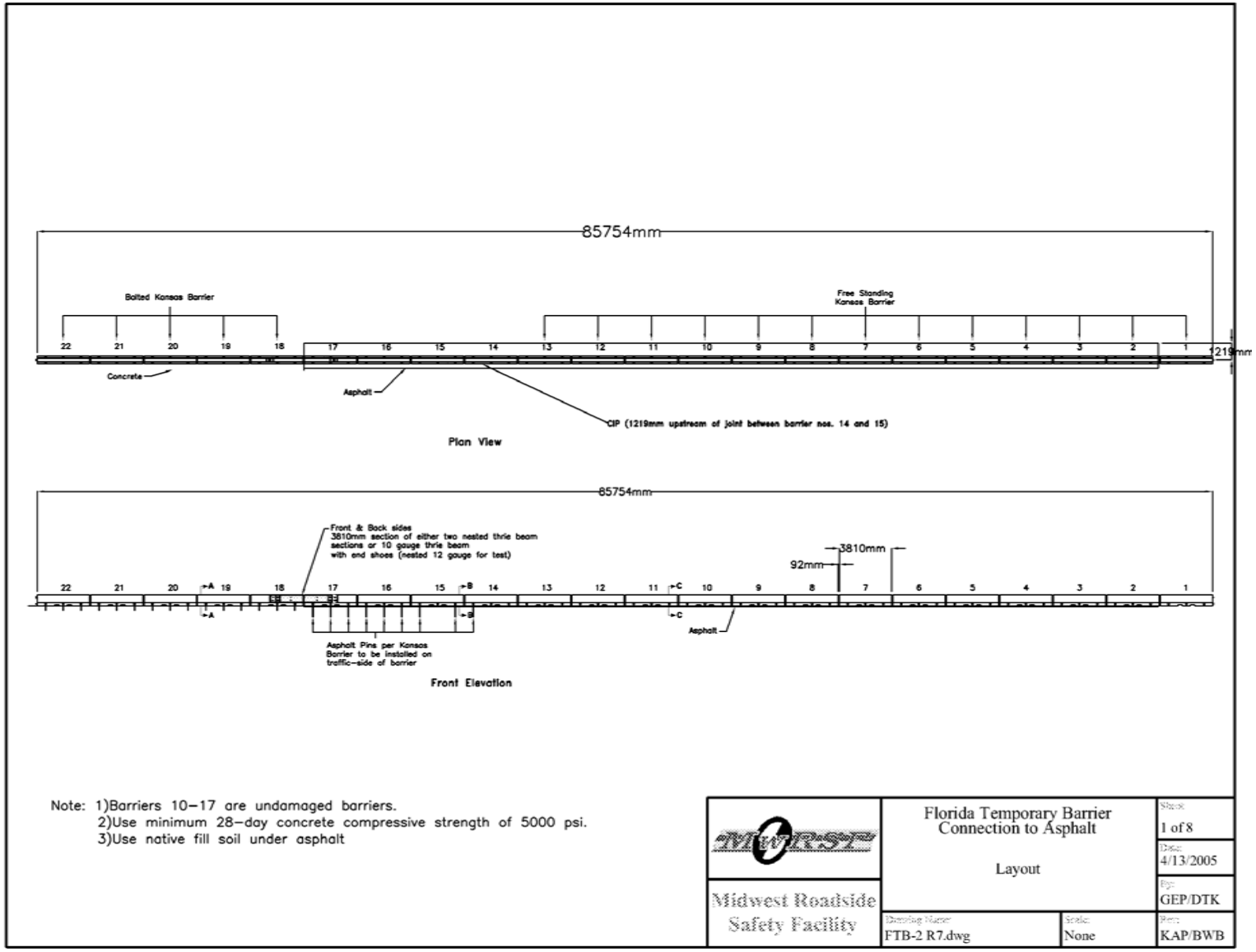

Figure 38. Free-Standing to Rigid Concrete Barrier Transition Details

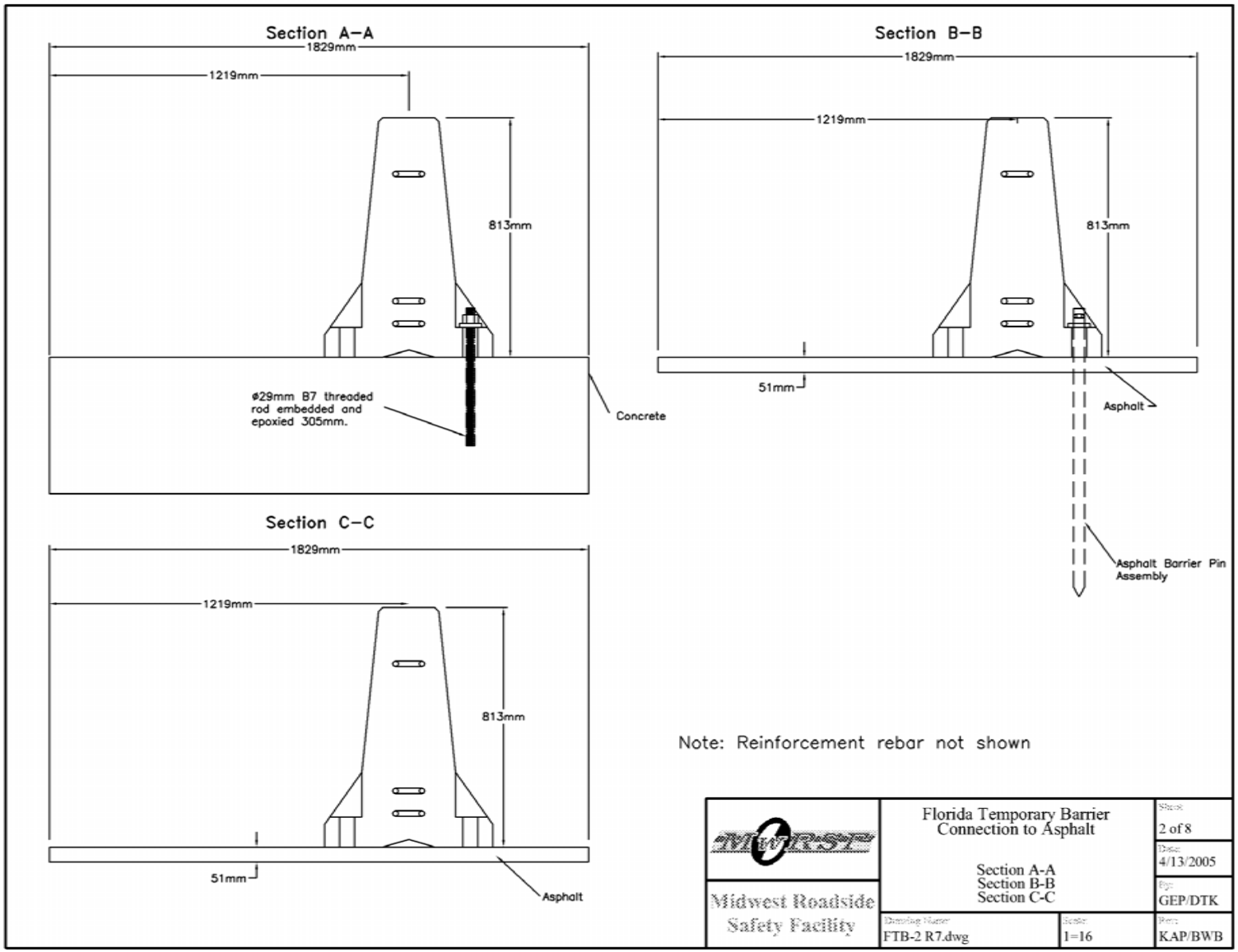

Figure 39. Free-Standing to Rigid Concrete Barrier Transition Details

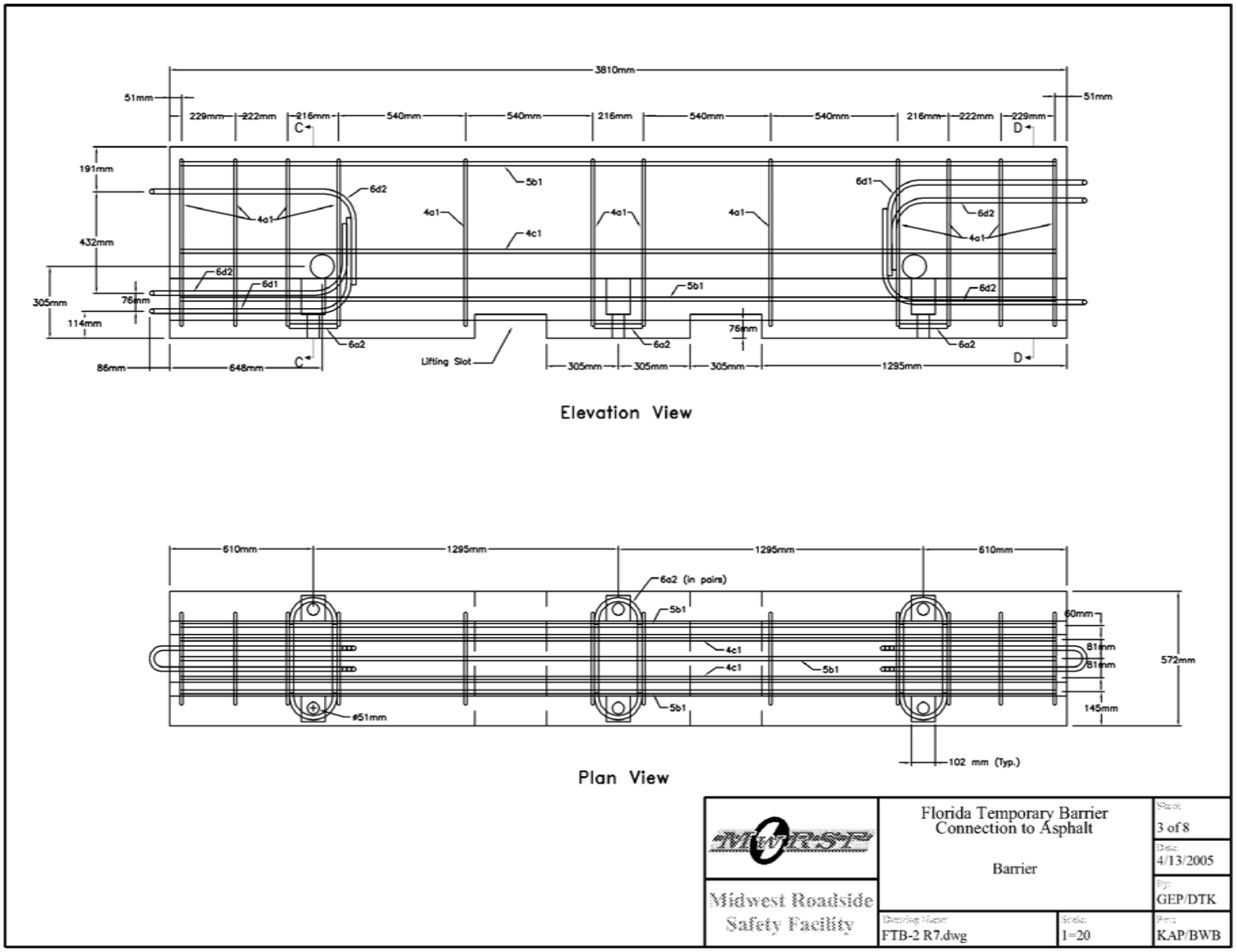

Figure 40. Free-Standing to Rigid Concrete Barrier Transition Details

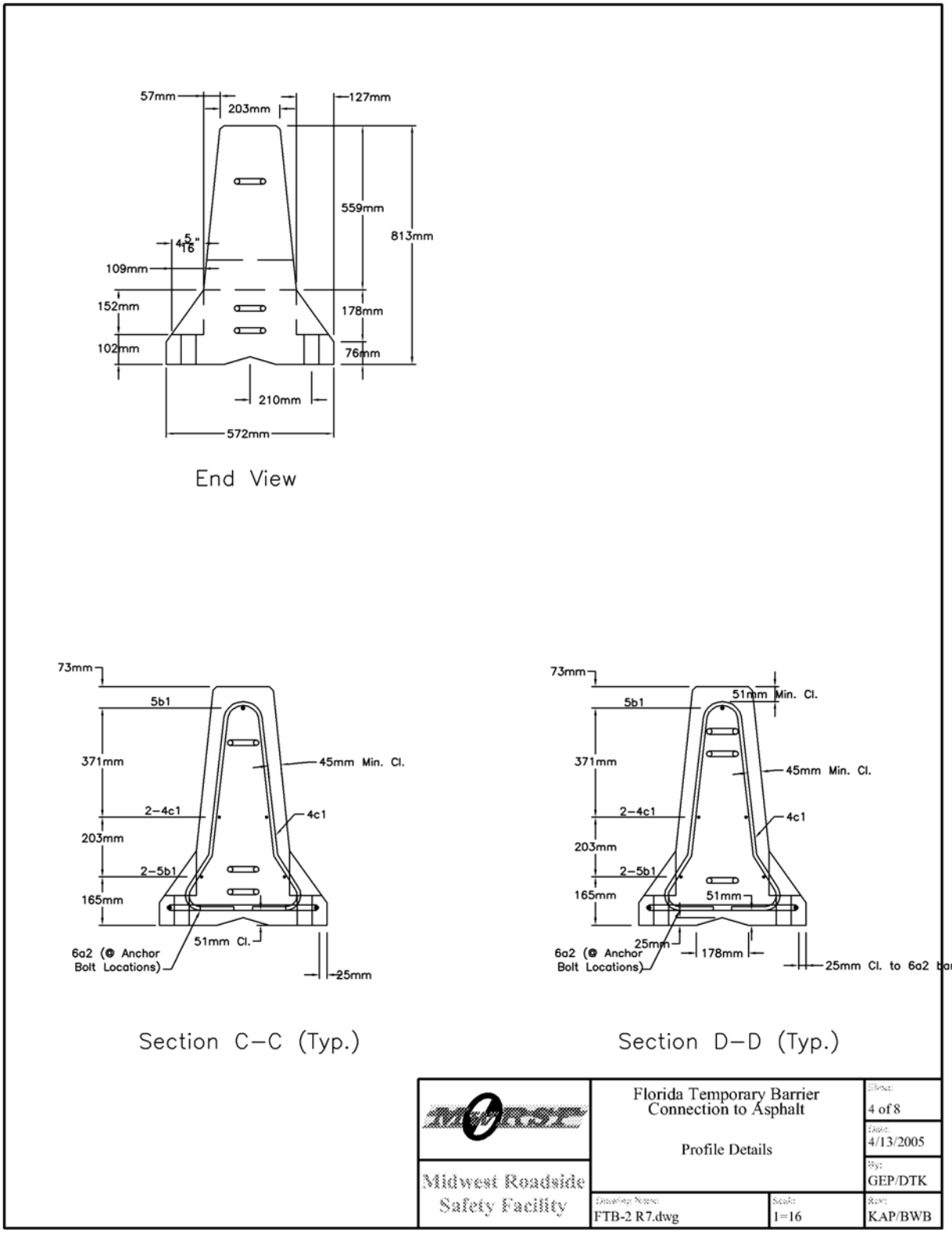

Figure 41. Free-Standing to Rigid Concrete Barrier Transition Details

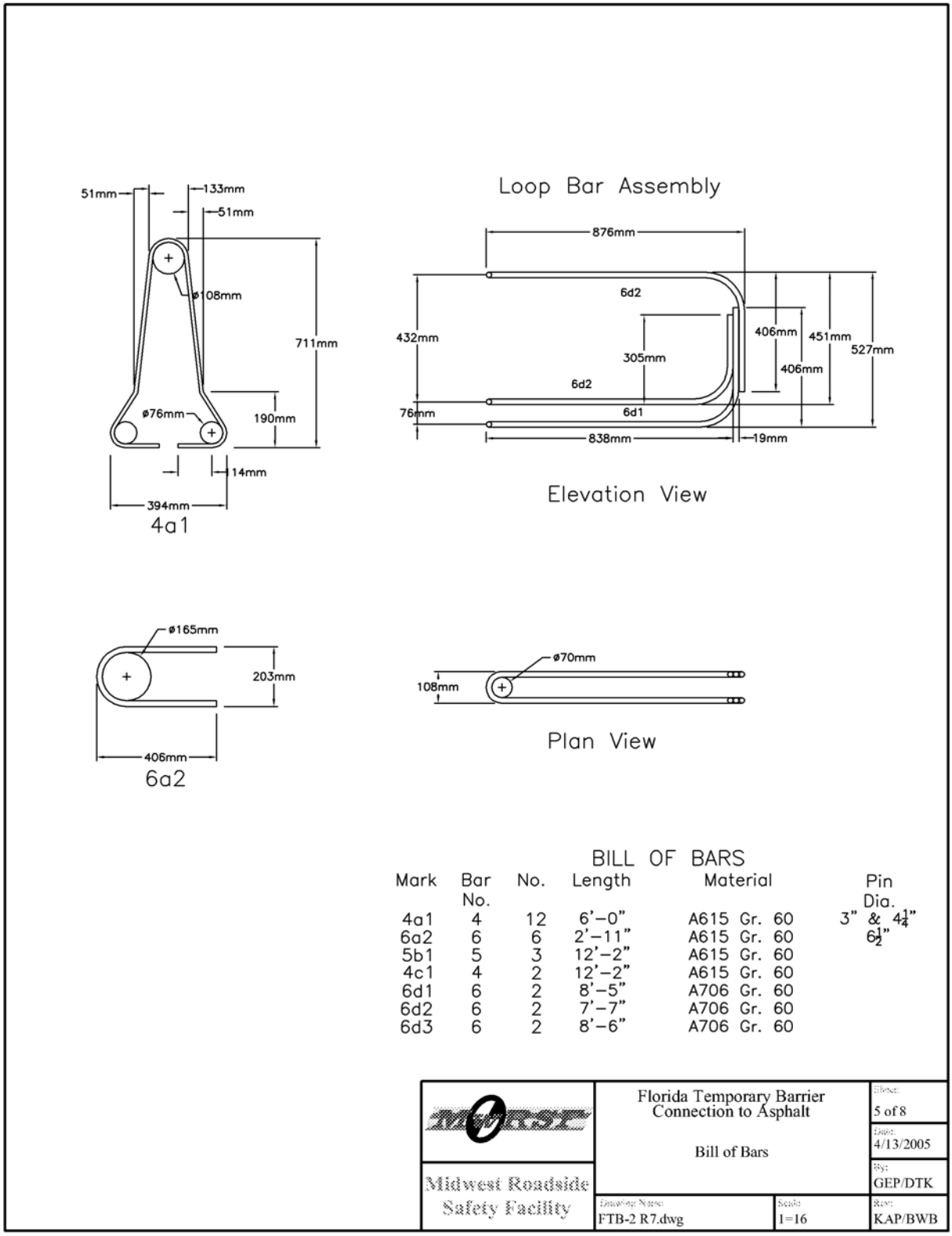

Figure 42. Free-Standing to Rigid Concrete Barrier Transition Details

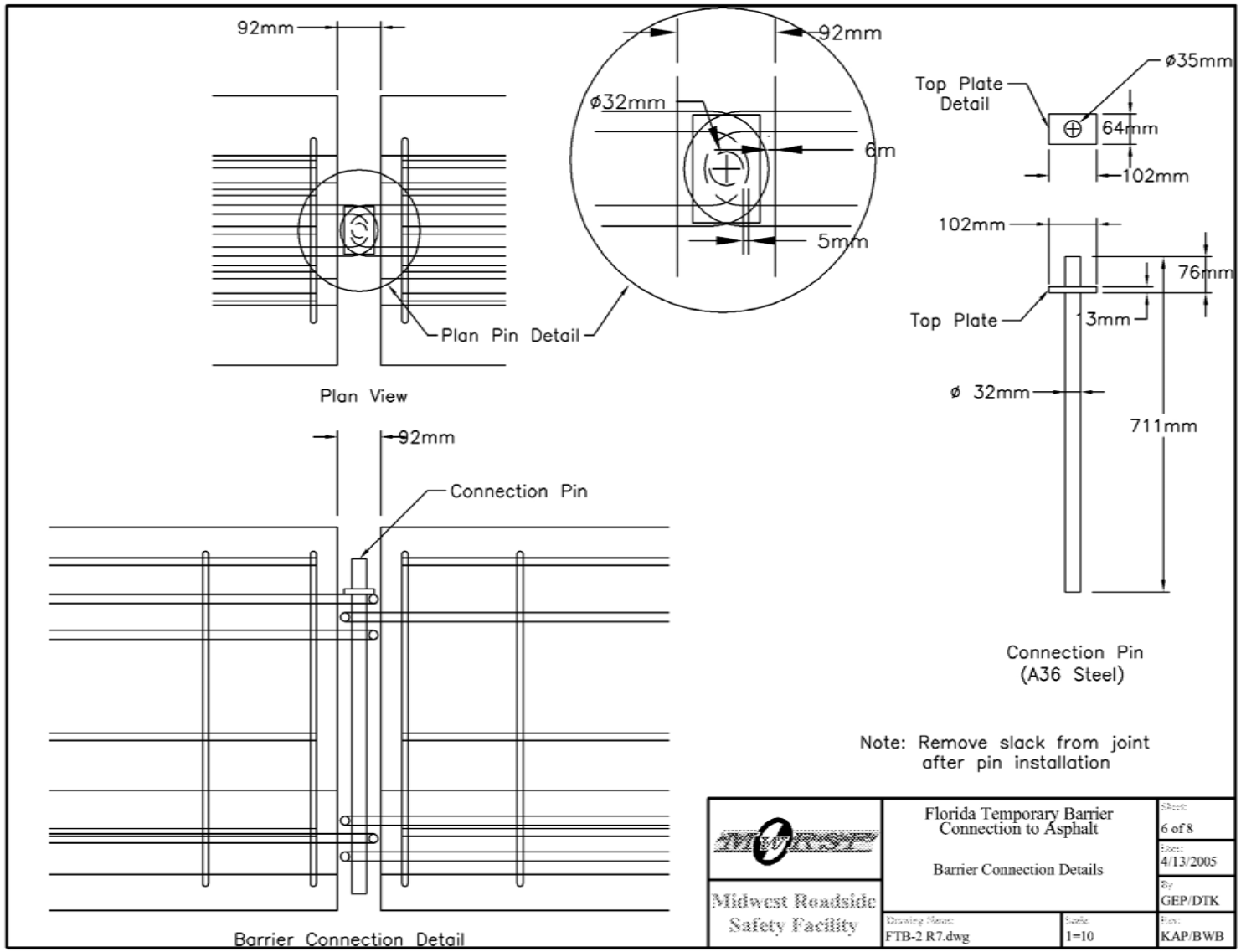

Figure 43. Free-Standing to Rigid Concrete Barrier Transition Details

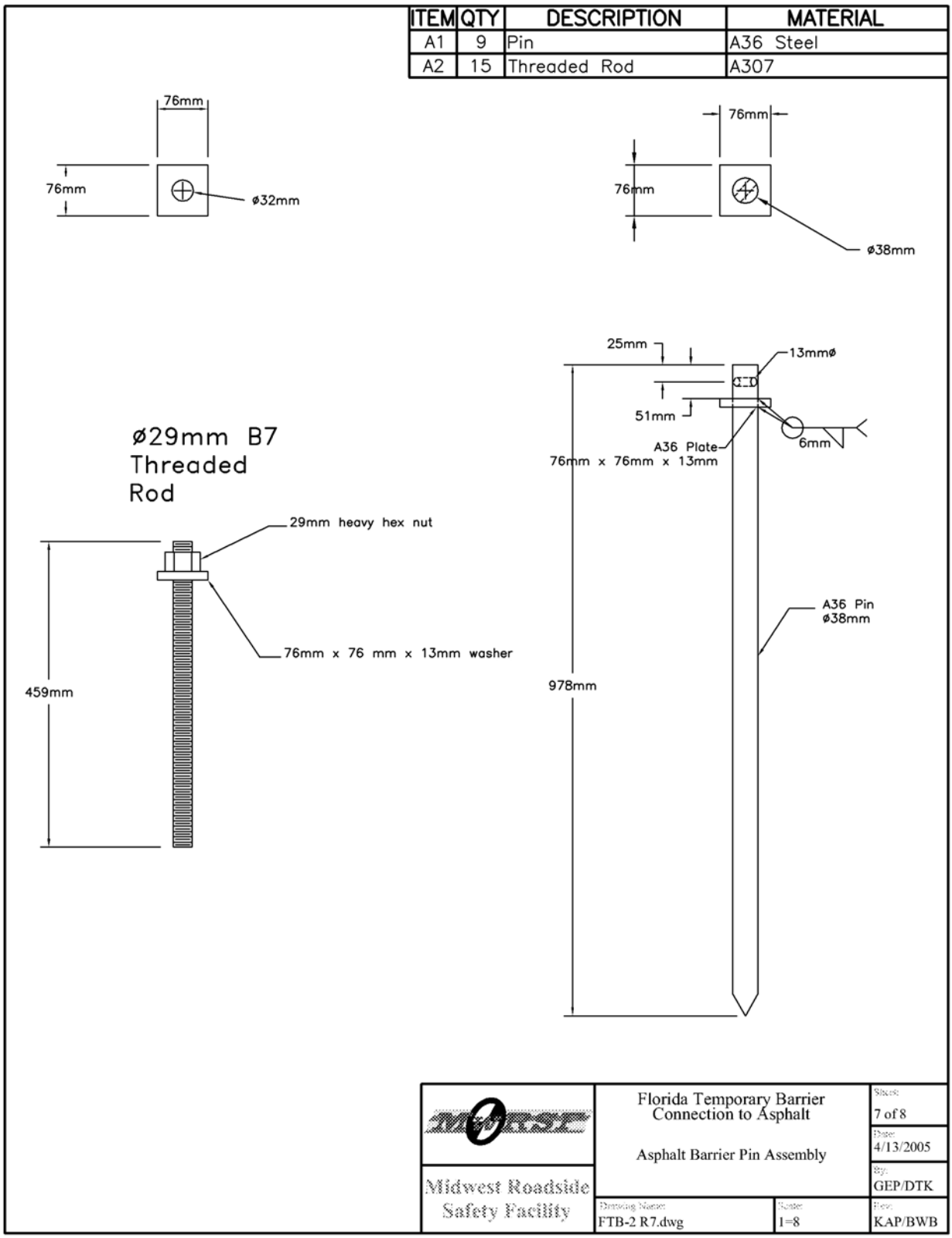

Figure 44. Free-Standing to Rigid Concrete Barrier Transition Details

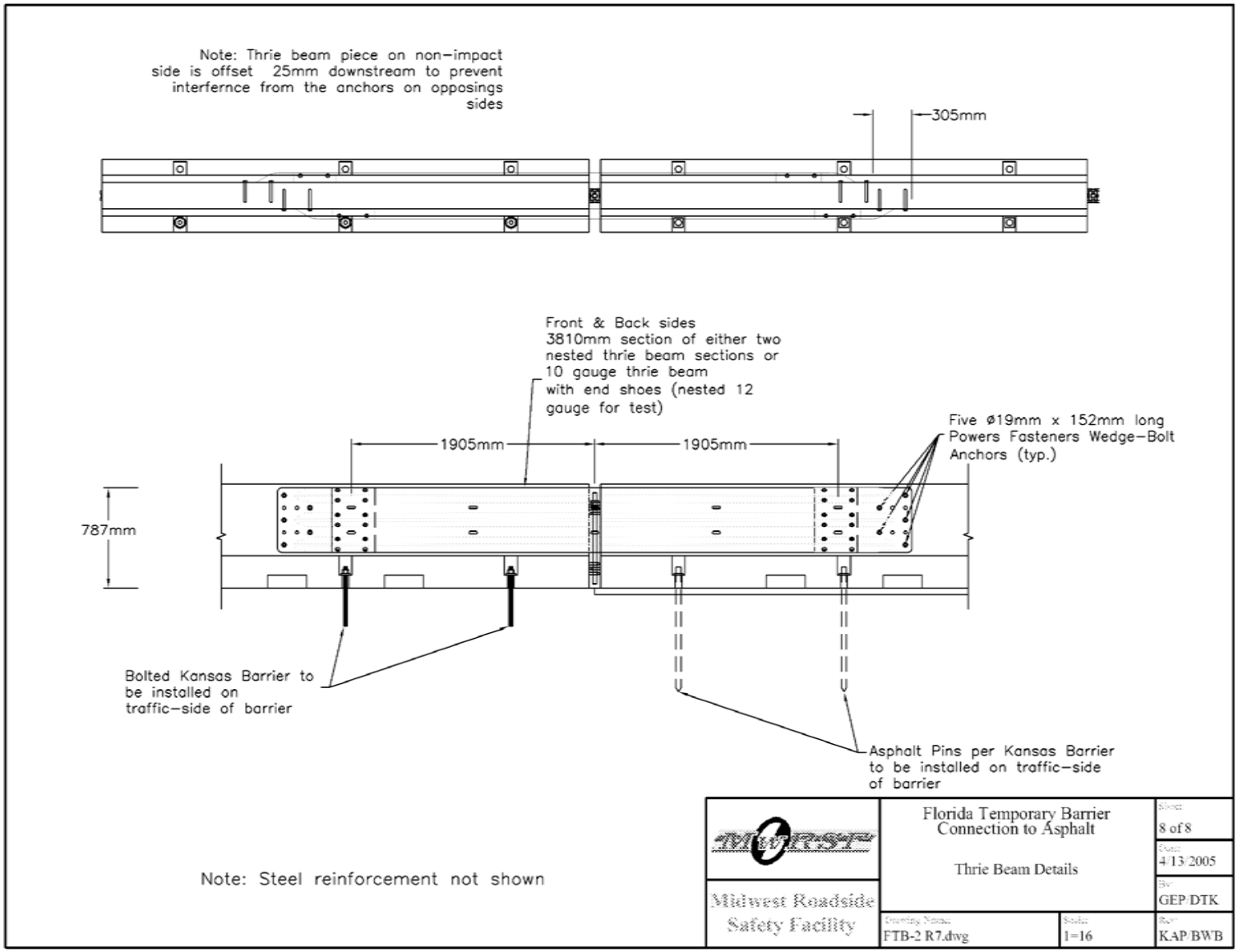

Figure 45. Free-Standing to Rigid Concrete Barrier Transition Details

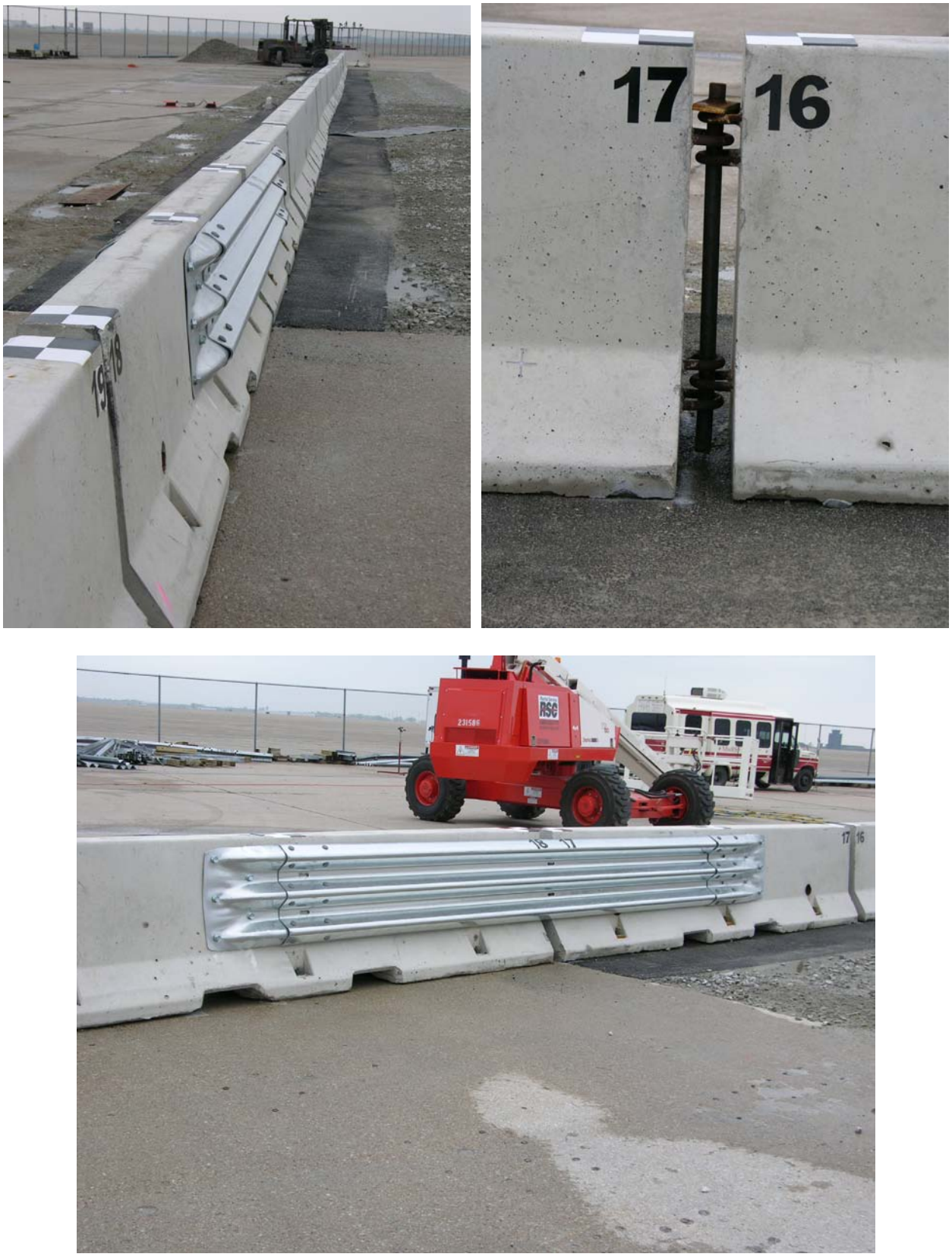

Figure 46. Free-Standing to Rigid Concrete Barrier Transition Photographs

9 FULL-SCALE TEST NO. FTB-2

9.1 Test No. FTB-2

For test no. FTB-2, a 2,030-kg (4,475 lbs) pickup truck impacted the asphalt tie-down temporary concrete barrier system at a speed of 102.7 km/hr (63.8 mph) and at an angle of 26.1 degrees. A summary of the test results and the sequential photographs are shown in Figure 47. The summary of the test results and sequential photographs in English units is shown in Appendix F. Additional sequential photographs are shown in Figure 48. Documentary photographs of the crash test are shown in Figure 49 through Figure 52.

9.2 Test Description

The impact point for this test was 1,219-mm upstream of the joint between barrier nos. 14 and 15, as shown in Figure 53. Immediately after impact, the impacted barrier segments began to deflect backwards, and the right-front corner of the pickup truck was deformed inward. The vehicle climbed the face of the barrier as it began to redirect causing it to pitch upward and roll to the left. By 0.242 sec, the pickup truck had redirected parallel to the barriers with a speed of 66.9 km/h (41.6 mph). As the vehicle continued to redirect, the left-front tire of the truck contacted the ground, which caused the vehicle to yaw counterclockwise. At 1.206 sec, the right-rear tire and the pickup truck box landed on the top of the barrier on the traffic side before exiting the system. After exiting the barrier at approximately 1.500 sec, the pickup truck continued to move downstream until coming to rest 62.4-m (204.7-ft) downstream and 1.4 m (4.6-ft) to the left of the original impact point. A summary of the test results and sequential photographs is shown in Figure 47.

9.3 System Damage

Damage to the transition was moderate, as shown in Figure 54 through Figure 56. Tire marks, scrapes, and cracking of the concrete were visible on barrier segment nos. 14 through 16. Barrier segment nos. 14 through 16 were deflected laterally. Barrier no. 15 was cracked and completely fractured through the midsection of the barrier, but the reinforcing steel remained intact. Deformation to several of the barrier joints and the tie-down pins was noted in the impact region. Several of the tie-down pins were pulled up between 13 to 102 mm (0.5 to 4 in.) due to barrier rotation. No movement of the tie-down pins was noted on the non-impacted barrier segments. Damaged concrete was observed near several of the vertical holes on the front face of the barriers in the impact region, but the reinforcing steel surrounding the holes remained intact and safely around the pins. The maximum permanent set and dynamic barrier deflections were measured to be 133 mm (5.25 in.) and 467 mm (18.375 in.), respectively.

9.4 Vehicle Damage

Vehicle damage was moderate, as shown in Figure 57 and Figure 58. The majority of the damage to the pickup truck was focused on the right-front corner and right side where the impact occurred, including the right-front bumper, fender, and suspension components. Scrapes and dents from vehicle contact with the barriers were observed on the lower portion of the truck bed and the right-side door of the vehicle. A large indentation was also visible on the right-front edge of the truck box. The right-front tire and the outside of the steel rim were disengaged from the main body of the wheel assembly during impact. Minimal damage was observed in the interior occupant compartment of the vehicle, and the maximum deformation of the passenger-side floor pan was 102 mm (4 in.). Details from the occupant compartment deformation measurements are located in Appendix G.

9.5 Occupant Risk Values

The longitudinal and lateral occupant impact velocities (OIV) were determined to be 5.04 m/s (16.5 ft/s) and 5.69 m/s (18.7 ft/s), respectively. The maximum 0.010-sec average occupant ridedown decelerations (ORD) in the longitudinal and lateral directions were 7.25 g's and 12.66 g's, respectively. It is noted that the occupant impact velocities and the occupant ridedown decelerations were within the suggested limits provided in NCHRP Report No. 350. Results are shown graphically in Appendix H. Roll, pitch, and yaw data were collected from film analysis and the rate gyroscope and are shown graphically in Appendix H.

9.6 Discussion

Following test no. FTB-2, a safety performance evaluation was conducted, and the transition between free-standing temporary barrier and rigid barrier was determined to be acceptable according to the NCHRP Report No. 350 criteria for test designation no. 3-21. It should be noted that the degree of vehicle roll and pitch observed in this test were a cause for concern, but they are not sufficient to cause the test to be unacceptable. This vehicle instability was due in part to barrier rotation, but was also largely due to the inherent vehicle instabilities caused by the sloped face of safety shape barriers. It is believed that barriers with a vertical shape front face would demonstrate markedly better vehicle stability when impacted. The vehicle instability observed during previous testing of free-standing F-shape temporary barriers [14] and the improved stability observed during testing of free-standing and tie-down vertical shape temporary barriers [15-16] seems to support this conclusion.

0.000 sec | 0.058 sec | 0.266 sec | 0.458 sec | 0.778 sec

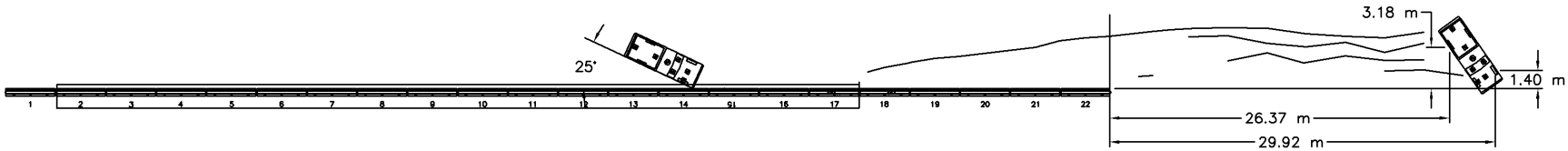

- Test Number FTB-2 (3-21)
- Date 4/20/05
- Test Article ..... F-shape PCB Approach Transition
- Total Length..... 62.34 m
- Overall Height..... 813 mm
- Barrier Elements ..... 22 Kansas F-shape PCB's
- Joint Connections..... 32-mm diameter by 712-mm long A36 steel pin with a 64x102x13-mm plate
- Tie-Down Anchors..... Three 38.1-mm dia. x 977.5-mm long A36 steel pins on the traffic side face only
- Soil Type..... Grading B - AASHTO M 147-65
- Vehicle Model..... 1998 GMC C2500
  - Curb..... 1,993 kg
  - Test Inertial ..... 2,030 kg
  - Gross Static ..... 2,030 kg
- Vehicle Speed
  - Impact..... 102.7 km/h
  - Exit ..... NA
- Vehicle Angle
  - Impact (trajectory) ..... 26.1 deg
  - Exit (trajectory) 9.8
- Vehicle Stability ..... Satisfactory
- Vehicle Snagging..... Minor
- Occupant Ridedown Deceleration (10 msec avg.)
  - Longitudinal ..... 7.25 g's < 20 g's
  - Lateral (not req.)..... 12.66 g's < 20 g's
- Occupant Impact Velocity
  - Longitudinal ..... 5.04 m/s < 12 m/s
  - Lateral (not req.)..... 5.69 m/s < 12 m/s
- THIV (not req.)..... 8.18 m/s < 12 m/s
- PHD (not req.) ..... 15.32 g's < 20 g's
- Vehicle Damage ..... Moderate
  - TAD 1-RFQ-4
  - SAE 1RFAW4
  - OCDI RF001100000
- Vehicle Stopping Distance..... 62.4 m downstream of impact 1.4 m from traffic side face
- Test Article Damage..... Moderate
- Maximum Deflection
  - Permanent Set ..... 133 mm
  - Dynamic ..... 467 mm (top of barrier)
- Working Width ..... 668 mm

Figure 47. Summary of Test Results and Sequential Photographs, Test FTB-2

0.000 sec

0.000 sec

0.176 sec

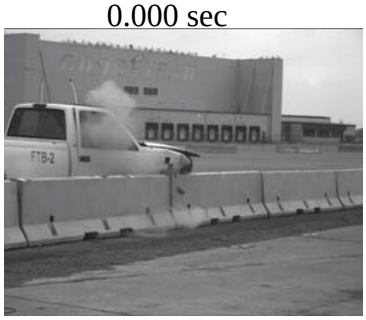

0.068 sec

0.300 sec

0.160 sec

0.486 sec

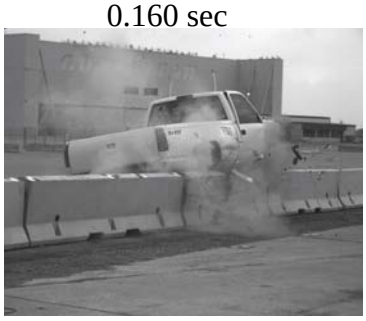

0.244 sec

1.252 sec

0.418 sec

Figure 48. Additional Sequential Photographs, Test FTB-2

Figure 49. Documentary Photographs, Test FTB-2

Figure 50. Documentary Photographs, Test FTB-2

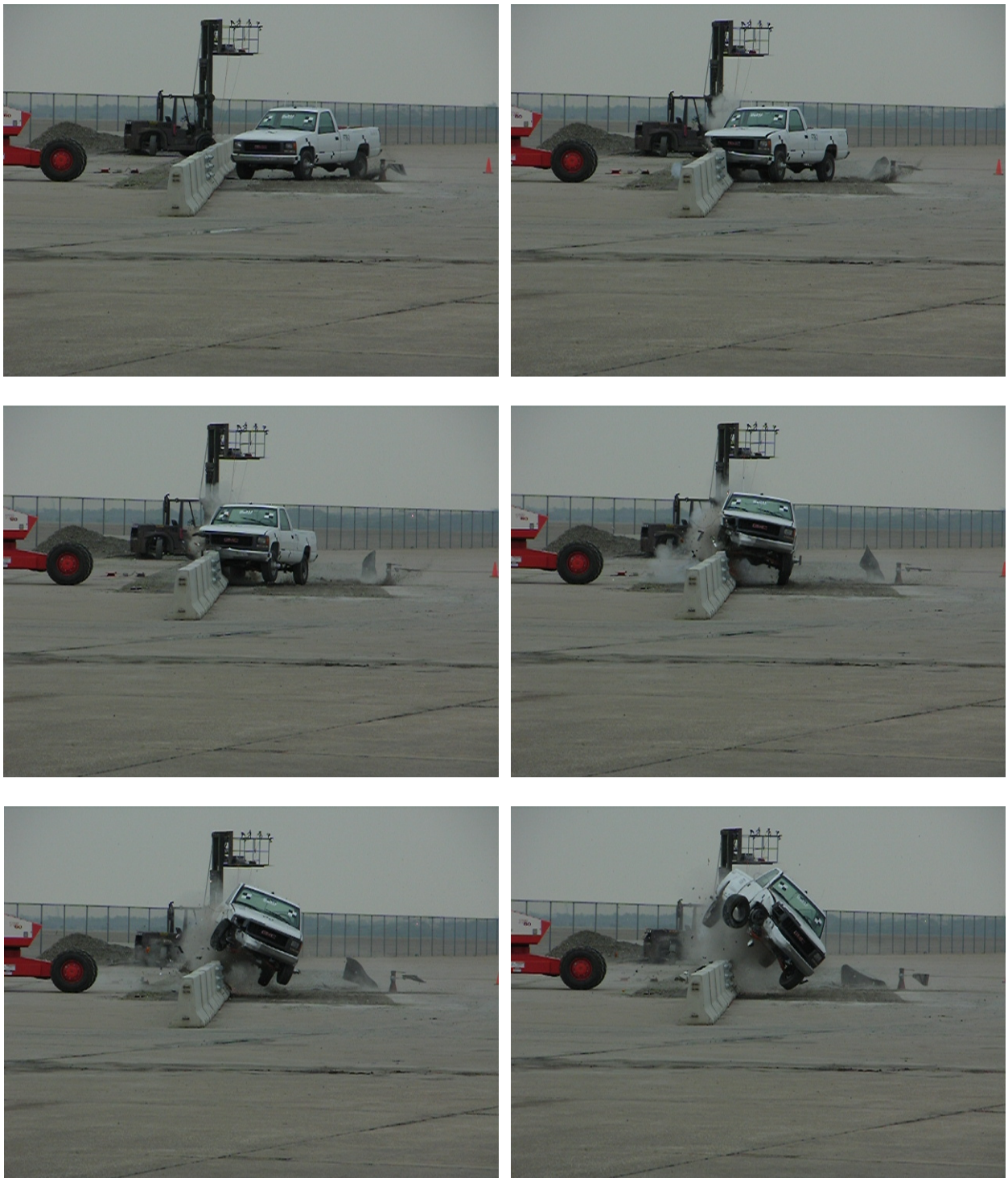

Figure 51. Documentary Photographs, Test FTB-2

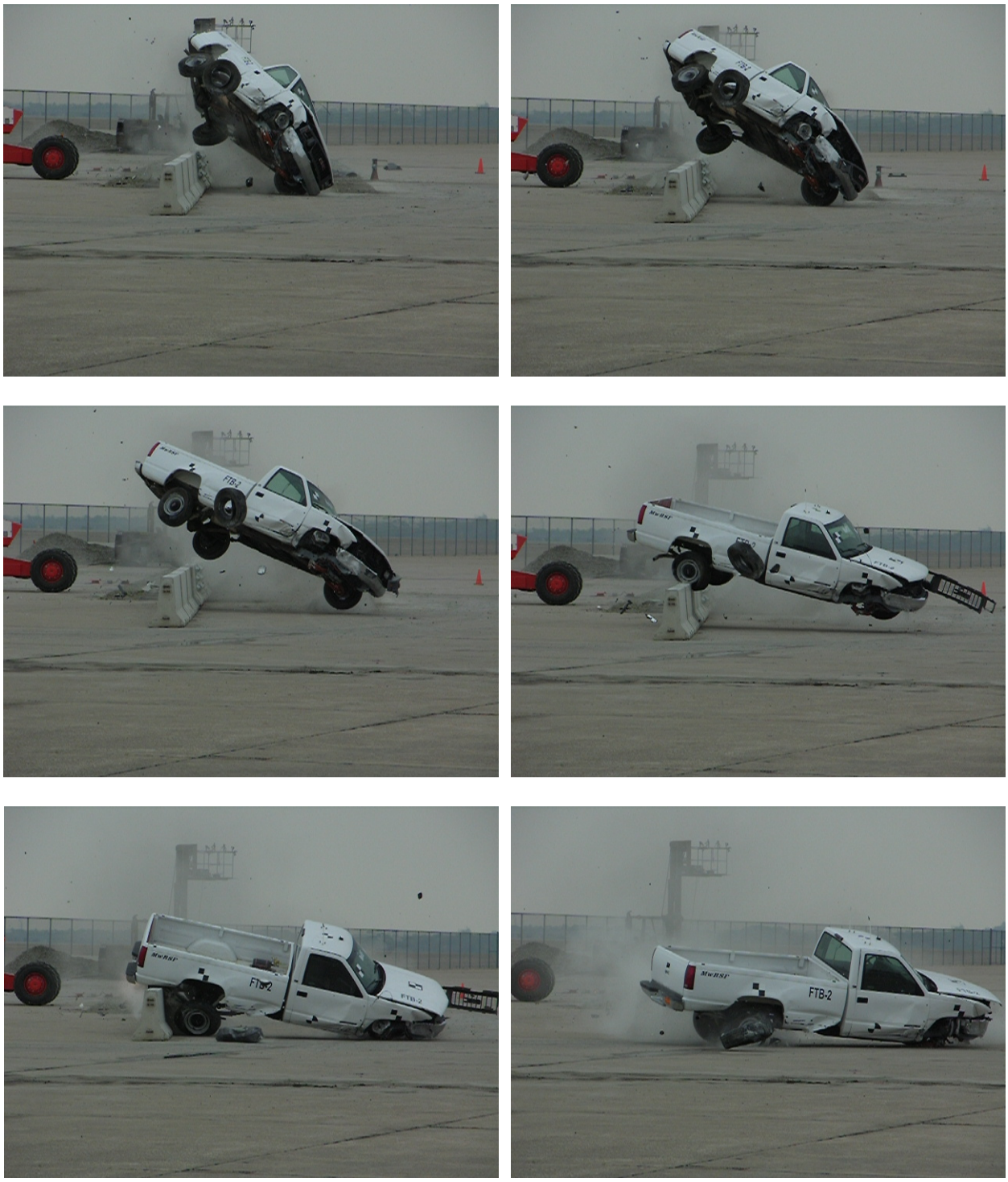

Figure 52. Documentary Photographs, Test FTB-2

Figure 53. Impact Location, Test No. FTB-2

Figure 54. System Damage, Test FTB-2

Figure 55. System Damage, Test FTB-2

Figure 56. System Damage, Test FTB-2

Figure 57. Vehicle Damage, Test FTB-2

Figure 58. Vehicle Damage, Test FTB-2

10 SUMMARY AND CONCLUSIONS

A tie-down system for use with temporary barriers on asphalt roadways and a transition between free-standing temporary barrier and rigid barrier were designed and successfully crash tested according to the TL-3 safety criteria set forth in NCHRP Report No. 350, as shown in Table 3. Both systems were designed for use with the Kansas F-shape temporary concrete barrier system. The tie-down system was designed to reduce barrier deflections from those observed during testing of comparable freestanding systems and to safely constrain deflected barriers installed in limited deflection applications on asphalt road surfaces. The transition was designed to create a safe approach section when connecting free-standing temporary barrier installations with rigid rail systems, such as concrete bridge rails.

The tie-down system utilized three 38.1-mm (1.5-in.) diameter x 914-mm (36-in.) long A36 steel pins with 76-mm x 76-mm x 13-mm (3-in. x 3-in. x 0.5-in.) A36 steel caps installed in holes on the front face of each barrier segment. The new tie-down design was then installed in combination with sixteen F-shape barriers and crash tested according to NCHRP Report No. 350 test designation 3-11. The results showed that the vehicle was safely redirected, and the test was judged acceptable according to the NCHRP Report No. 350 criteria. Barrier deflections for the system were reduced, and all of the barriers in the system were safely restrained on the asphalt road surface.

The temporary barrier approach transition to rigid barrier varied the barrier stiffness in the transition region through strategic application of the previously designed asphalt tie-downs and the placement of either 10-gauge or nested 12 gauge thrie beam across the joint between the final barrier in the transition and the rigid barrier. Two potential CIP locations were identified for the system, but one was ruled out based on previous experience with temporary barrier and tie-

down barrier deflections. Computer simulation with LS-DYNA was used to locate the final CIP for the full-scale crash test. The system was tested according to NCHRP Report No. 350 test designation 3-21. The results showed that the vehicle was safely redirected, and the test was judged acceptable according to the NCHRP Report No. 350 criteria.

Table 3. Test Summary

Test No.	Test Designation and Description	Actual Impact Conditions		Occupant Risk				Comments	Assessment
		Speed (km/h)	Angle (Deg.)	OIV (m/s)		RA (g's)			
				Long.	Lat.	Long.	Lat.		
FTB-1	Test 3-11 – Pickup truck redirection	98.7	25.4	3.93	5.73	18.89	14.00	The vehicle was safely and smoothly redirected.	**PASS**
FTB-2	Test 3-21 - Pickup truck transition	102.7	26.1	5.04	5.69	7.25	12.66	The vehicle was safely and smoothly redirected.	**PASS**

11 RECOMMENDATIONS

The tie-down and transition systems described herein provide designers with improved flexibility and safety when installing temporary concrete barrier. These designs can be coupled with the previously developed F-shape temporary barrier tie-down systems for concrete surfaces to adapt to a wide range of installations. In addition, the transition is the first temporary barrier transition designed to have been successfully tested according the NCHRP Report No. 350 criteria. There are some comments however that need to be made regarding the use of these designs.

The asphalt tie-down system for use with F-shape temporary concrete barriers was tested with a clear gap of 152 mm (6 in.) between the back side of the barriers and the edge of the vertical drop-off. Therefore, this distance is recommended as the minimum safe distance that the barrier system should be installed from the edge of the asphalt roadway. This 152-mm (6-in.) distance from the back side of the barrier does not reflect the distance for safe installation of the tie-down system adjacent to a rigid hazard. For this type of installation, designers must consider the working width of the system obtained during the full-scale testing. It is also important to note that the tie-down barriers should be installed on an asphalt surface with a minimum of 51 mm (2 in.) of asphalt cover to insure that the barriers are free to move laterally.

The tie-down and transition systems described herein were designed for use with the Kansas F-shape temporary concrete barrier system, and therefore, they should not be used with other temporary barrier systems or joint connections without further study. Although it is very likely that this tie-down system can be adapted to other approved temporary barrier systems, it is necessary to utilize some criteria to aid in that determination. They are as follows:

1. Joints between barrier segments must have comparable or greater torsional rigidity about the longitudinal barrier axis when compared to that of the as-tested configuration.
2. Alternative barrier segment lengths would be acceptable as long as they are at least 3.81-m long and utilize an equivalent or greater number of anchors per foot of barrier length. With shorter barrier lengths, it is believed that additional barrier rotation will occur due to the greater number of joints, thus resulting in the propensity for increased climbing and rollover.
3. Alternative barrier segments should have comparable mass per unit length.
4. Alternative barrier segments should have equal or greater reinforcement than the F-shape barrier described herein. This reinforcement recommendation is to include the longitudinal steel, shear stirrups, and containment steel bars surrounding the anchor boxes used with the vertical anchor rods.
5. The shape of alternative barrier segments may require further study. Past research has shown that the F-shape provides slightly improved results over those observed using the New Jersey shape barrier. Therefore, further study may be needed to assure safe performance when applying the designs to other barrier shapes.

The approach transition design between free-stranding and rigid concrete barrier detailed in this report should be applied when designers are attaching free-standing temporary barrier to rigid concrete barriers or tie-down temporary barrier systems that provide a high degree of constraint on lateral deflection. This requires that the approach transition be applied when free-standing F-shape temporary barriers are connected to rigid concrete barrier, the bolt-through tie-down system designed for use on concrete roadways, or the asphalt pin tie-down system developed as part of this research. When the approach transition is used in conjunction with the

bolt-through tie-down system designed for use on concrete roadways or the asphalt pin tie-down system, the thrie beam guardrail on the downstream end of the transition is not necessary due to the similar stiffness and deflection levels of the tie-down barriers and the transition. Use of the thrie beam sections is required when the system is attached to rigid barriers to reduce the potential for vehicle snag. The approach transition does not need to be applied when free-standing barriers are attached to the steel strap tie-down system designed for use on concrete roadways and bridge decks.

The final recommendations for the systems relate to the transition design. First, thirteen free-standing barriers were installed upstream of the transition for the full-scale testing. The number of free-standing barrier was increased over the eight barriers typically used in order to account for increased loading of the upstream end due to the constrained barriers downstream. It is recommended that a minimum of thirteen free-standing barriers be used upstream of the transition until further research can be conducted into the numbers of upstream barriers required to provide sufficient upstream anchorage. Finally, the researchers believe that the bolt-through tie-down developed previously could be safely applied for transitions on concrete surfaces using the configuration developed here. The asphalt and bolt-through concrete tie-down systems are believed to possess similar lateral restraint and thus can be interchanged in the transition design as needed.

The development of both the asphalt pin tie-down and the approach transition was conducted in close coordination with the Florida Department of Transportation. As such, the Florida Department of Transportation has developed details and standard plans that address many of the above recommendations as well as other design and installation issues not covered in this report. Florida Department of Transportation has graciously agreed to allow their standard

plans to be published as part of this research report to provide additional guidance for installation of the F-shape temporary concrete barrier and its various tie-down and transition applications. These details are located in Appendix I.

12 REFERENCES

1. Bielenberg, B.W., Faller, R.K., Reid, J.D., Holloway, J.C., Rohde, J.R., and Sicking, D.L., *Development of a Tie-Down System for Temporary Concrete Barriers*, Final Report to the Midwest States Regional Pooled Fund, Report No. TRP-03-115-02, Midwest Roadside Safety Facility, University of Nebraska-Lincoln, Lincoln, NE, June 2002.

2. Bielenberg, B.W., Faller, R.K., Reid, J.D., Rohde, J.R., and Sicking, D.L., *Design and Testing of Tie-Down Systems for Temporary Barriers*, Paper No. 03-3146, Transportation Research Record No. 1851, Transportation Research Board, Washington D.C., November 2003.

3. Polivka, K.A., Faller, R.K., Rohde, J.R., Holloway, J.C., Bielenberg, B.W., and Sicking, D.L., *Development and Evaluation of a Tie-Down System for the Redesigned F-Shape Concrete Temporary Barrier*, Final Report to the Midwest State's Regional Pooled Fund Program, Transportation Research Report No. TRP-03-134-03, Project No. SPR-3(017)-Year 13, Project Code: RPFP-03-06, Midwest Roadside Safety Facility, University of Nebraska-Lincoln, August 22, 2003.

4. Ross, H.E., Sicking, D.L., Zimmer, R.A. and Michie, J.D., *Recommended Procedures for the Safety Performance Evaluation of Highway Features*, National Cooperative Highway Research Program (NCHRP) Report No. 350, Transportation Research Board, Washington, D.C., 1993.

5. Jewel, J., Weldon, G., and Peter, R., *Compliance Crash Testing of K-Rail Used in Semi-Permanent Installations*, Report No. 59-680838, Division of Materials Engineering and Testing Services, CALTRANS, Sacramento, CA, October 1999.

6. Mak, K.K., and Sicking, D.L., *Rollover Caused by Concrete Safety Shape Barrier - Volume I: Technical Report and Volume II: Appendices*, Report Nos. FHWA-RD-88-219/220, Performed for the Office of Safety and Traffic Operations R&D, Federal Highway Administration, Performed by the Texas Transportation Institute, Texas A&M University, January 1989.

7. Bronstad, M.E., Calcote, L.R., and Kimball, C.E., Jr., *Concrete Median Barrier Research - Vol. 2 Research Report*, Report No. FHWA-RD-77-4, Submitted to the Offices of Research and Development, Federal Highway Administration, Performed by Southwest Research Institute, San Antonio, TX, March 1976.

8. Buth, C.E., Campise, W.L., Griffin III, L.I., Love, M.L., and Sicking, D.L., *Performance Limits of Longitudinal Barrier Systems - Volume I: Summary Report*, FHWA/RD-86/153, Final Report to the Federal Highway Administration, Office of Safety and Traffic Operations R&D, Performed by Texas Transportation Institute, Texas A&M University, May 1986.

9. Fortuniewicz, J.S., Bryden, J.E., and Phillips, R.G., *Crash Tests of Portable Concrete Median Barrier for Maintenance Zones*, Report No. FHWA/NY/RR-82/102, Final Report to the Office of Research, Development, and Technology, Federal Highway Administration, Performed by the Engineering Research and Development Bureau, New York State Department of Transportation, December 1982.

10. Buth, C.E., Hirsch, T.J., and McDevitt, C.F., *Performance Level 2 Bridge Railings*, Transportation Research Record No. 1258, Transportation Research Board, National Research Council, Washington D.C., 1990.

11. Hinch, J., Yang, T-L, and Owings, R., *Guidance Systems for Vehicle Testing*, ENSCO, Inc., Springfield, VA, 1986.

12. Halquist, J. O., *LS-DYNA Keyword Users Manual: Version 940*, Livermore California, Livermore Software Technology Corporation, June 1997.

13. Polivka, K.A., Sicking, D.L., and Reid, J.D., *Deflections Limits for Temporary Concrete Barriers*, Revised Final Report to the Midwest State's Regional Pooled Fund Program, Transportation Research Report No. TRP-03-113-02, Project No. SPR-3(017)-Year 9, Midwest Roadside Safety Facility, University of Nebraska-Lincoln, June 18, 2003.

14. Faller, R.K., Rohde, J.R., Rosson, B.T., Smith, R.P., and Addink, K.H., *Development of a TL-3 F-Shape Temporary Concrete Median Barrier*, Report No. TRP-03-64-96, Midwest Roadside Safety Facility, University of Nebraska-Lincoln, Lincoln, NE., December 1996.

15. Polivka, K.A., Bielenberg B.W., Faller, R.K., Reid, J.D., Holloway, J.C., Rohde, J.R., and Sicking, D.L., *Development of a Steel H-Section Temporary Barrier for Use in Limited Deflection Applications*, In Progress Report to the Midwest States Regional Pooled Fund, Report No. TRP-03-120-02, Midwest Roadside Safety Facility, University of Nebraska-Lincoln, Lincoln, NE, August 2002.

16. Post, E.R., Faller, R.K., Pfeifer, B.G., and Holloway, J.C., *Full-Scale Vehicle Crash Test on the Iowa Steel Temporary Barrier Rail*, Report No. TRP-03-20-89, Midwest Roadside Safety Facility, University of Nebraska-Lincoln, Lincoln, NE., December 1989.

17. *Vehicle Damage Scale for Traffic Investigators*, Second Edition, Technical Bulletin No. 1, Traffic Accident Data (TAD) Project, National Safety Council, Chicago, Illinois, 1971.

18. *Collision Deformation Classification – Recommended Practice J224 March 1980*, Handbook Volume 4, Society of Automotive Engineers (SAE), Warrendale, Pennsylvania, 1985.

13 APPENDICES

APPENDIX A - Asphalt Pin Tie-Down, English Units

Figure A-1. Asphalt Pin Tie-Down Design Details 97
Figure A-2. Asphalt Pin Tie-Down Design Details 98
Figure A-3. Asphalt Pin Tie-Down Design Details 99
Figure A-4. Asphalt Pin Tie-Down Design Details 100
Figure A-5. Asphalt Pin Tie-Down Design Details 101
Figure A-6. Asphalt Pin Tie-Down Design Details 102
Figure A-7. Asphalt Pin Tie-Down Design Details 103

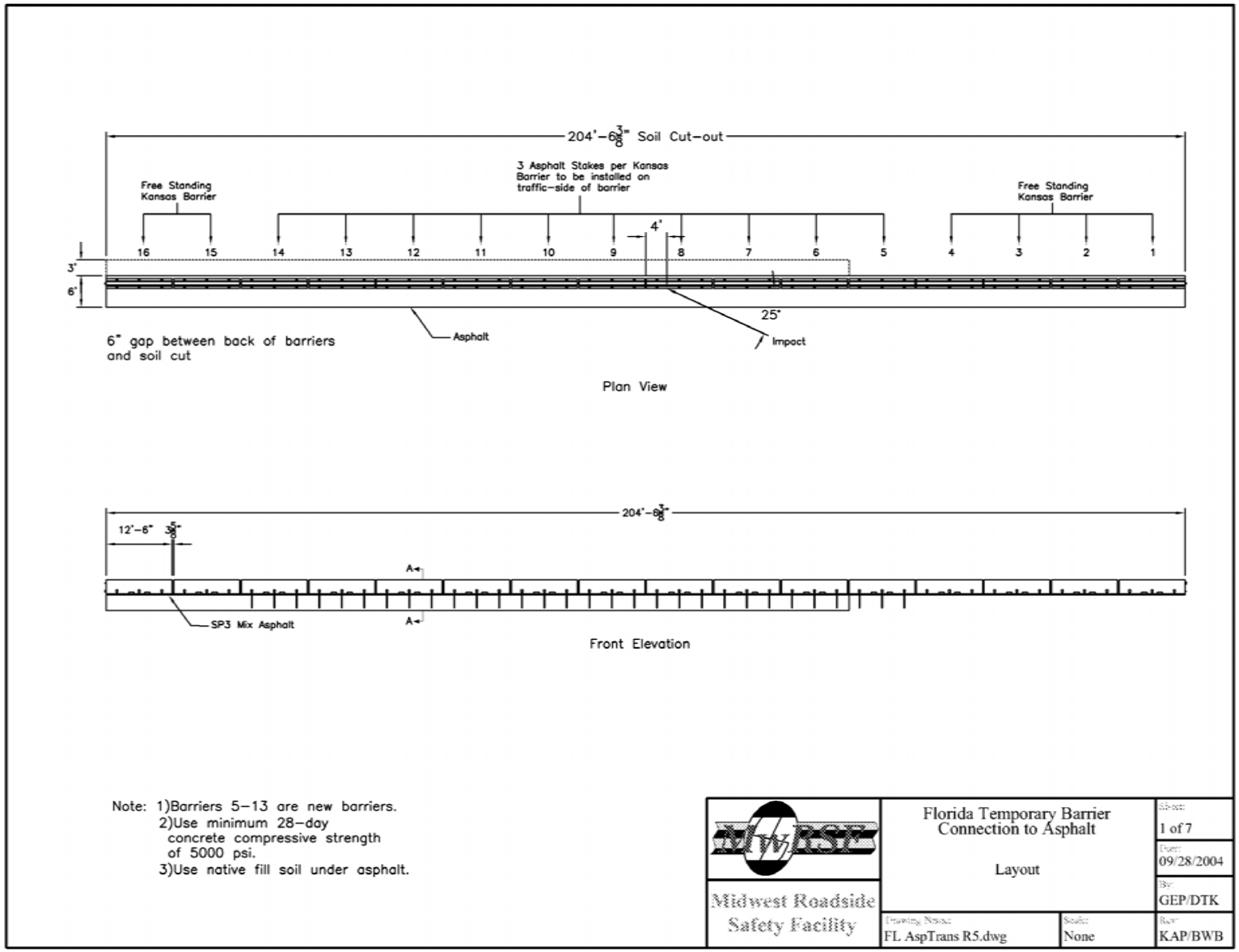

Figure A-1. Asphalt Pin Tie-Down Design Details

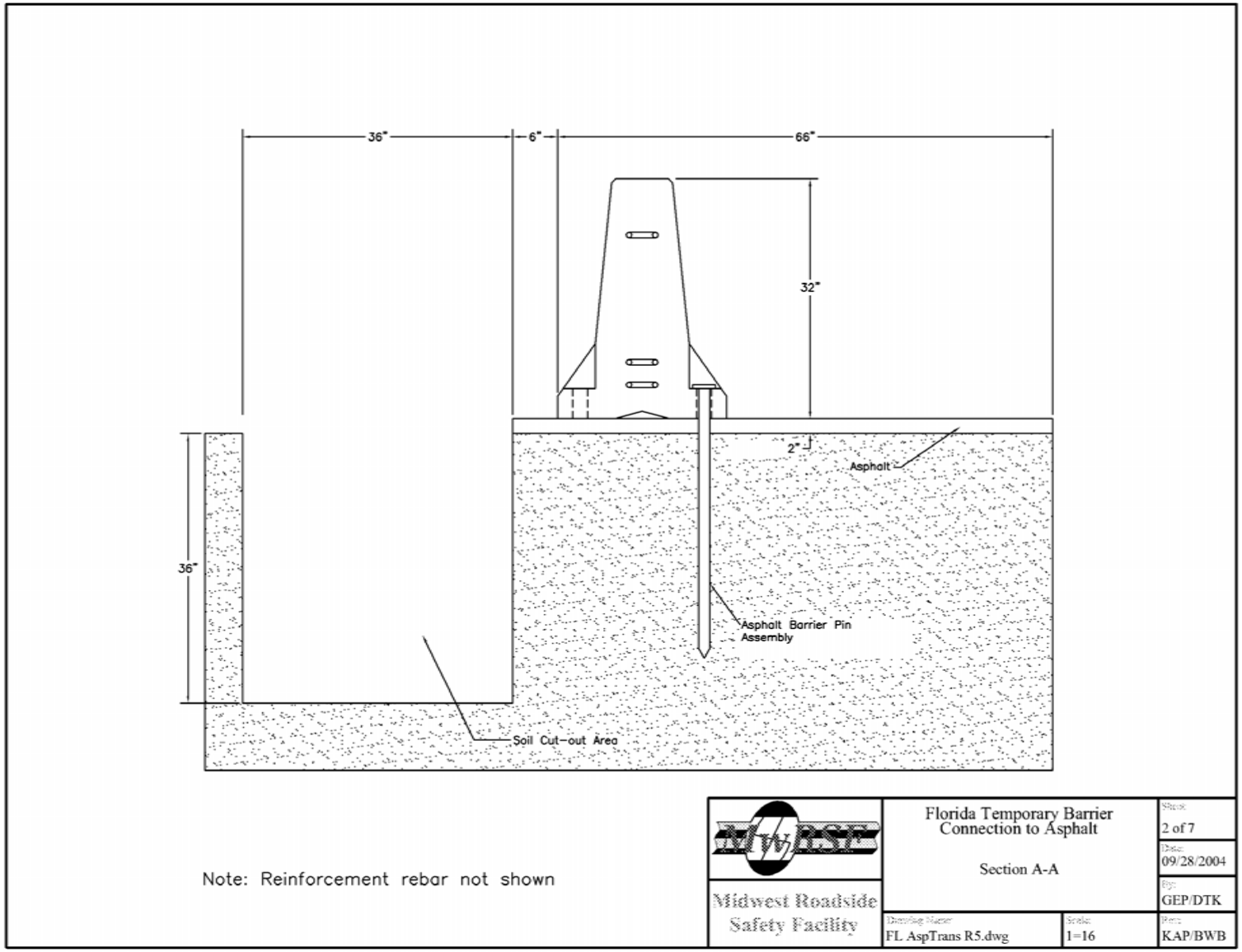

Figure A-2. Asphalt Pin Tie-Down Design Details

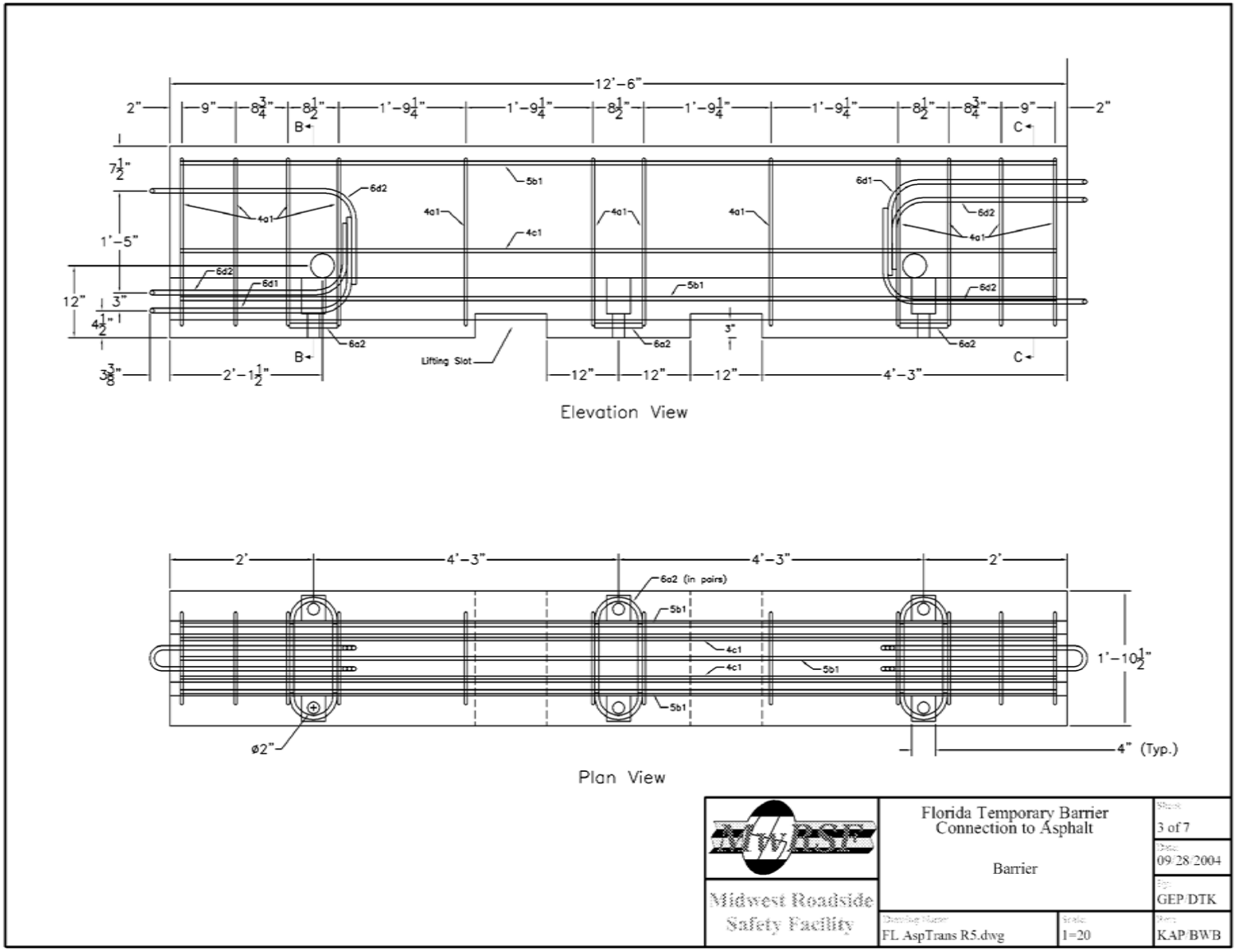

Figure A-3. Asphalt Pin Tie-Down Design Details

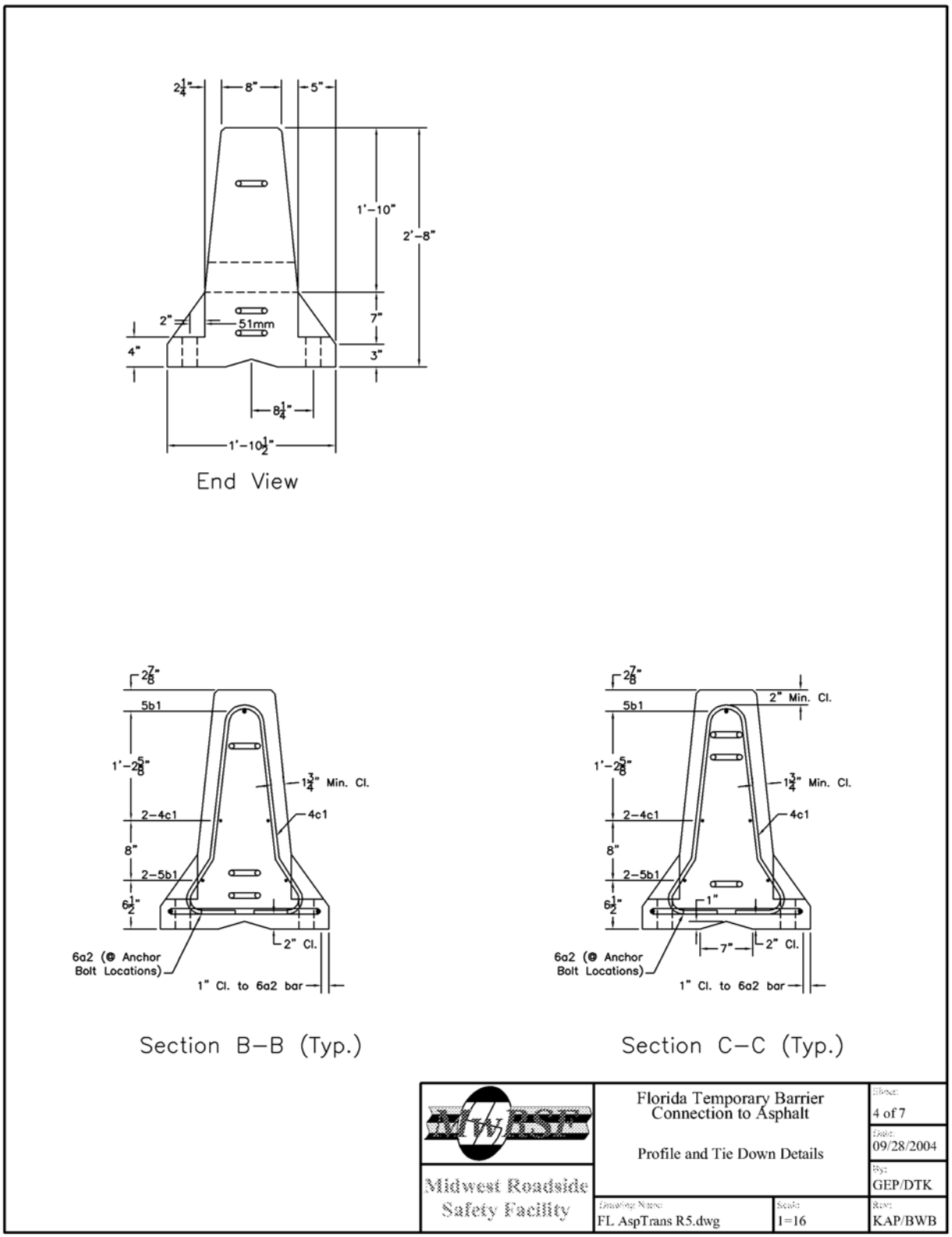

Figure A-4. Asphalt Pin Tie-Down Design Details

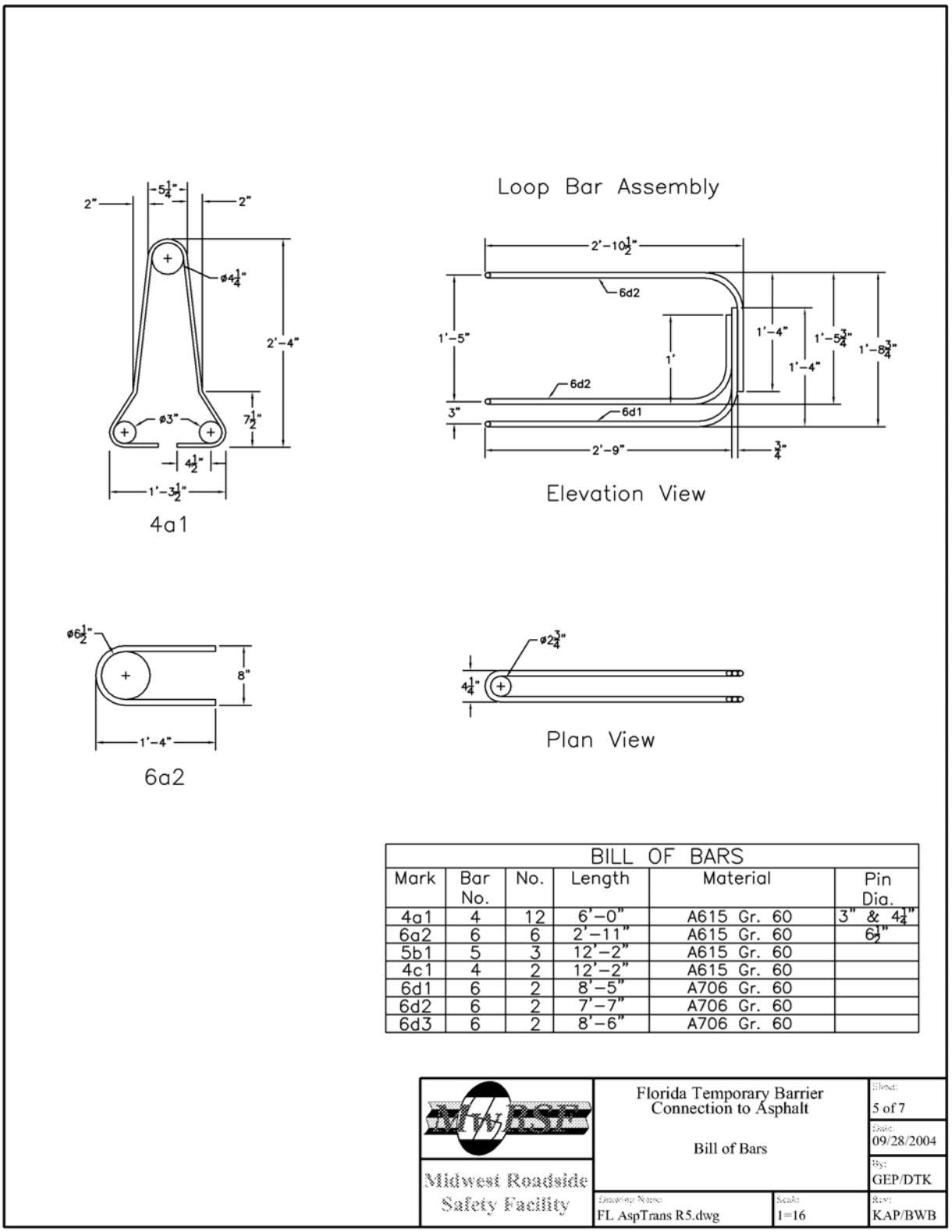

Figure A-5. Asphalt Pin Tie-Down Design Details

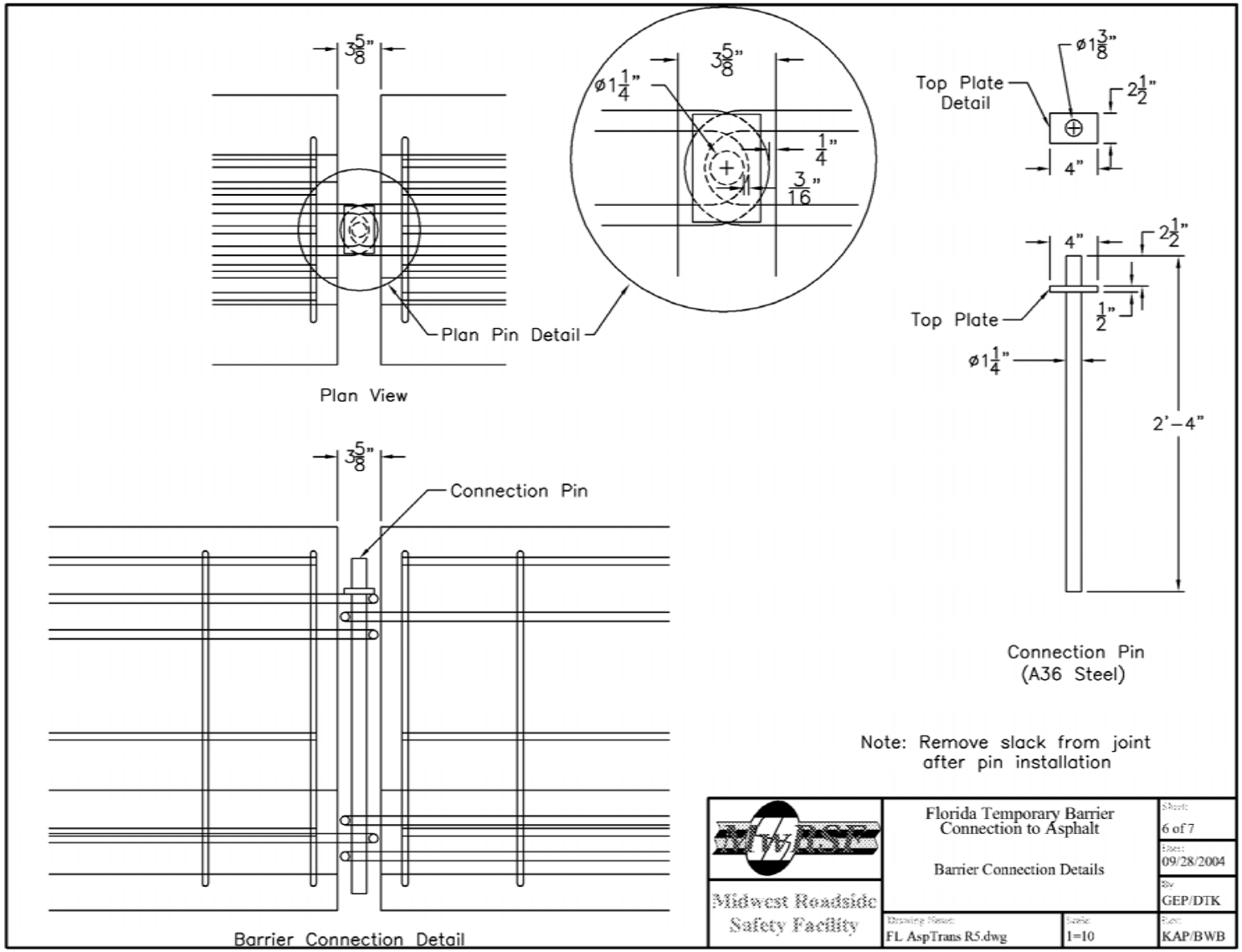

Figure A-6. Asphalt Pin Tie-Down Design Details

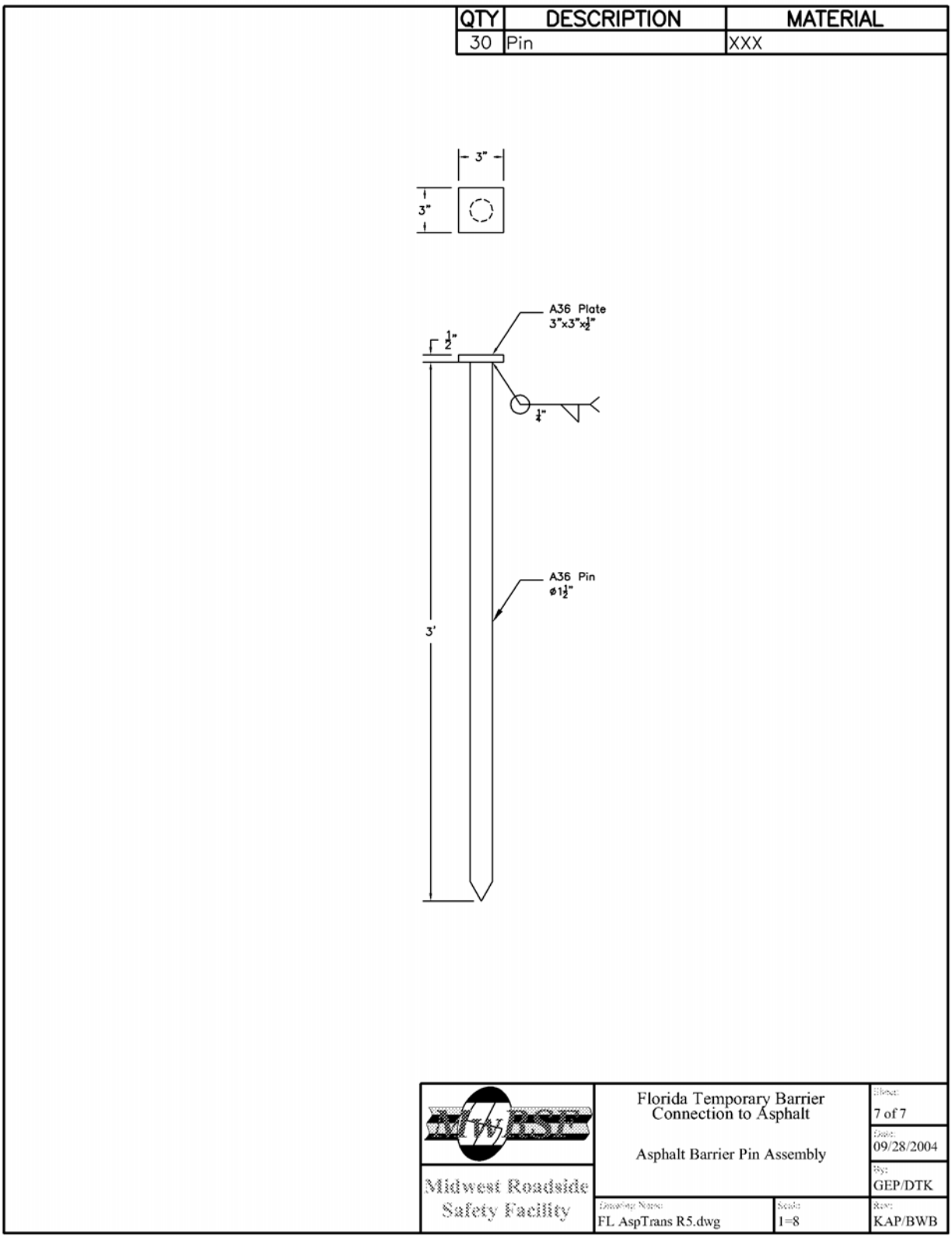

Figure A-7. Asphalt Pin Tie-Down Design Details

APPENDIX B - Test Summary Sheet in English Units, Test No. FTB-1

Figure B-1. Summary of Test Results and Sequential Photographs, Test FTB-1 105

0.000 sec | 0.152 sec | 0.350 sec | 0.500 sec | 0.768 sec

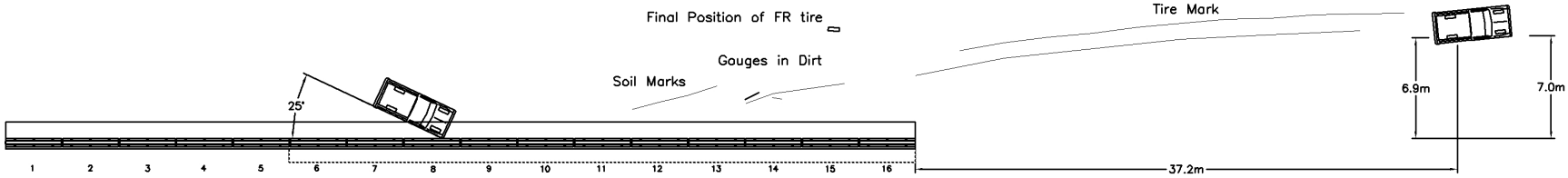

- Test Number FTB-1 (3-11)
- Date 9/27/04
- Test Article ..... F-shape PCB Asphalt Pin Tie-Down
- Total Length..... 204.5 ft
- Overall Height..... 32 in.
- Placement..... 6 in. from the edge of a 36 in. vertical drop
- Barrier Elements ..... 16 Kansas F-shape PCB's
- Joint Connections..... 1.25-in. diameter by 28-in. long A36 steel pin with a 2.5x4x0.5-in. plate
- Tie-Down Anchors..... Three 1.5-in. dia. x 36-in. long A36 steel pins per barrier on the traffic side face only
- Soil Type..... Grading B - AASHTO M 147-65
- Vehicle Model..... 1998 GMC C2500
  - Curb..... 4,308 lbs
  - Test Inertial ..... 4433 lbs
  - Gross Static ..... 4433 lbs
- Vehicle Speed
  - Impact..... 61.3 mph
  - Exit ..... NA
- Vehicle Angle
  - Impact (trajectory)..... 25.4 deg
  - Exit (trajectory) ..... NA
- Vehicle Stability ..... Satisfactory
- Vehicle Snagging..... Minor
- Occupant Ridedown Deceleration (10 msec avg.)
  - Longitudinal ..... 18.89 g's < 20 g's
  - Lateral (not req.)..... 14.00 g's < 20 g's
- Occupant Impact Velocity
  - Longitudinal ..... 12.89 ft/s < 39.4 ft/s
  - Lateral (not req.)..... 18.80 ft/s < 39.4 ft/s
- THIV (not req.)..... 24.93 ft/s
- PHD (not req.) ..... 23.57 g's
- Vehicle Damage ..... Moderate
  - TAD 1-RFQ-3
  - SAE 1RFAW3
  - OCDI..... RF001100000
- Vehicle Stopping Distance..... 228.7-ft downstream of impact 22.6-ft from traffic side face
- Test Article Damage..... Moderate
- Maximum Deflection
  - Permanent Set ..... 11.1 in.
  - Dynamic..... 21.8 in. (top of barrier)
- Working Width..... 44.3 in.

Figure B-1. Summary of Test Results and Sequential Photographs, Test FTB-1

APPENDIX C - Occupant Compartment Deformation, Test No. FTB-1

Figure C-1. Occupant Compartment Deformation, Test No. FTB-1 107
Figure C-2. OCDI, Test No. FTB-1 108

VEHICLE PRE/POST CRUSH INFO
Set-1

TEST: FTB-1
VEHICLE: 1998/GMC/WHITE

Note: If impact is on driver side need to enter negative number for Y

POINT	X	Y	Z	X'	Y'	Z'	DEL X	DEL Y	DEL Z
1	53	6	0	52.5	6	0.75	-0.5	0	0.75
2	55.5	14.75	-4.125	55	13.75	-3.75	-0.5	-1	0.375
3	55.5	22	-4.125	53.5	20.5	-3	-2	-1.5	1.125
4	55.25	29.25	-3.75	53.75	27.75	-3	-1.5	-1.5	0.75
5	48	6	-2.25	47.75	6	-1.25	-0.25	0	1
6	49.5	14.75	-7.5	49.5	13.25	-7.5	0	-1.5	0
7	49.5	21.75	-7	49.5	20.75	-7	0	-1	0
8	49	29.25	-6.5	48.75	27.75	-6.25	-0.25	-1.5	0.25
9	43.75	6	-3	43.5	6	-2	-0.25	0	1
10	45.5	14.25	-7.75	45.25	13.25	-7.25	-0.25	-1	0.5
11	45.25	21.25	-7.25	45.25	20.25	-7.5	0	-1	-0.25
12	44.75	27.75	-7	45	27	-7.5	0.25	-0.75	-0.5
13	39.5	6	-3.5	39.25	6	-2.5	-0.25	0	1
14	40.5	14.5	-8	40.5	13.25	-7.5	0	-1.25	0.5
15	40.75	21.5	-7.5	41	20.5	-7.75	0.25	-1	-0.25
16	40	27.75	-7.25	40	27	-7.5	0	-0.75	-0.25
17	34	6.25	-4.5	33.5	6	-3.5	-0.5	-0.25	1
18	34.25	14.5	-8	34.5	13.25	-7.5	0.25	-1.25	0.5
19	35	21.25	-7.25	35	20.5	-7.25	0	-0.75	0
20	35	28	-7.25	35	26.75	-7.5	0	-1.25	-0.25
21	28.5	5.75	-5	28.25	5.75	-4	-0.25	0	1
22	30	15	-8.25	29.75	14.25	-8	-0.25	-0.75	0.25
23	30.5	21.25	-7.75	30.5	20.25	-7.75	0	-1	0
24	30	28.75	-7.25	30	27.25	-7.5	0	-1.5	-0.25
25	22.25	5.5	-5.5	22	5.5	-5	-0.25	0	0.5
26	23.5	14	-8.75	23.75	13.5	-8.25	0.25	-0.5	0.5
27	24	19.75	-8	24.25	19.25	-7.75	0.25	-0.5	0.25
28	24.25	28.25	-7.25	24.25	27.5	-7.25	0	-0.75	0
29									
30									

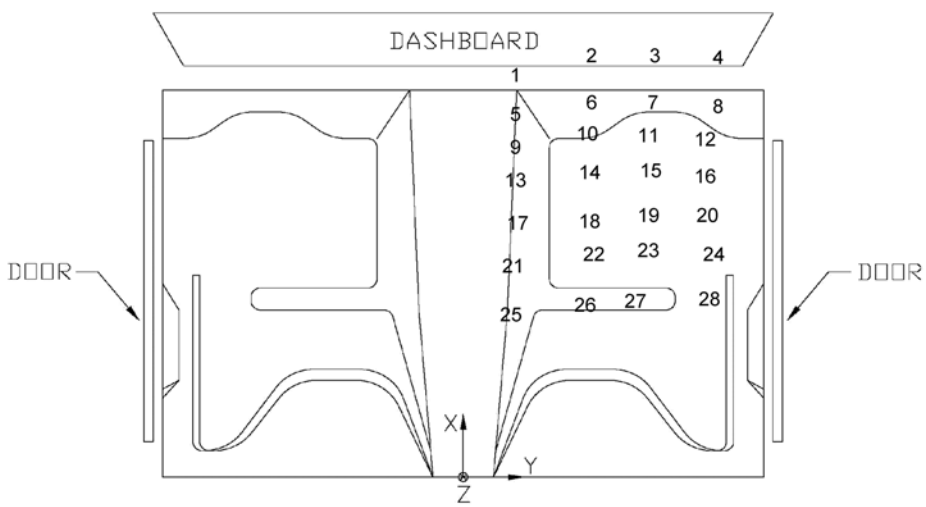

Figure C-1. Occupant Compartment Deformation, Test No. FTB-1

Occupant Compartment Deformation Index (OCDI)

Test No. FTB-1
Vehicle Type: 2000p

OCDI = XXABCDEFGHI

XX = location of occupant compartment deformation

A = distance between the dashboard and a reference point at the rear of the occupant compartment, such as the top of the rear seat or the rear of the cab on a pickup

B = distance between the roof and the floor panel

C = distance between a reference point at the rear of the occupant compartment and the motor panel

D = distance between the lower dashboard and the floor panel

E = interior width

F = distance between the lower edge of right window and the upper edge of left window

G = distance between the lower edge of left window and the upper edge of right window

H= distance between bottom front corner and top rear corner of the passenger side window

I= distance between bottom front corner and top rear corner of the driver side window

Severity Indices

0 - if the reduction is less than 3%
1 - if the reduction is greater than 3% and less than or equal to 10 %
2 - if the reduction is greater than 10% and less than or equal to 20 %
3 - if the reduction is greater than 20% and less than or equal to 30 %
4 - if the reduction is greater than 30% and less than or equal to 40 %

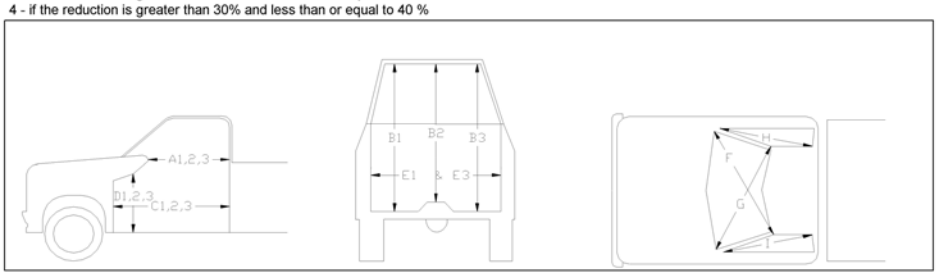

where,
1 = Passenger Side
2 = Middle
3 = Driver Side

Location:

Measurement	Pre-Test (in.)	Post-Test (in.)	Change (in.)	% Difference	Severity Index
A1	41.00	41.25	0.25	0.61	0
A2	41.50	41.75	0.25	0.60	0
A3	40.00	40.00	0.00	0.00	0
B1	46.88	47.00	0.13	0.27	0
B2	42.88	42.75	-0.13	-0.29	0
B3	47.00	47.50	0.50	1.06	0
C1	57.50	57.50	0.00	0.00	0
C2	54.50	54.25	-0.25	-0.46	0
C3	57.50	55.00	-2.50	-4.35	1
D1	17.00	17.25	0.25	1.47	0
D2	15.75	15.75	0.00	0.00	0
D3	16.63	17.75	1.13	6.77	1
E1	62.38	61.25	-1.13	-1.80	0
E3	64.00	63.75	-0.25	-0.39	0
F	58.75	58.75	0.00	0.00	0
G	58.75	58.75	0.00	0.00	0
H	42.00	41.50	-0.50	-1.19	0
I	41.50	41.50	0.00	0.00	0

Note: Maximum sevrity index for each variable (A-I) is used for determination of final OCDI value

XX A B C D E F G H I
Final OCDI: RF 0 0 1 1 0 0 0 0 0

Figure C-2. OCDI, Test No. FTB-1

APPENDIX D - Accelerometer and Rate Gyro Analysis Test, No. FTB-1

Figure D-1. Graph of Longitudinal Acceleration, Test No. FTB-1 110
Figure D-2. Graph of Longitudinal Occupant Impact Velocity, Test No. FTB-1 111
Figure D-3. Graph of Longitudinal Occupant Displacement, Test No. FTB-1 112
Figure D-4. Graph of Lateral Acceleration, Test No. FTB-1 113
Figure D-5. Graph of Lateral Occupant Impact Velocity, Test No. FTB-1..... 114
Figure D-6. Graph of Lateral Occupant Displacement, Test No. FTB-1 115
Figure D-7. Angular Displacements, Test No. FTB-1..... 116

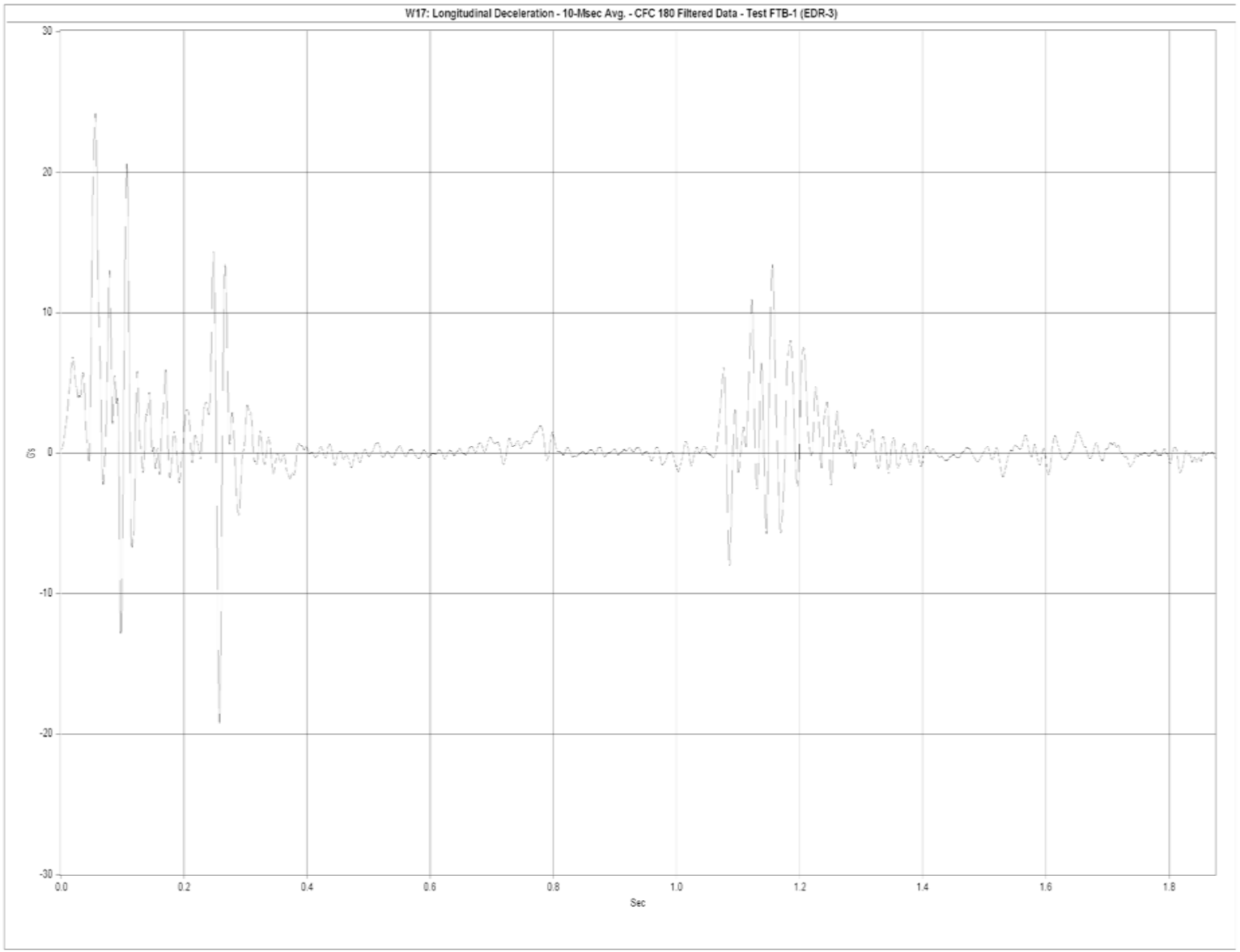

Figure D-1. Graph of Longitudinal Acceleration, Test No. FTB-1

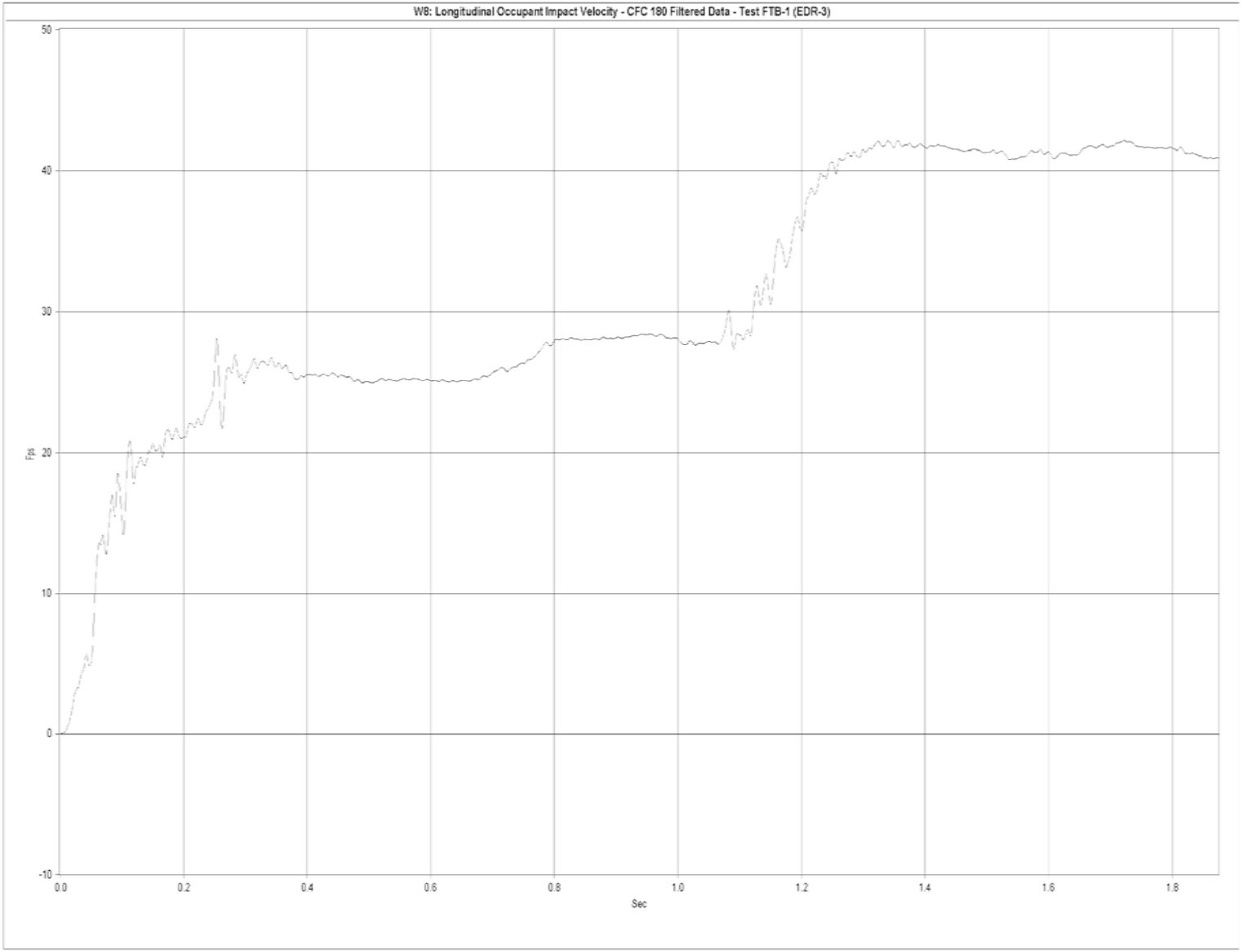

Figure D-2. Graph of Longitudinal Occupant Impact Velocity, Test No. FTB-1

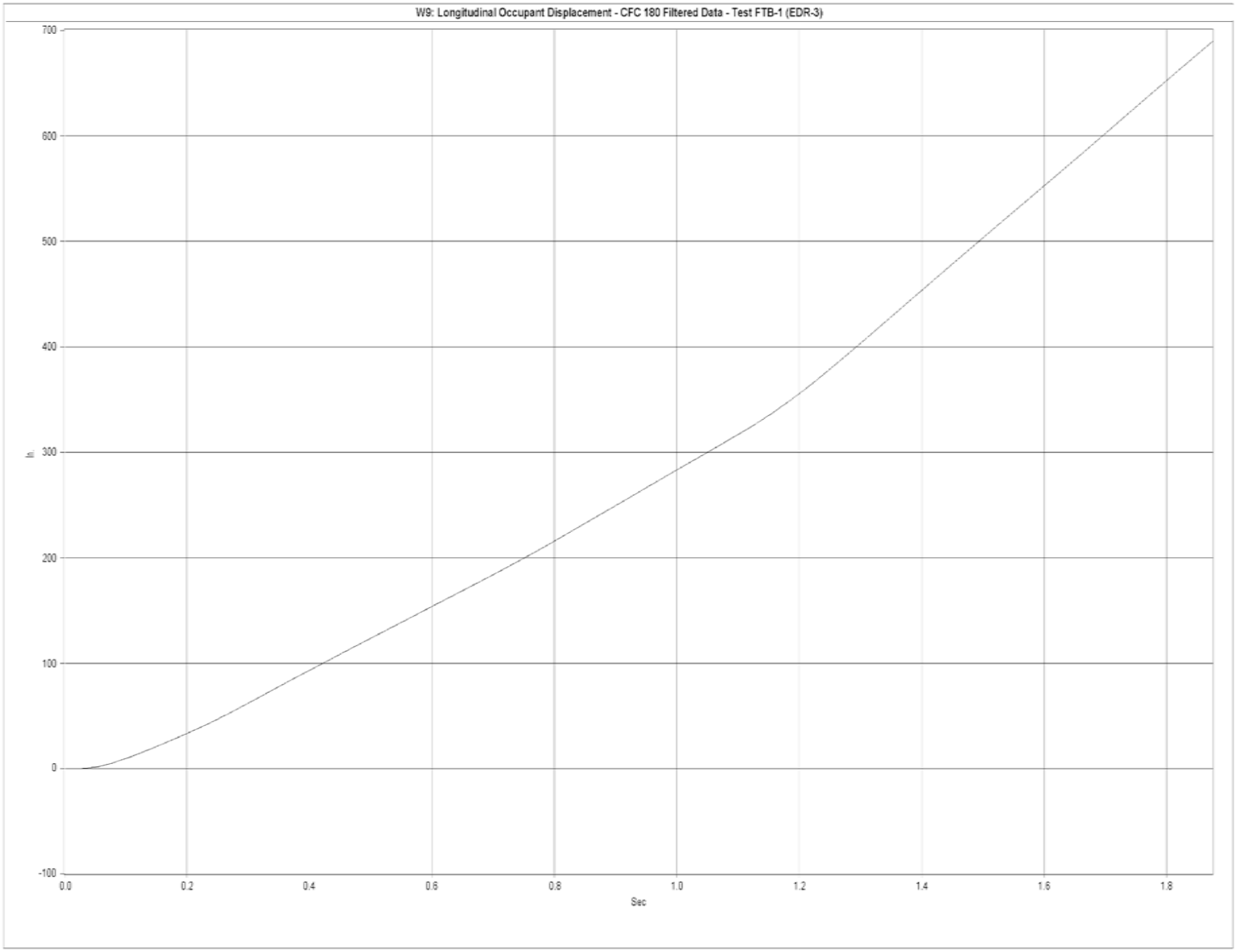

Figure D-3. Graph of Longitudinal Occupant Displacement, Test No. FTB-1

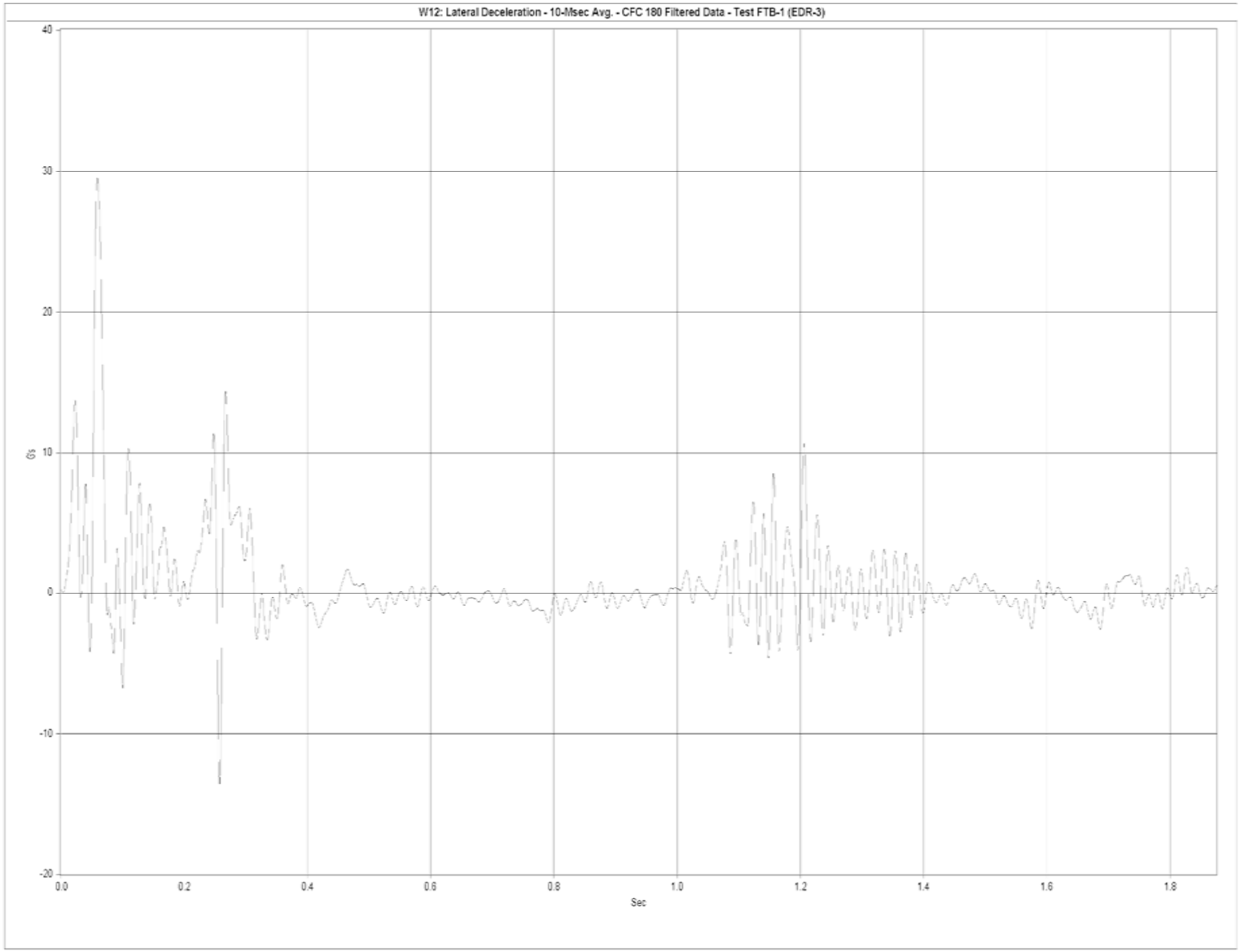

Figure D-4. Graph of Lateral Acceleration, Test No. FTB-1

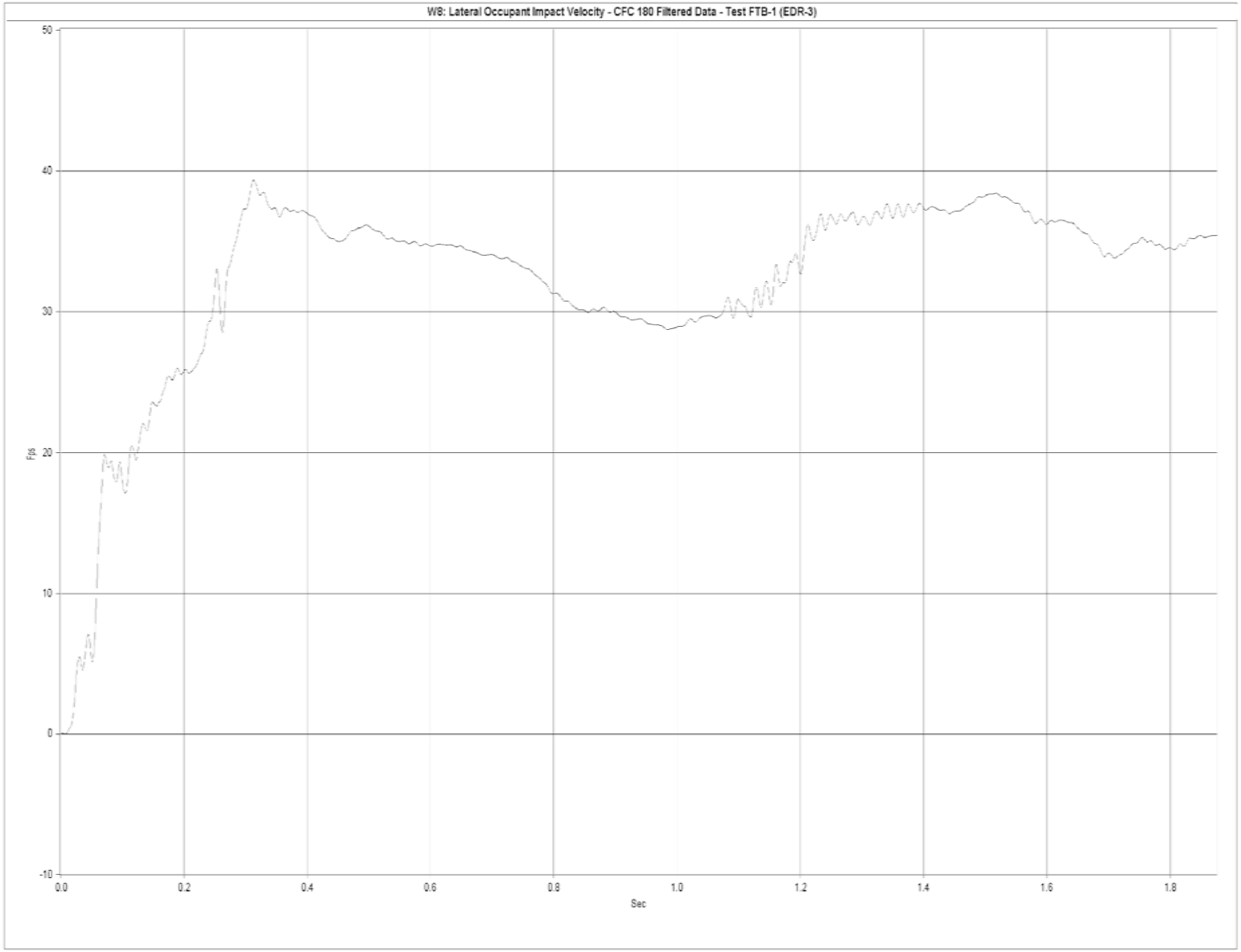

Figure D-5. Graph of Lateral Occupant Impact Velocity, Test No. FTB-1

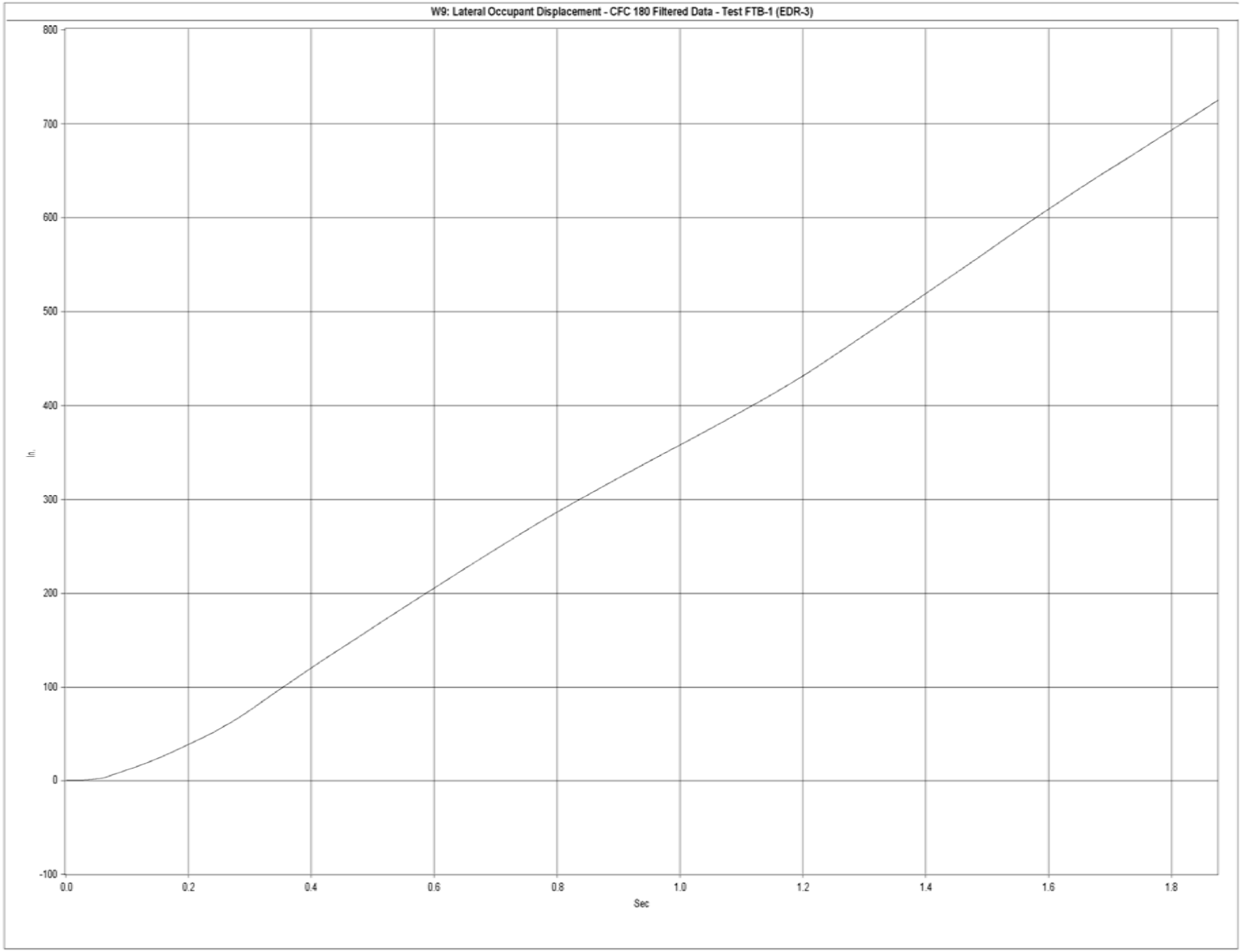

Figure D-6. Graph of Lateral Occupant Displacement, Test No. FTB-1

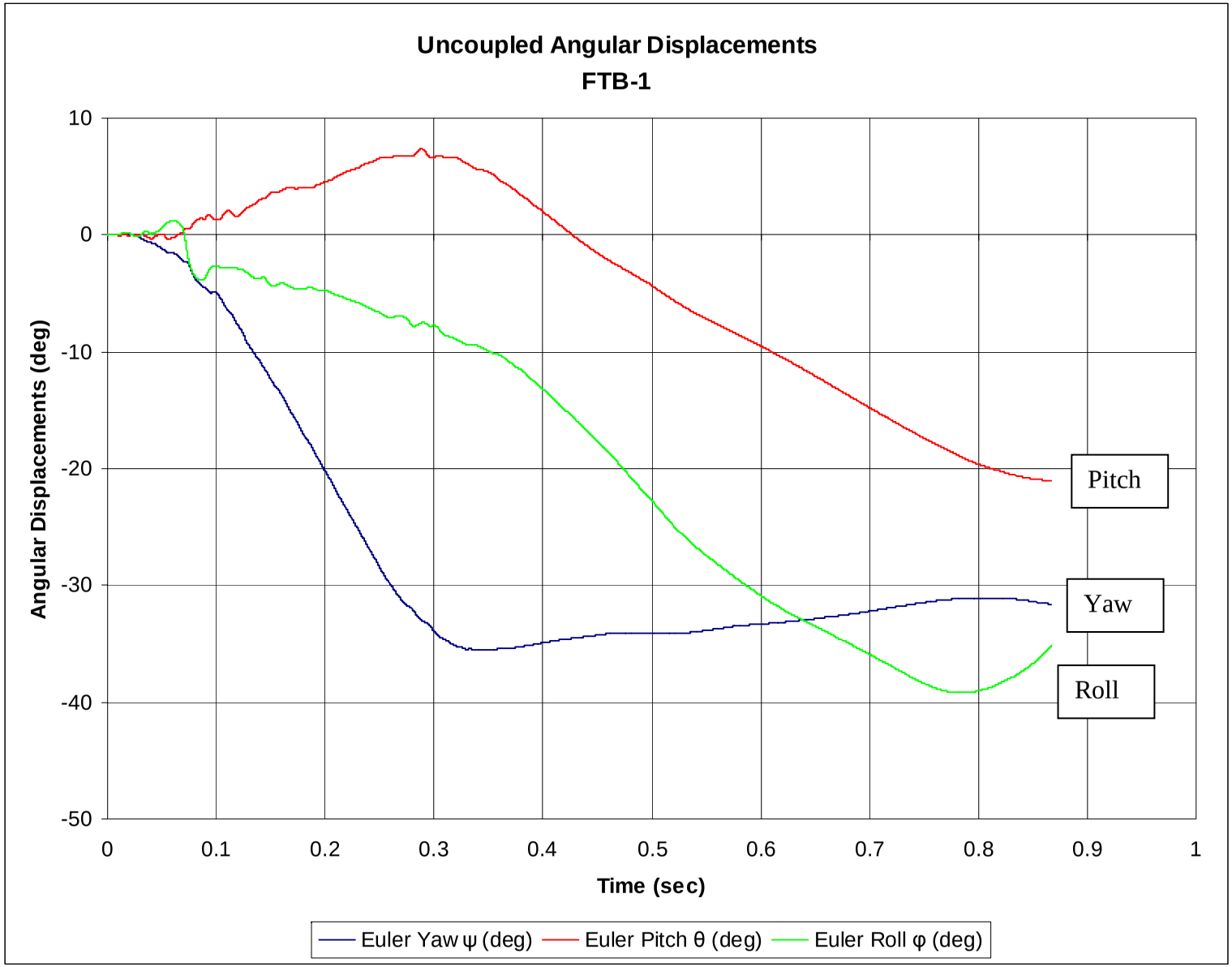

Figure D-7. Angular Displacements, Test No. FTB-1

APPENDIX E - Free-Standing to Rigid Barrier Transition Details, English Units

Figure E-1. Free Standing to Rigid Barrier Transition Design Details..... 118
Figure E-2. Free Standing to Rigid Barrier Transition Design Details..... 119
Figure E-3. Free Standing to Rigid Barrier Transition Design Details..... 120
Figure E-4. Free Standing to Rigid Barrier Transition Design Details..... 121
Figure E-5. Free Standing to Rigid Barrier Transition Design Details..... 122
Figure E-6. Free Standing to Rigid Barrier Transition Design Details..... 123
Figure E-7. Free Standing to Rigid Barrier Transition Design Details..... 124
Figure E-8. Free Standing to Rigid Barrier Transition Design Details..... 125

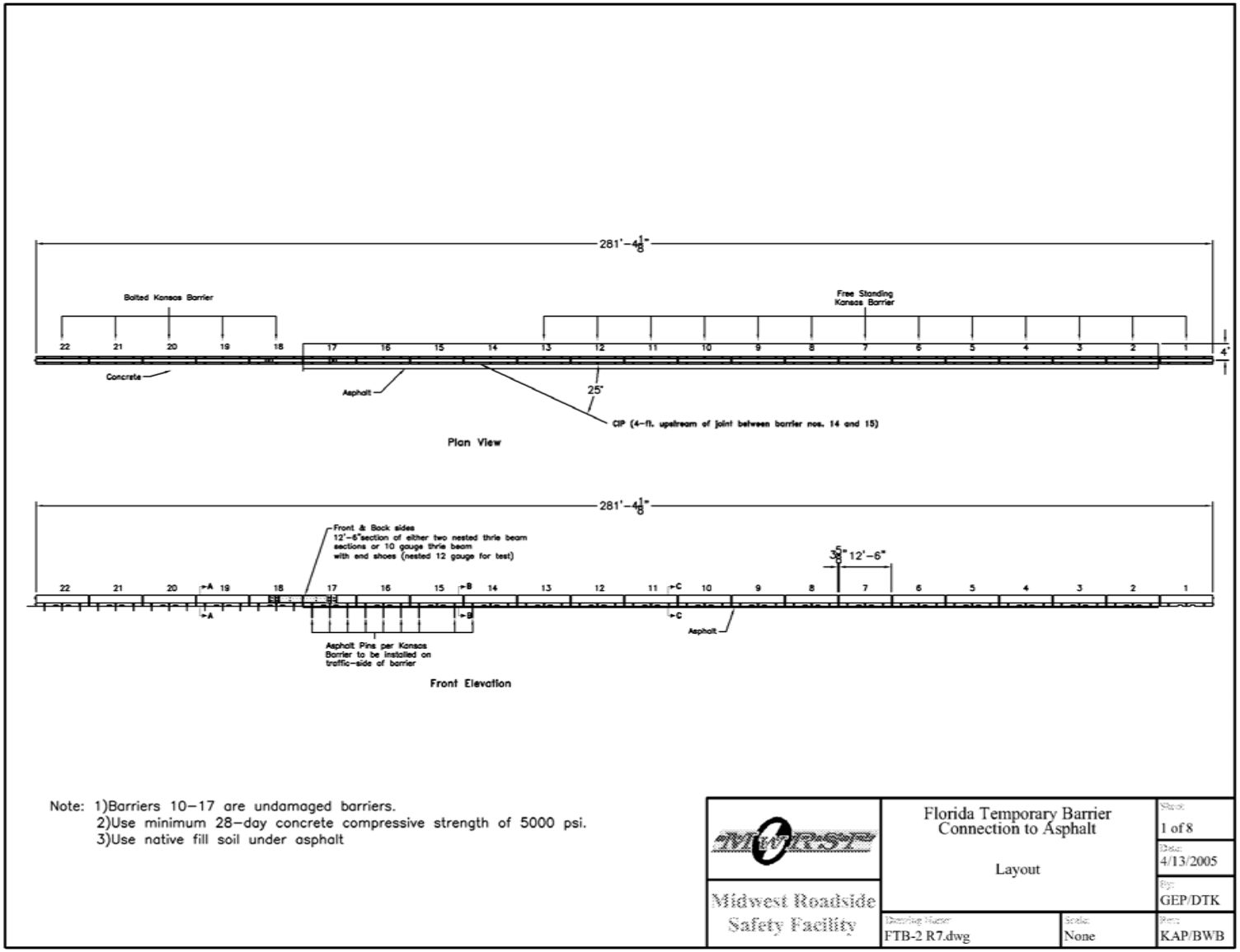

Figure E-1. Free Standing to Rigid Barrier Transition Design Details

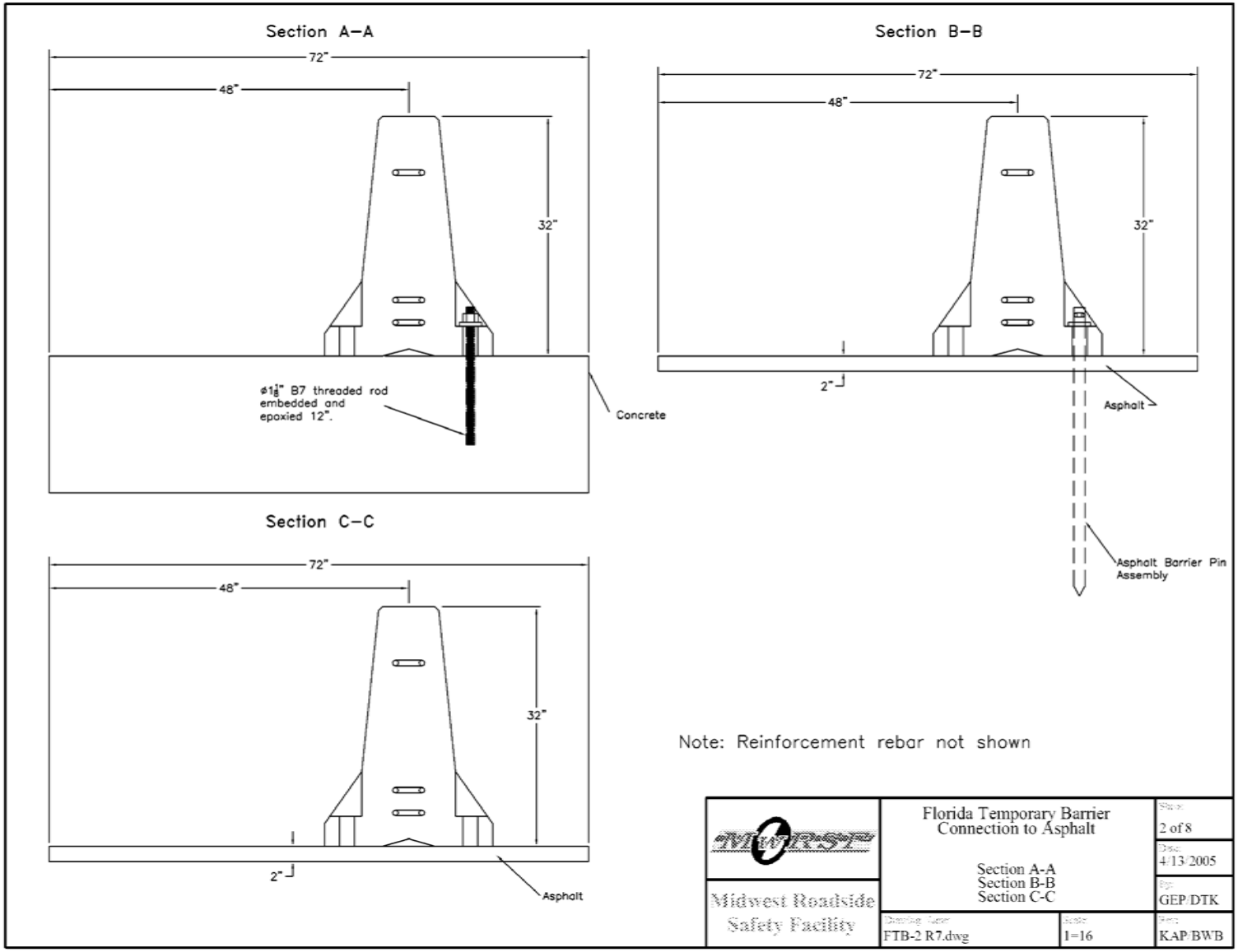

Figure E-2. Free Standing to Rigid Barrier Transition Design Details

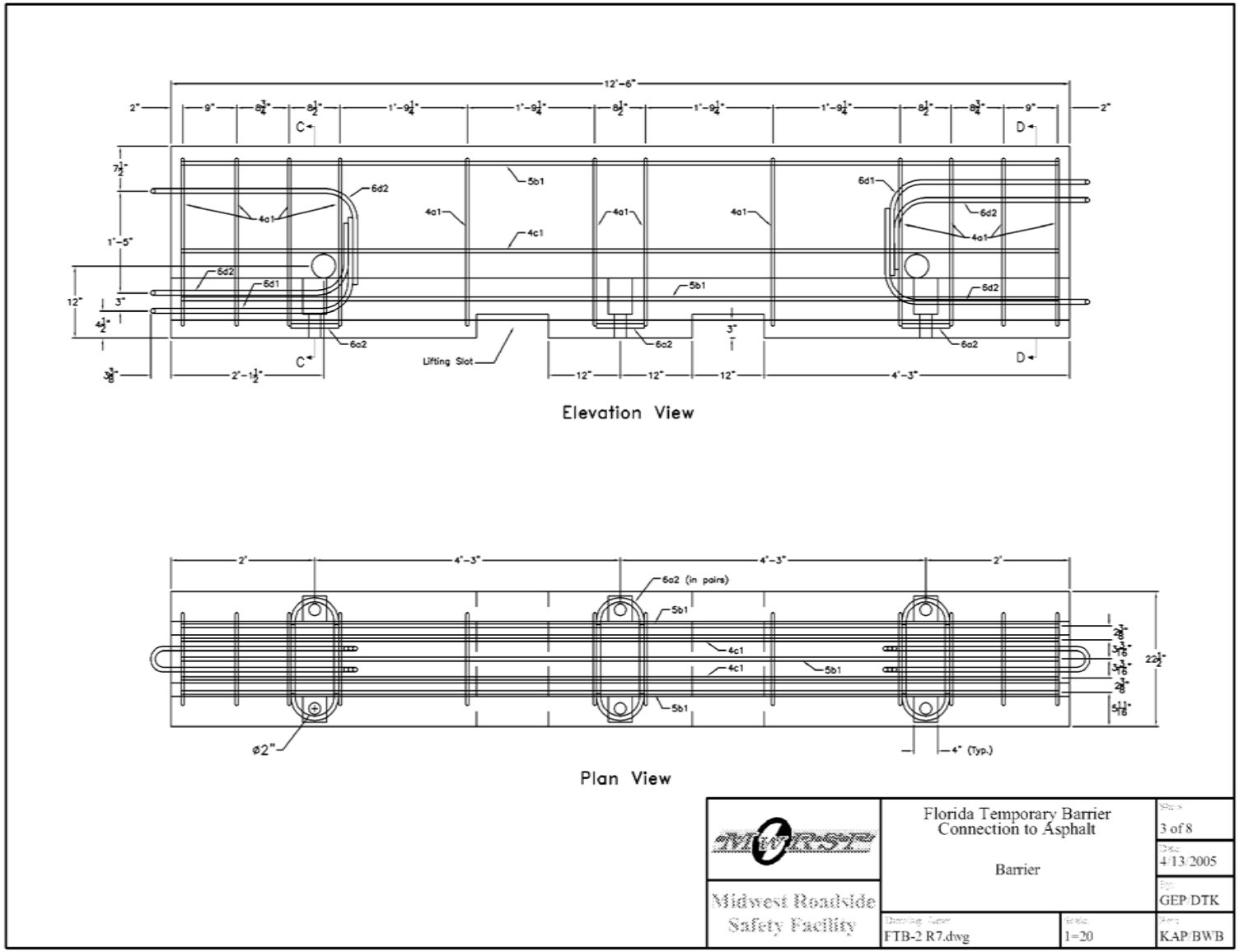

Figure E-3. Free Standing to Rigid Barrier Transition Design Details

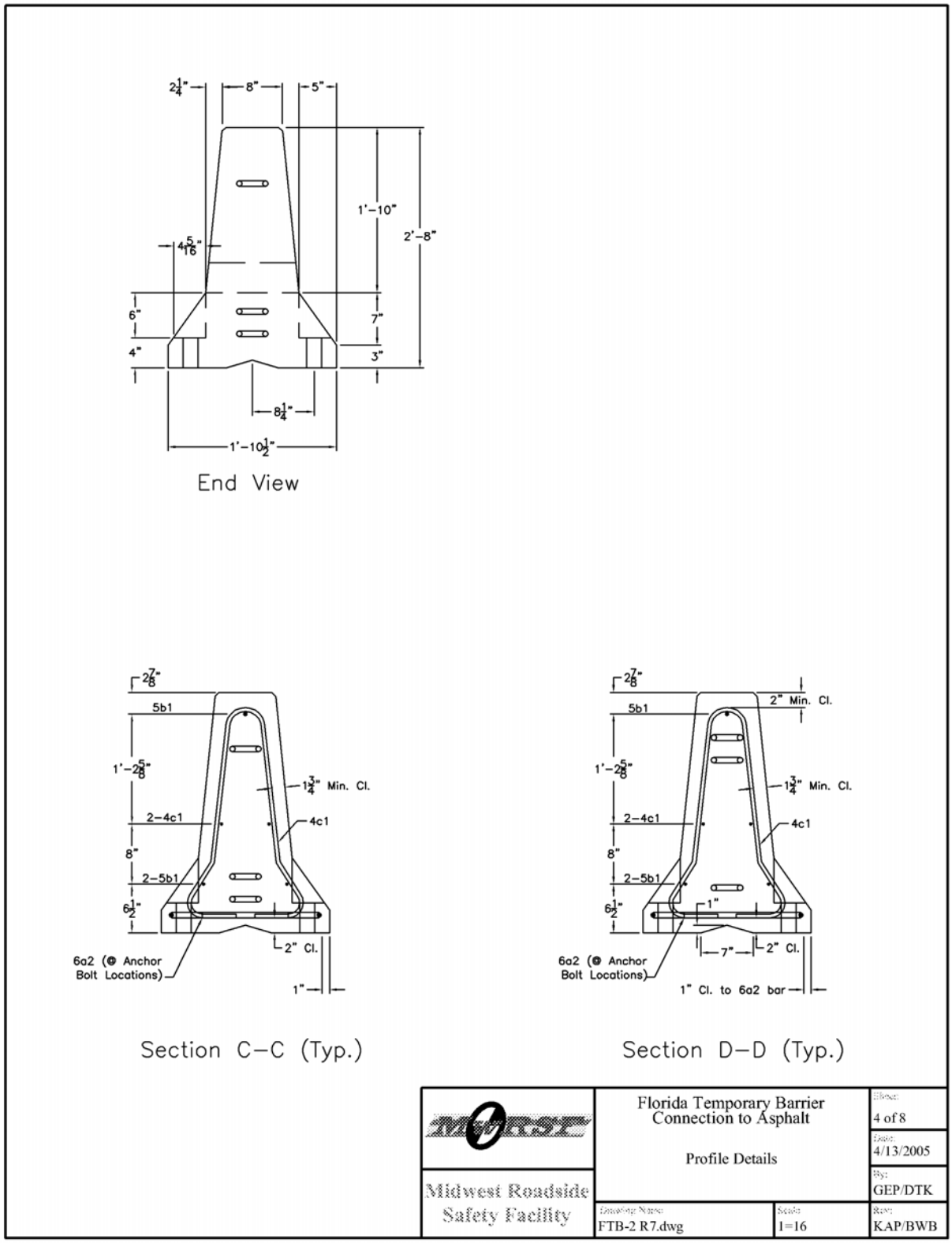

Figure E-4. Free Standing to Rigid Barrier Transition Design Details

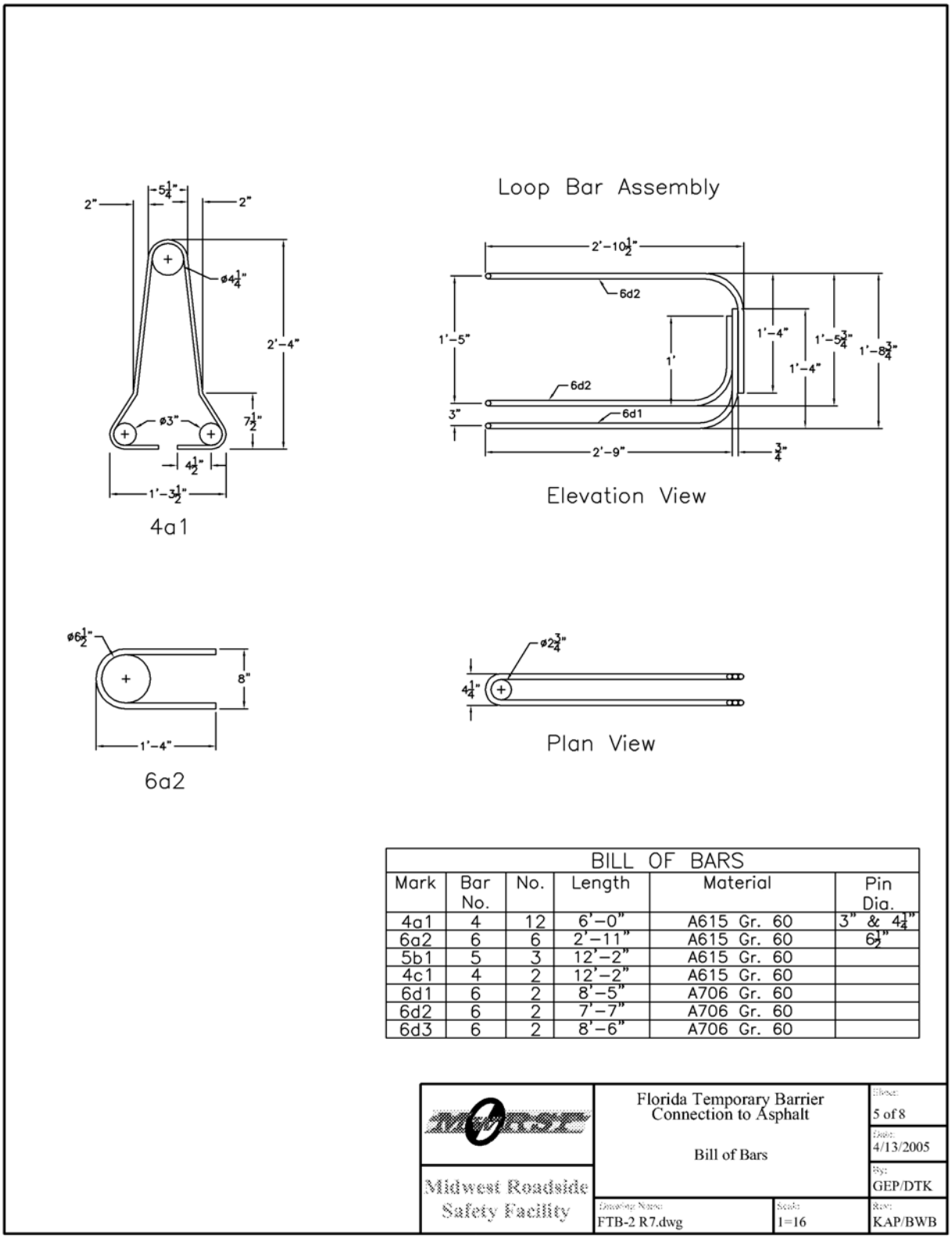

BILL OF BARS

Mark	Bar No.	No.	Length	Material	Pin Dia.
4a1	4	12	6'-0"	A615 Gr. 60	3" & 4 1/4"
6a2	6	6	2'-11"	A615 Gr. 60	6 1/2"
5b1	5	3	12'-2"	A615 Gr. 60	
4c1	4	2	12'-2"	A615 Gr. 60	
6d1	6	2	8'-5"	A706 Gr. 60	
6d2	6	2	7'-7"	A706 Gr. 60	
6d3	6	2	8'-6"	A706 Gr. 60	

Figure E-5. Free Standing to Rigid Barrier Transition Design Details

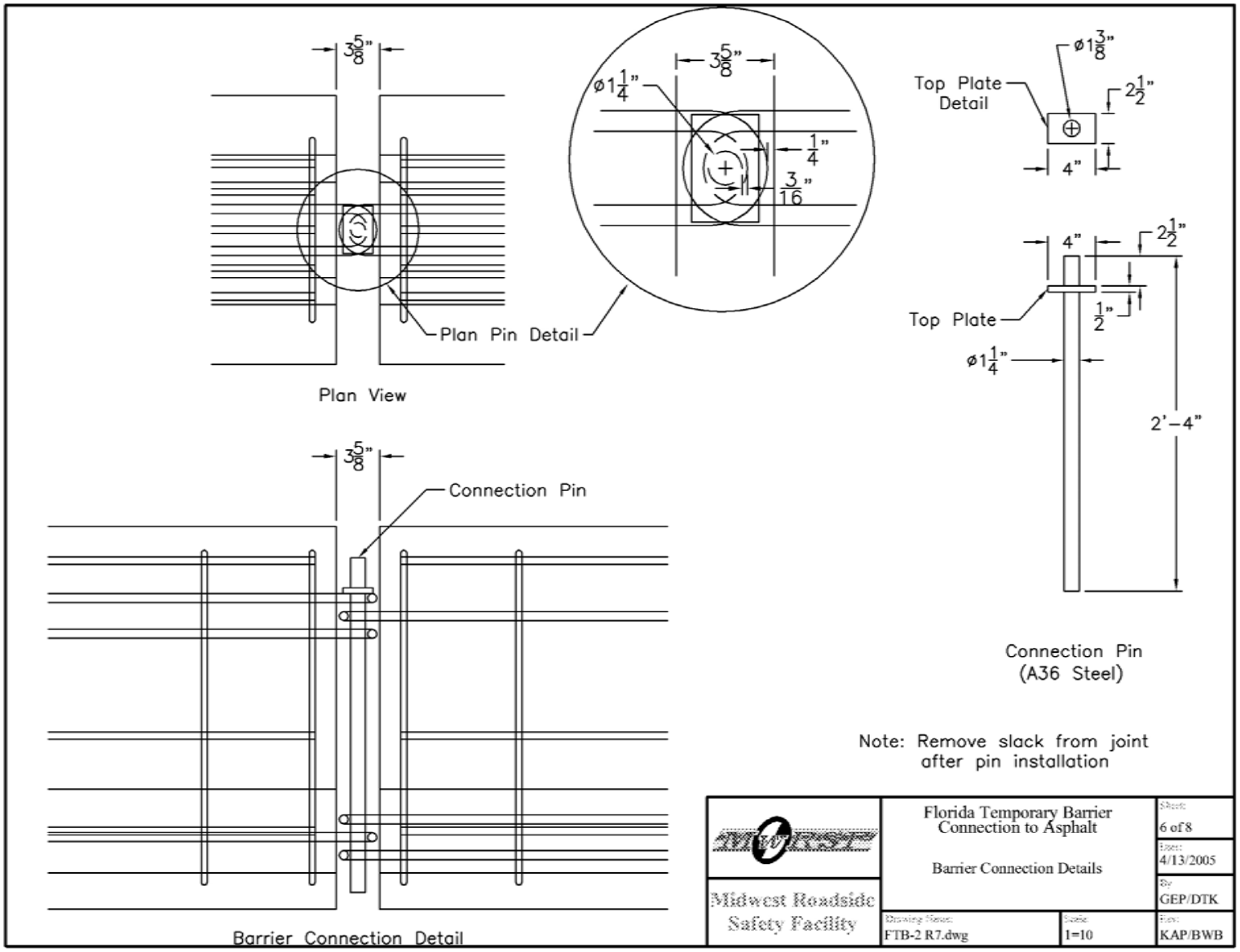

Figure E-6. Free Standing to Rigid Barrier Transition Design Details

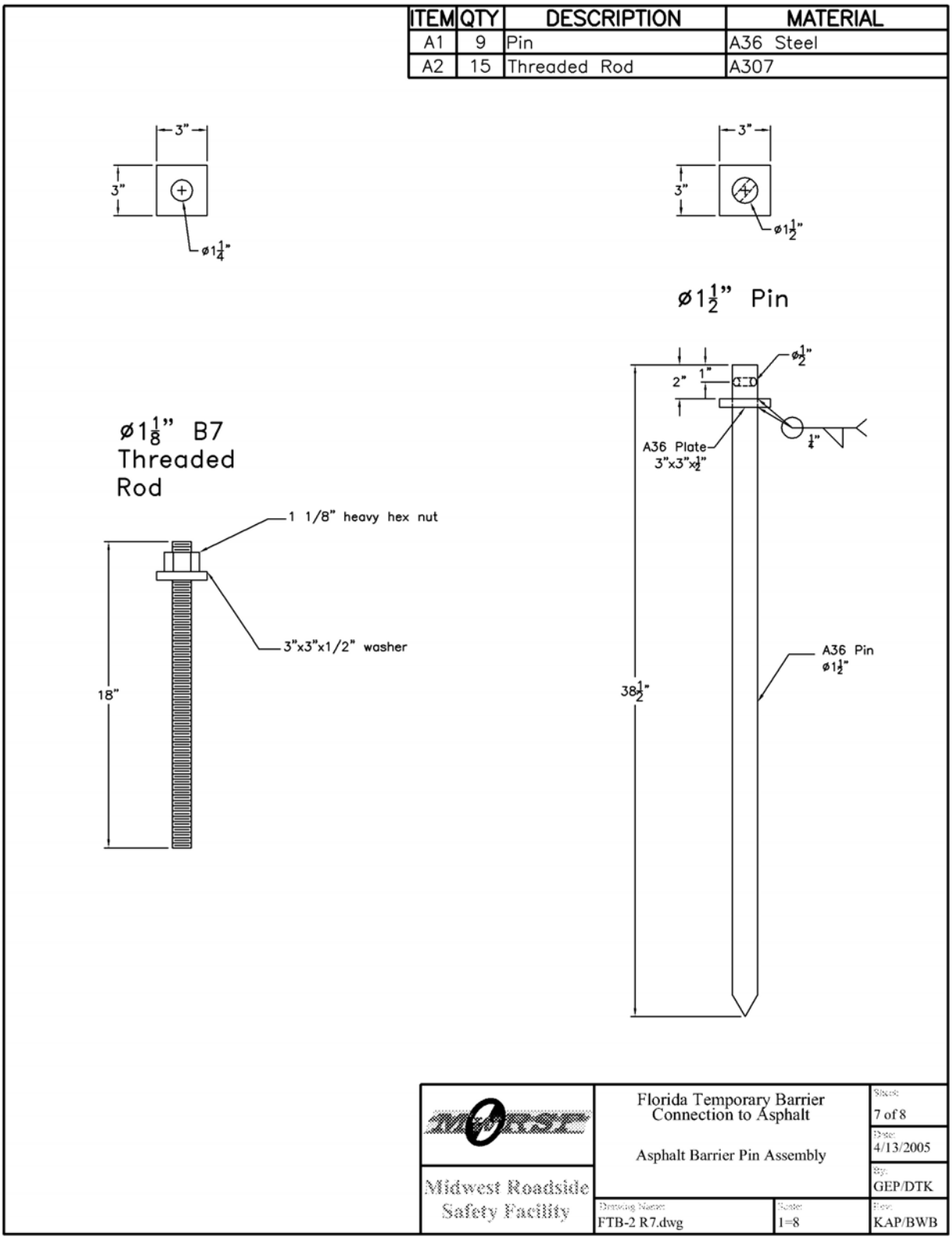

Figure E-7. Free Standing to Rigid Barrier Transition Design Details

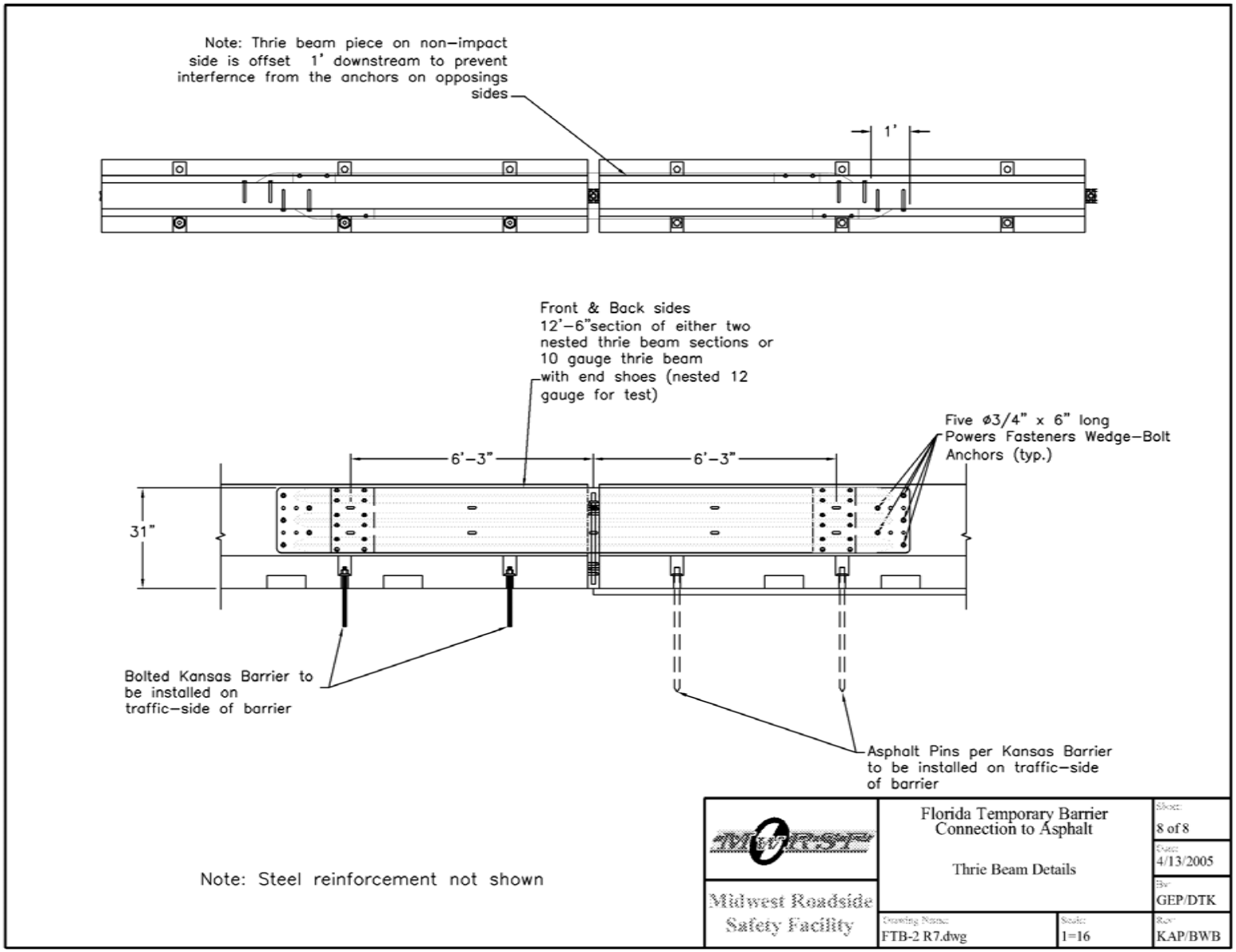

Figure E-8. Free Standing to Rigid Barrier Transition Design Details

APPENDIX F - Test Summary Sheet in English Units, Test No. FTB-2

Figure F-1. Summary of Test Results and Sequential Photographs, Test FTB-2..... 127

0.000 sec | 0.058 sec | 0.266 sec | 0.458 sec | 0.778 sec

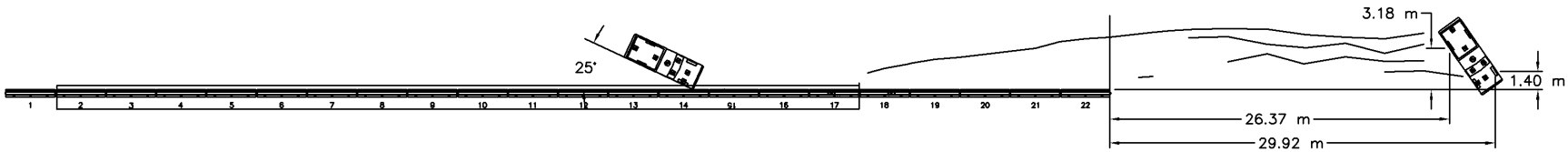

- Test Number FTB-2 (3-21)
- Date 4/20/05
- Test Article ..... F-shape PCB Approach Transition
- Total Length..... 204.5 ft
- Overall Height..... 32 in.
- Barrier Elements ..... 22 Kansas F-shape PCB's
- Joint Connections..... 1.25-i.n diameter by 28-in. long A36 steel pin with a 2.5x4x0.5-in. plate
- Tie-Down Anchors..... Three 1.5-in. dia. x 38.5-in. long A36 steel pins on the traffic side face only
- Soil Type..... Grading B - AASHTO M 147-65
- Vehicle Model..... 1998 GMC C2500
  - Curb..... 4.394 lbs
  - Test Inertial ..... 4,475 lbs
  - Gross Static ..... 4,475 lbs
- Vehicle Speed
  - Impact..... 63.8 mph
  - Exit ..... NA
- Vehicle Angle
  - Impact (trajectory) ..... 26.1 deg
  - Exit (trajectory) 9.8
- Vehicle Stability ..... Satisfactory
- Vehicle Snagging..... Minor
- Occupant Ridedown Deceleration (10 msec avg.)
  - Longitudinal ..... 7.25 g's < 20 g's
  - Lateral (not req.)..... 12.66 g's < 20 g's
- Occupant Impact Velocity
  - Longitudinal ..... 16.54 ft/s < 39.4 ft/s
  - Lateral (not req.)..... 18.67 ft/s < 39.4 ft/s
- THIV (not req.)..... 26.84 ft/s
- PHD (not req.) ..... 15.32 g's
- Vehicle Damage ..... Moderate
  - TAD 1-RFQ-4
  - SAE 1RFAW4
  - OCDI RF001100000
- Vehicle Stopping Distance..... 204.7 ft downstream of impact 4.6 ft from traffic side face
- Test Article Damage..... Moderate
- Maximum Deflection
  - Permanent Set ..... 5.2 in.
  - Dynamic ..... 18.4 in. (top of barrier)
- Working Width..... 26.3 in.

Figure F-1. Summary of Test Results and Sequential Photographs, Test FTB-2

APPENDIX G - Occupant Compartment Deformation, Test No. FTB-2

Figure G-1. Occupant Compartment Deformation, Test No. FTB-2..... 129
Figure G-2. OCDI, Test No. FTB-2..... 130

VEHICLE PRE/POST CRUSH INFO
Set-2

TEST: FTB-2
VEHICLE: 2000p

Note: If impact is on driver side need to enter negative number for Y

POINT	X	Y	Z	X'	Y'	Z'	DEL X	DEL Y	DEL Z
1	50.5	36.25	2.5	47.75	36	1.5	-2.75	-0.25	-1
2	51.25	31.75	3.25	47.25	30.75	1.25	-4	-1	-2
3	51	26.75	3	48.25	26	2	-2.75	-0.75	-1
4	49.75	21	2.5	49.5	21	2.75	-0.25	0	0.25
5	45.75	12.75	0	45.4	12.75	0	-0.35	0	0
6	44.75	37.75	6.75	44	36.5	7	-0.75	-1.25	0.25
7	45.5	32	7.25	44.75	30.75	8	-0.75	-1.25	0.75
8	45.75	27	7.25	45	25.5	8	-0.75	-1.5	0.75
9	45	21.25	7.25	45.5	20	7.5	0.5	-1.25	0.25
10	42.5	13	1.75	42.25	12.75	1.5	-0.25	-0.25	-0.25
11	40	37.5	8	40	36.25	9.75	0	-1.25	1.75
12	39.5	32.75	7.75	39.25	31.25	8.5	-0.25	-1.5	0.75
13	39.5	26.5	8	39.25	25.25	8.5	-0.25	-1.25	0.5
14	39.5	21	7.75	39	19.75	8	-0.5	-1.25	0.25
15	37.5	12.5	2.25	37.25	12.25	2	-0.25	-0.25	-0.25
16	35.25	37.5	8.25	35	36	9.5	-0.25	-1.5	1.25
17	35	33	8	34.5	31.5	8.5	-0.5	-1.5	0.5
18	35.25	26.75	8	35	25.5	8	-0.25	-1.25	0
19	35	20.5	8	34.75	19.5	8	-0.25	-1	0
20	33.75	13	2.75	33.5	12.75	2.5	-0.25	-0.25	-0.25
21	30	37.75	8.5	30	36.25	9.5	0	-1.5	1
22	29.25	32.5	8	29	31.5	8.75	-0.25	-1	0.75
23	29.25	25.5	8	29.25	24.5	8.25	0	-1	0.25
24	30	20	8	29.75	19	8	-0.25	-1	0
25	29	12.25	3	28.75	12	3.75	-0.25	-0.25	0.75
26	20.5	36.25	8.25	20.25	35.5	8.75	-0.25	-0.75	0.5
27	20.5	23.75	8	20	23	8	-0.5	-0.75	0
28	20	12	4.5	19.5	11.75	4.5	-0.5	-0.25	0
29									
30									

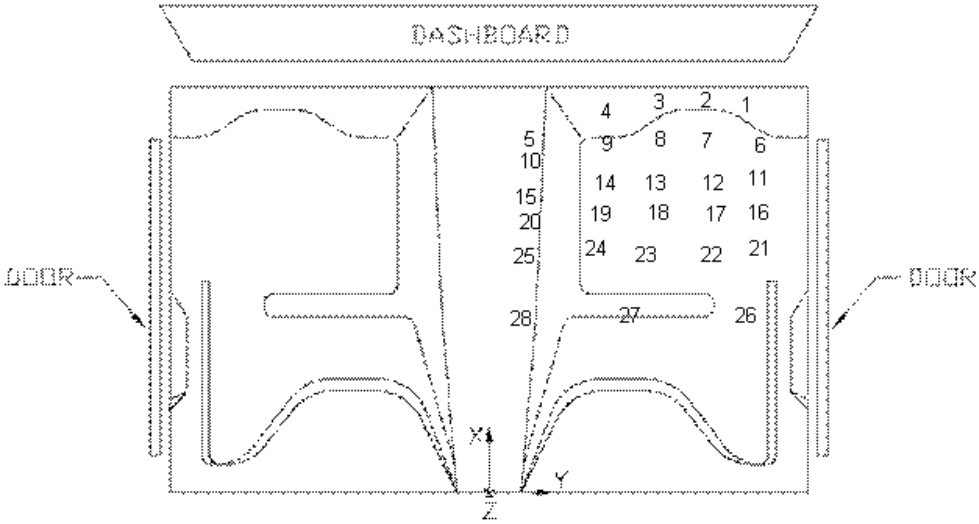

Figure G-1. Occupant Compartment Deformation, Test No. FTB-2

Occupant Compartment Deformation Index (OCDI)

Test No. FTB-2
Vehicle Type: 2000p

OCDI = XXABCDEFGHI

XX = location of occupant compartment deformation

A = distance between the dashboard and a reference point at the rear of the occupant compartment, such as the top of the rear seat or the rear of the cab on a pickup

B = distance between the roof and the floor panel

C = distance between a reference point at the rear of the occupant compartment and the motor panel

D = distance between the lower dashboard and the floor panel

E = interior width

F = distance between the lower edge of right window and the upper edge of left window

G = distance between the lower edge of left window and the upper edge of right window

H= distance between bottom front corner and top rear corner of the passenger side window

I= distance between bottom front corner and top rear corner of the driver side window

Severity Indices

0 - if the reduction is less than 3%
1 - if the reduction is greater than 3% and less than or equal to 10 %
2 - if the reduction is greater than 10% and less than or equal to 20 %
3 - if the reduction is greater than 20% and less than or equal to 30 %
4 - if the reduction is greater than 30% and less than or equal to 40 %

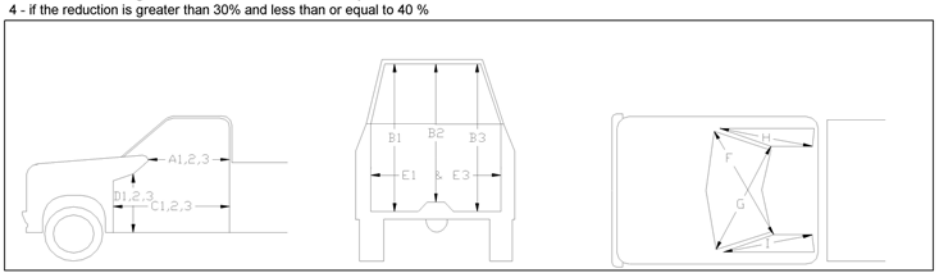

where,
1 = Passenger Side
2 = Middle
3 = Driver Side

Location:

Measurement	Pre-Test (in.)	Post-Test (in.)	Change (in.)	% Difference	Severity Index
A1	39.75	39.75	0.00	0.00	0
A2	40.25	40.00	-0.25	-0.62	0
A3	40.00	39.75	-0.25	-0.63	0
B1	46.00	45.50	-0.50	-1.09	0
B2	42.00	41.75	-0.25	-0.60	0
B3	45.50	45.75	0.25	0.55	0
C1	57.75	57.75	0.00	0.00	0
C2	52.50	52.00	-0.50	-0.95	0
C3	57.00	53.75	-3.25	-5.70	1
D1	16.25	16.75	0.50	3.08	1
D2	14.00	14.00	0.00	0.00	0
D3	18.75	18.75	0.00	0.00	0
E1	62.50	61.50	-1.00	-1.60	0
E3	63.50	63.50	0.00	0.00	0
F	56.75	56.75	0.00	0.00	0
G	57.00	57.00	0.00	0.00	0
H	41.50	41.25	-0.25	-0.60	0
I	41.00	41.00	0.00	0.00	0

Note: Maximum sevrity index for each variable (A-I) is used for determination of final OCDI value

XX A B C D E F G H I
Final OCDI: RF 0 0 1 1 0 0 0 0 0

Figure G-2. OCDI, Test No. FTB-2

APPENDIX H - Accelerometer and Rate Gyro Analysis, Test No. FTB-2

Figure H-1. Graph Longitudinal Acceleration, Test No. FTB-2 132
Figure H-2. Graph of Longitudinal Occupant Impact Velocity, Test No. FTB-2 133
Figure H-3. Graph of Longitudinal Occupant Displacement, Test No. FTB-2 134
Figure H-4. Graph of Lateral Acceleration, Test No. FTB-2 135
Figure H-5. Graph of Lateral Occupant Impact Velocity, Test No. FTB-2..... 136
Figure H-6. Graph of Lateral Occupant Displacement, Test No. FTB-2 137

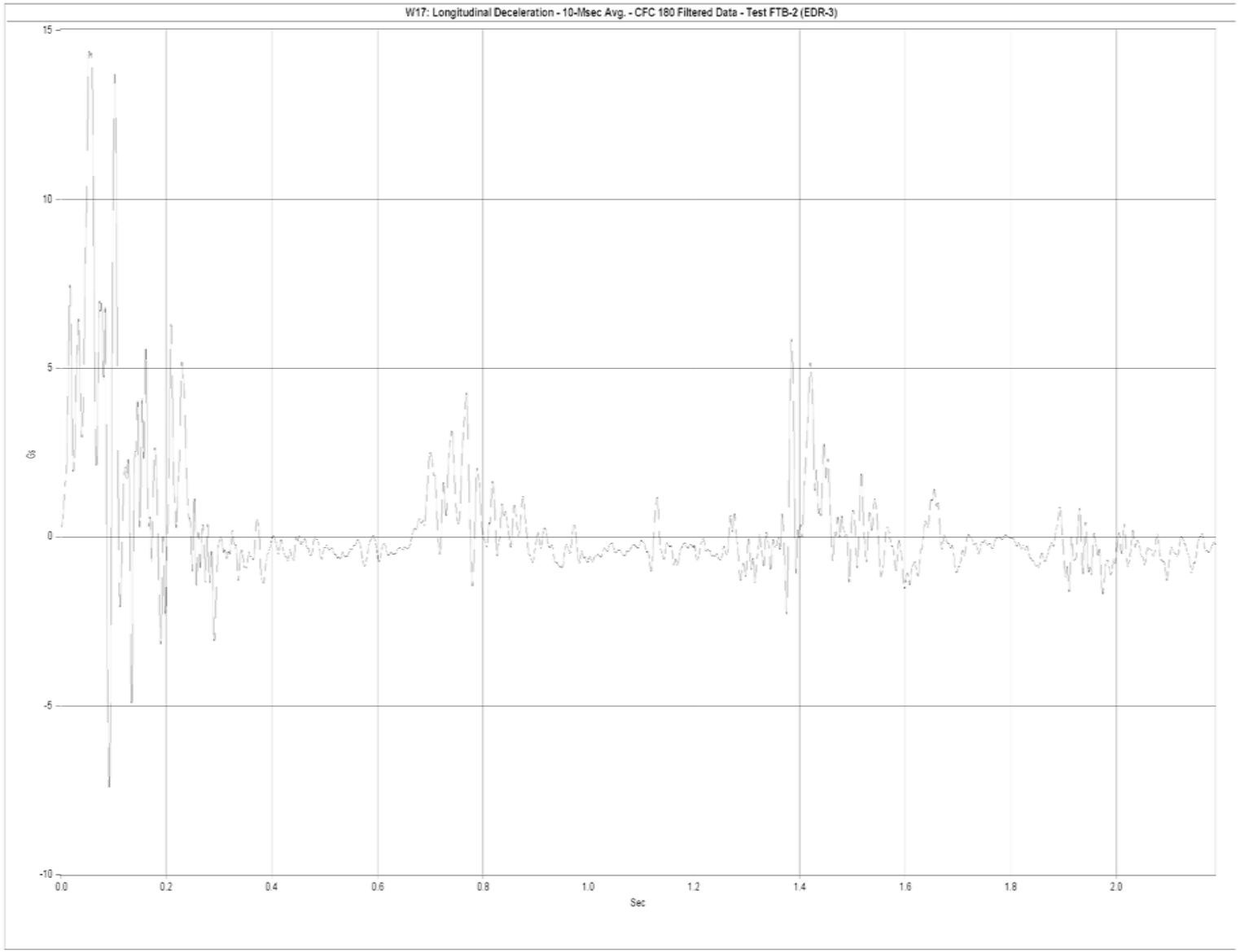

Figure H-1. Graph Longitudinal Acceleration, Test No. FTB-2

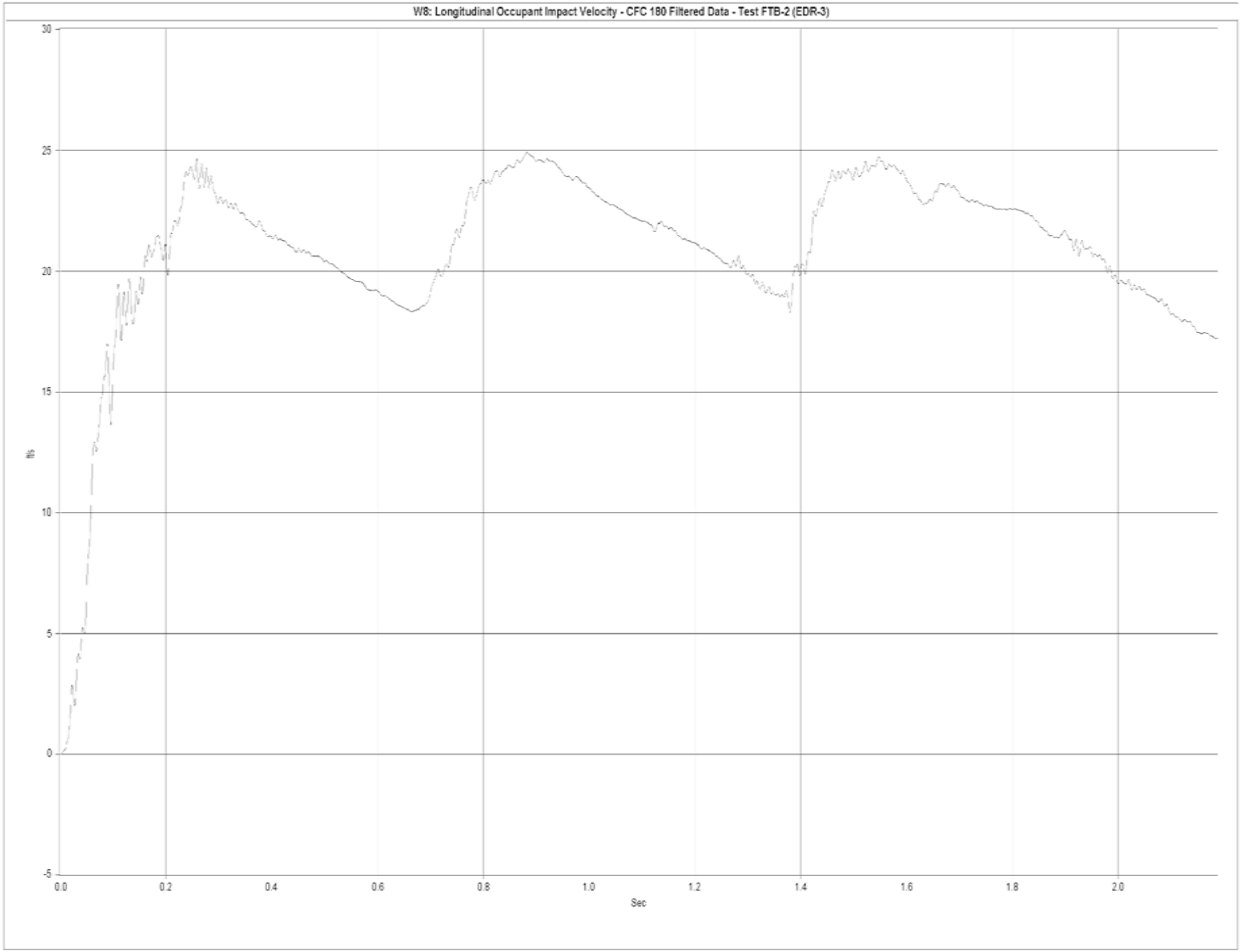

Figure H-2. Graph of Longitudinal Occupant Impact Velocity, Test No. FTB-2

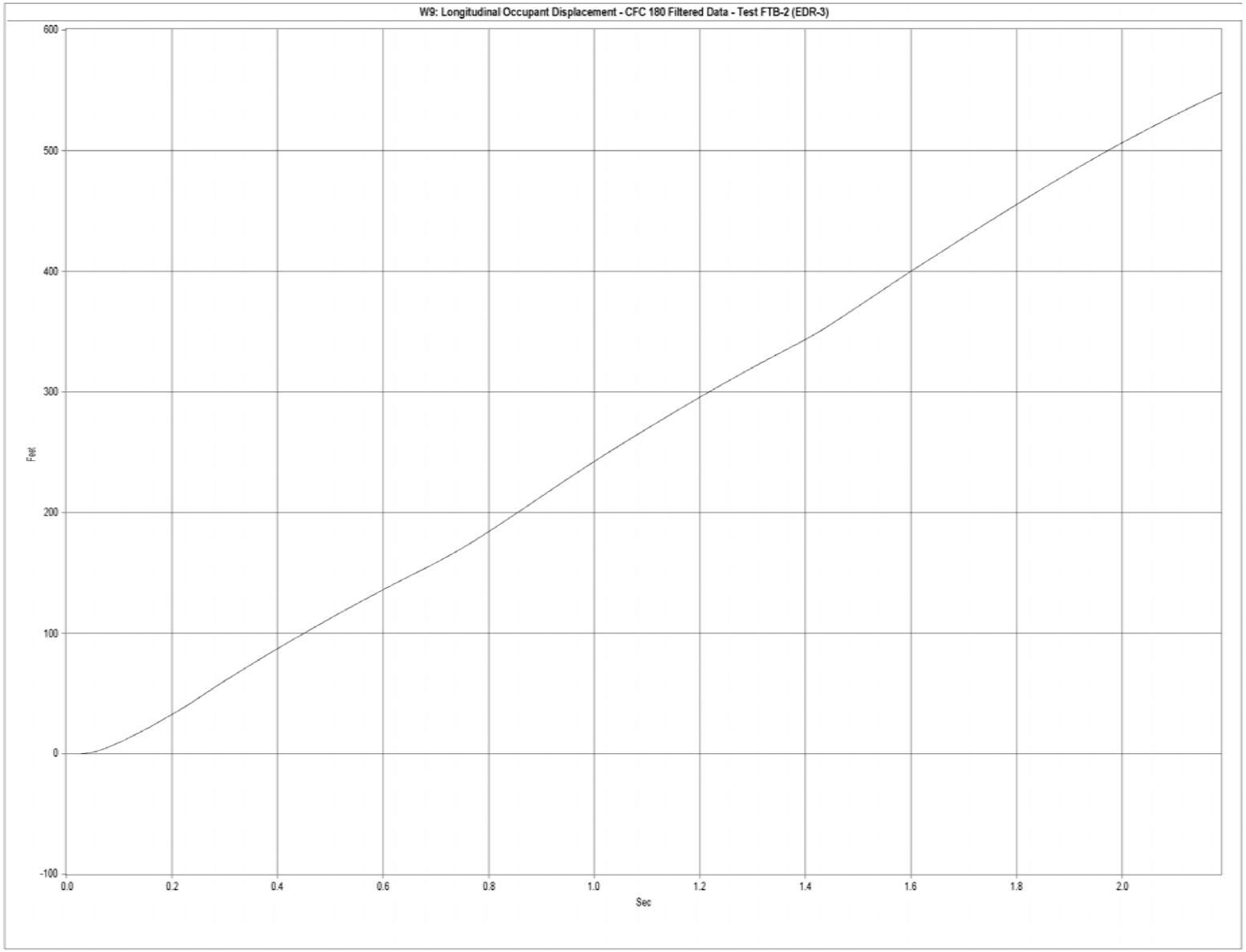

Figure H-3. Graph of Longitudinal Occupant Displacement, Test No. FTB-2

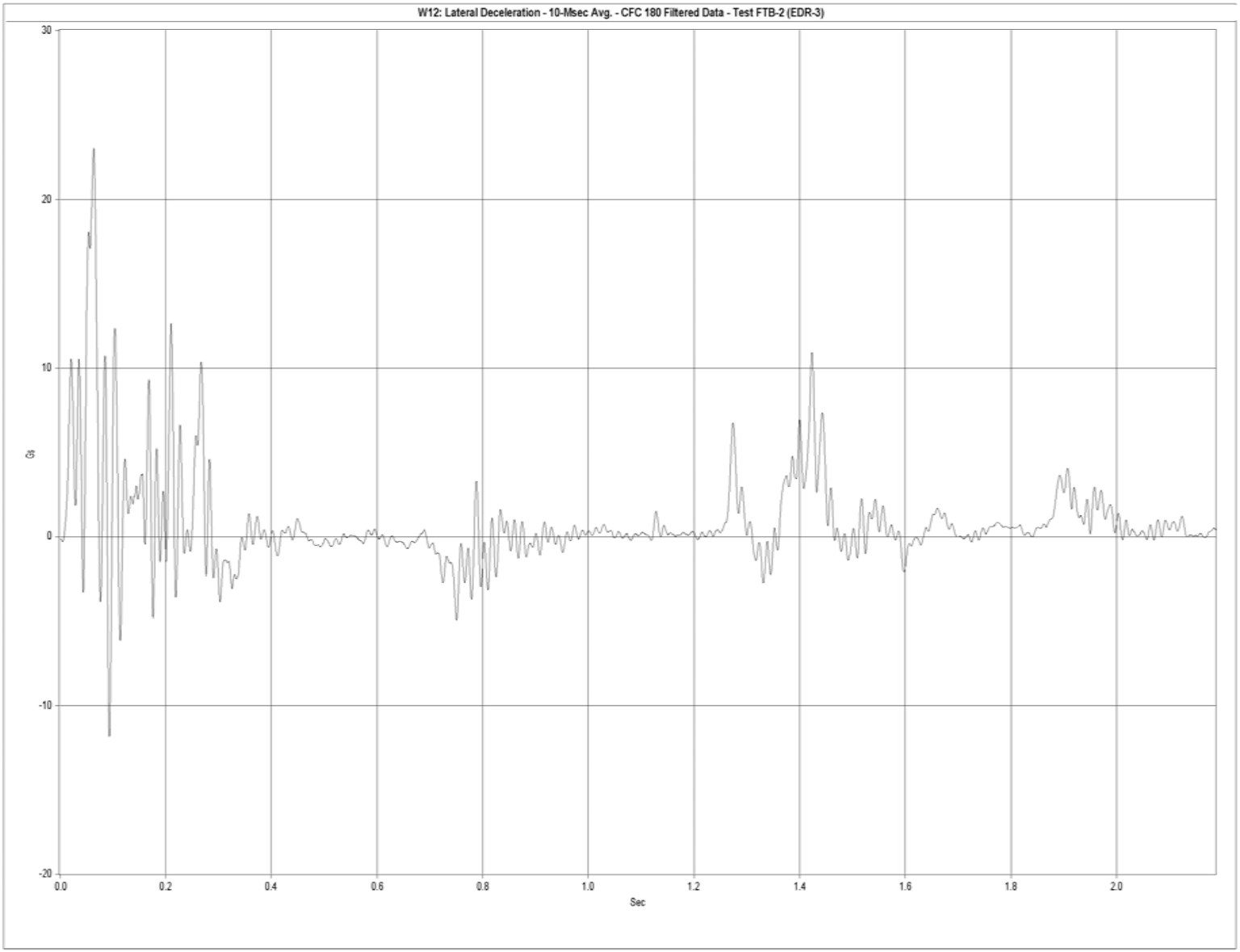

Figure H-4. Graph of Lateral Acceleration, Test No. FTB-2

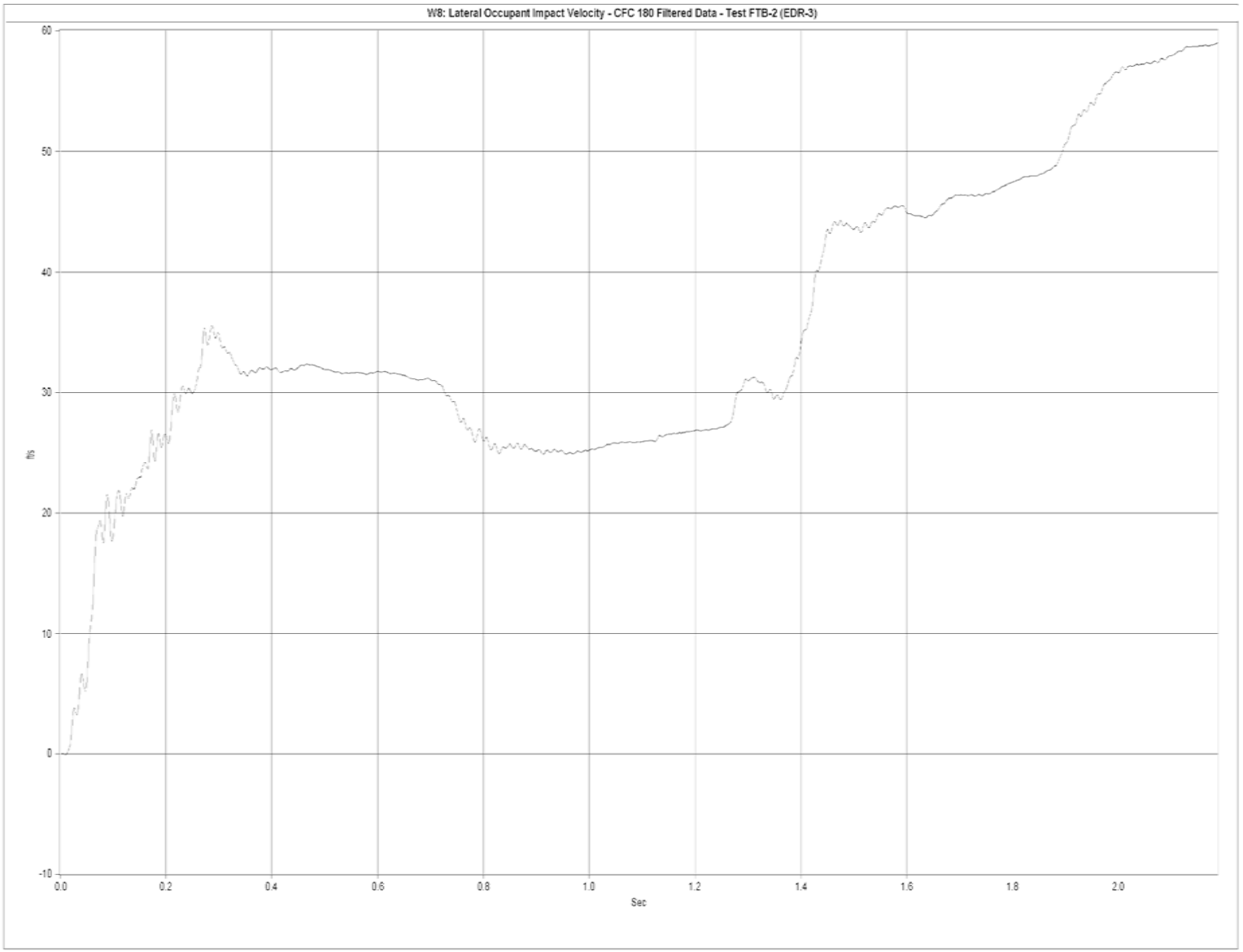

Figure H-5. Graph of Lateral Occupant Impact Velocity, Test No. FTB-2

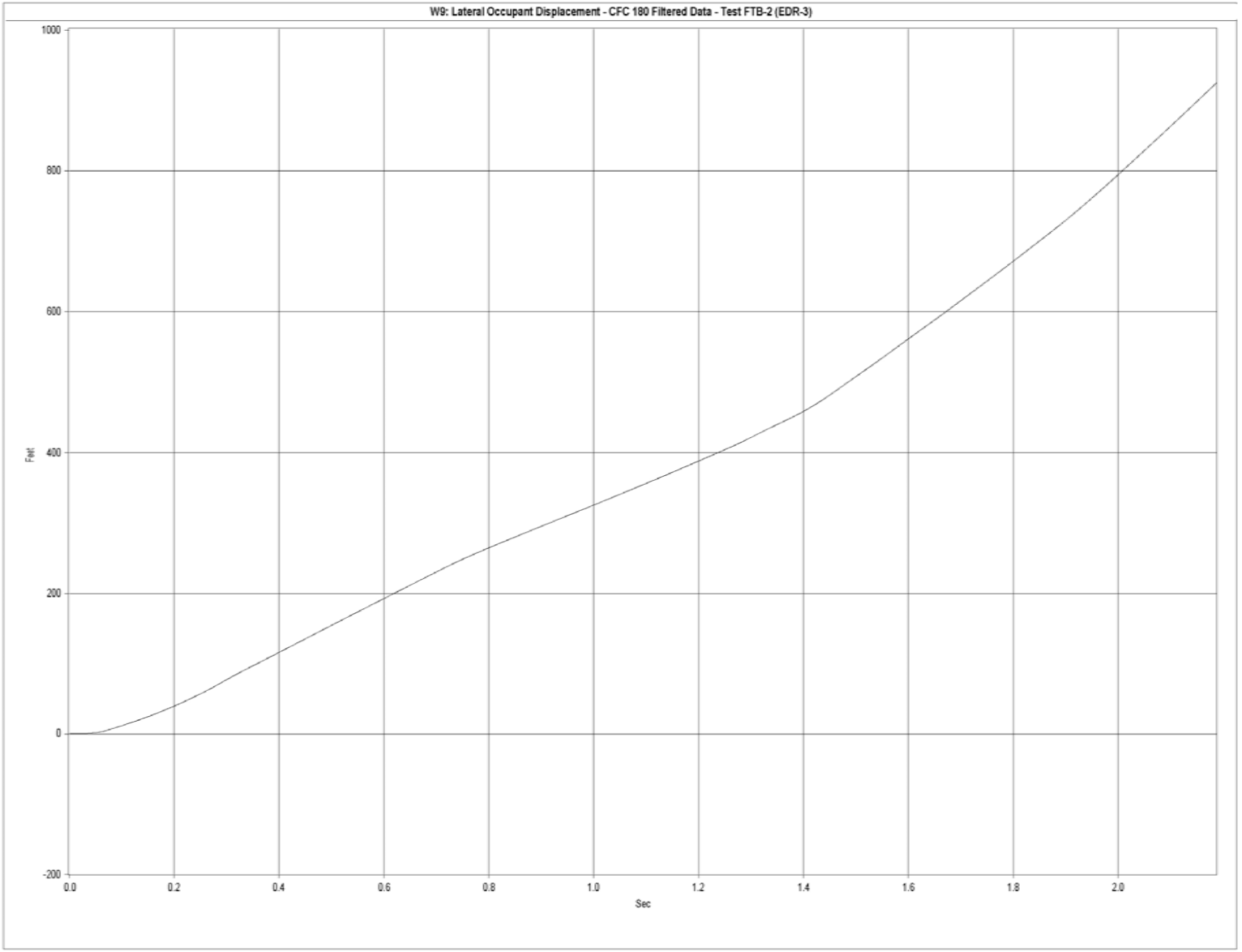

Figure H-6. Graph of Lateral Occupant Displacement, Test No. FTB-2

APPENDIX I - Florida Department of Transportation – F-shape PCB Standards

Figure I-1. Florida Department of Transportation – F-shape PCB Standards 139
Figure I-2. Florida Department of Transportation – F-shape PCB Standards 140
Figure I-3. Florida Department of Transportation – F-shape PCB Standards 141
Figure I-4. Florida Department of Transportation – F-shape PCB Standards 142
Figure I-5. Florida Department of Transportation – F-shape PCB Standards 143
Figure I-6. Florida Department of Transportation – F-shape PCB Standards 144
Figure I-7. Florida Department of Transportation – F-shape PCB Standards 145
Figure I-8. Florida Department of Transportation – F-shape PCB Standards 146
Figure I-9. Florida Department of Transportation – F-shape PCB Standards 147
Figure I-10. Florida Department of Transportation – F-shape PCB Standards 148
Figure I-11. Florida Department of Transportation – F-shape PCB Standards 149
Figure I-12. Florida Department of Transportation – F-shape PCB Standards 150
Figure I-13. Florida Department of Transportation – F-shape PCB Standards 151
Figure I-14. Florida Department of Transportation – F-shape PCB Standards 152

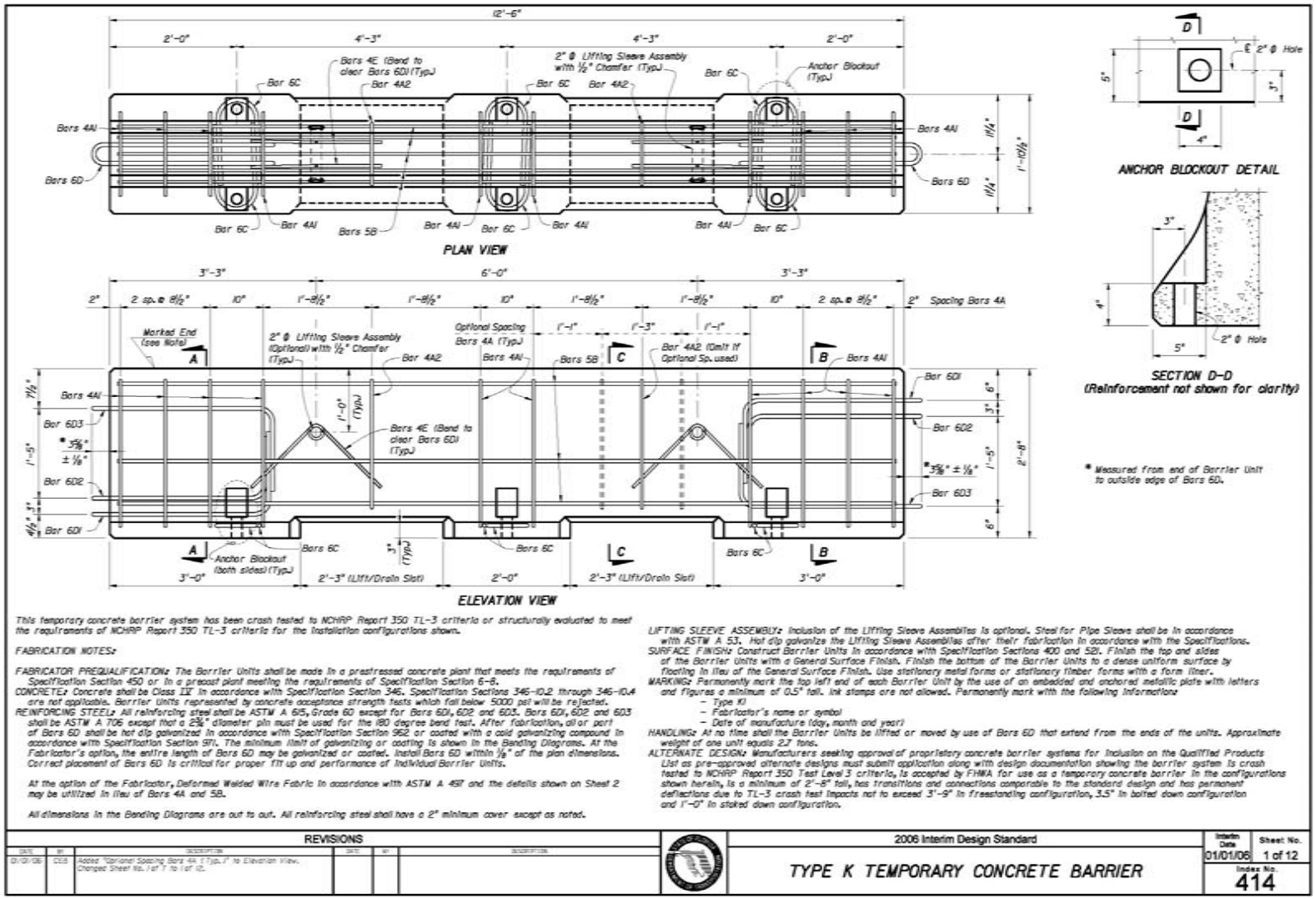

Figure I-1. Florida Department of Transportation – F-shape PCB Standards

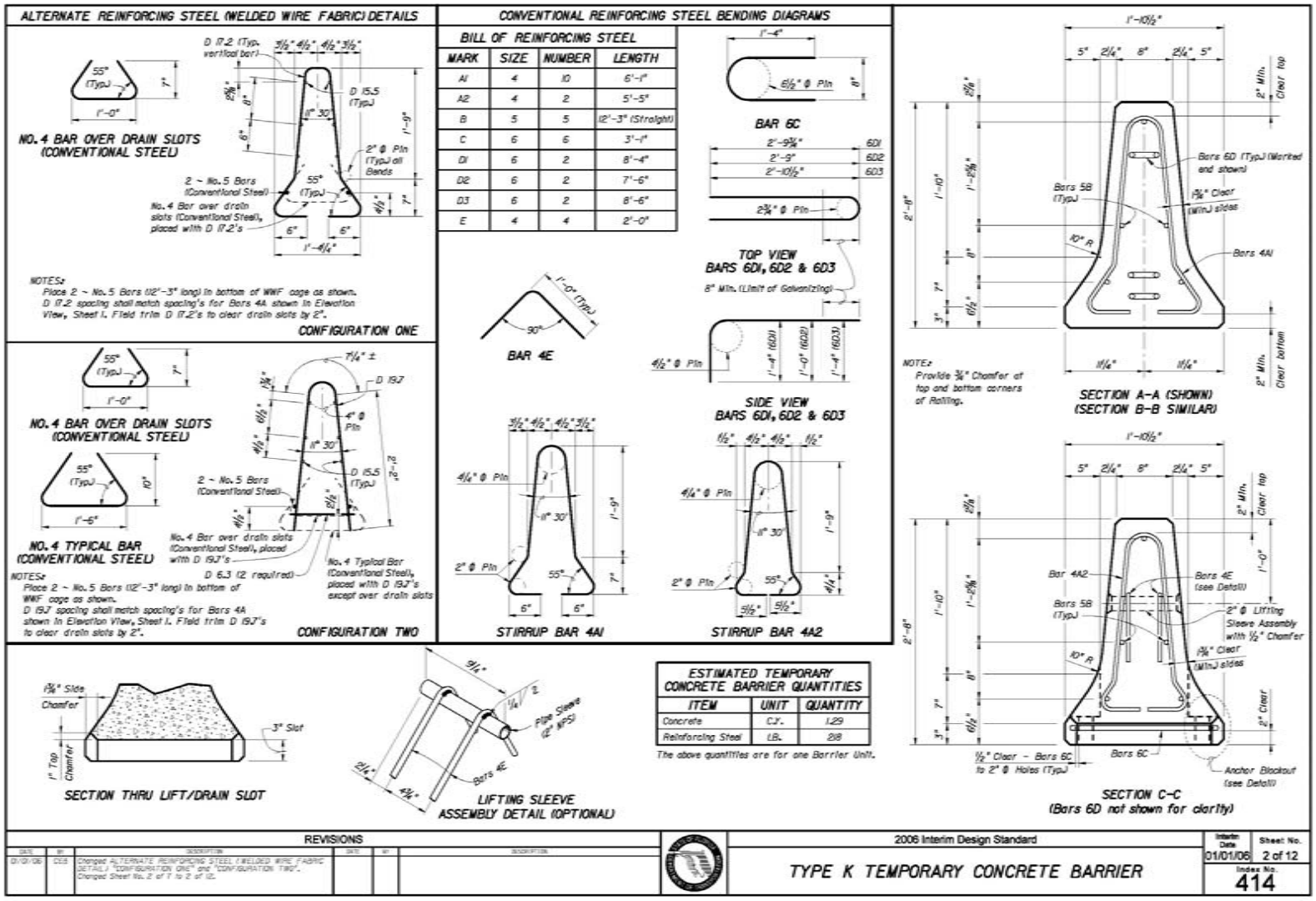

Figure I-2. Florida Department of Transportation – F-shape PCB Standards

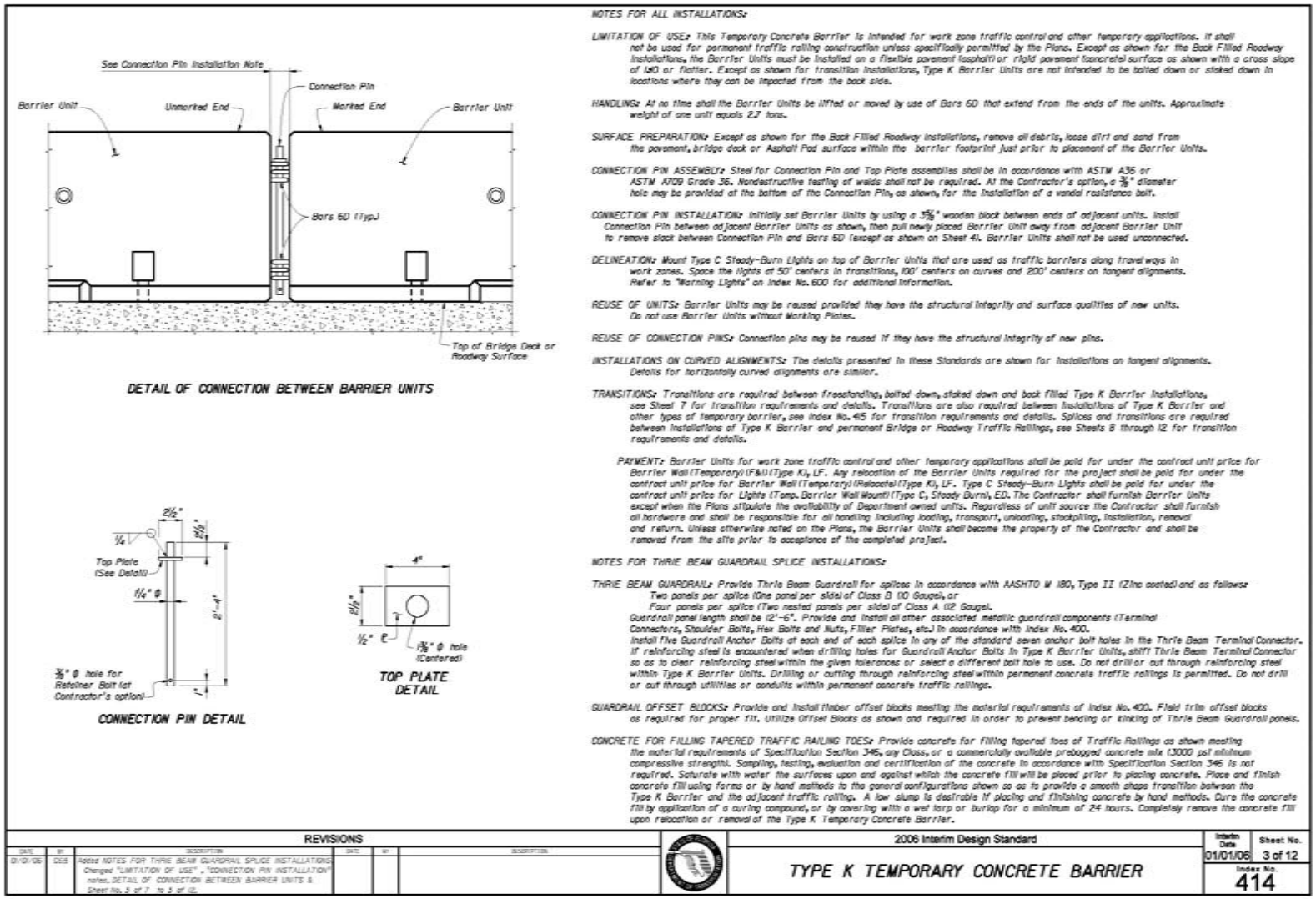

Figure I-3. Florida Department of Transportation – F-shape PCB Standards

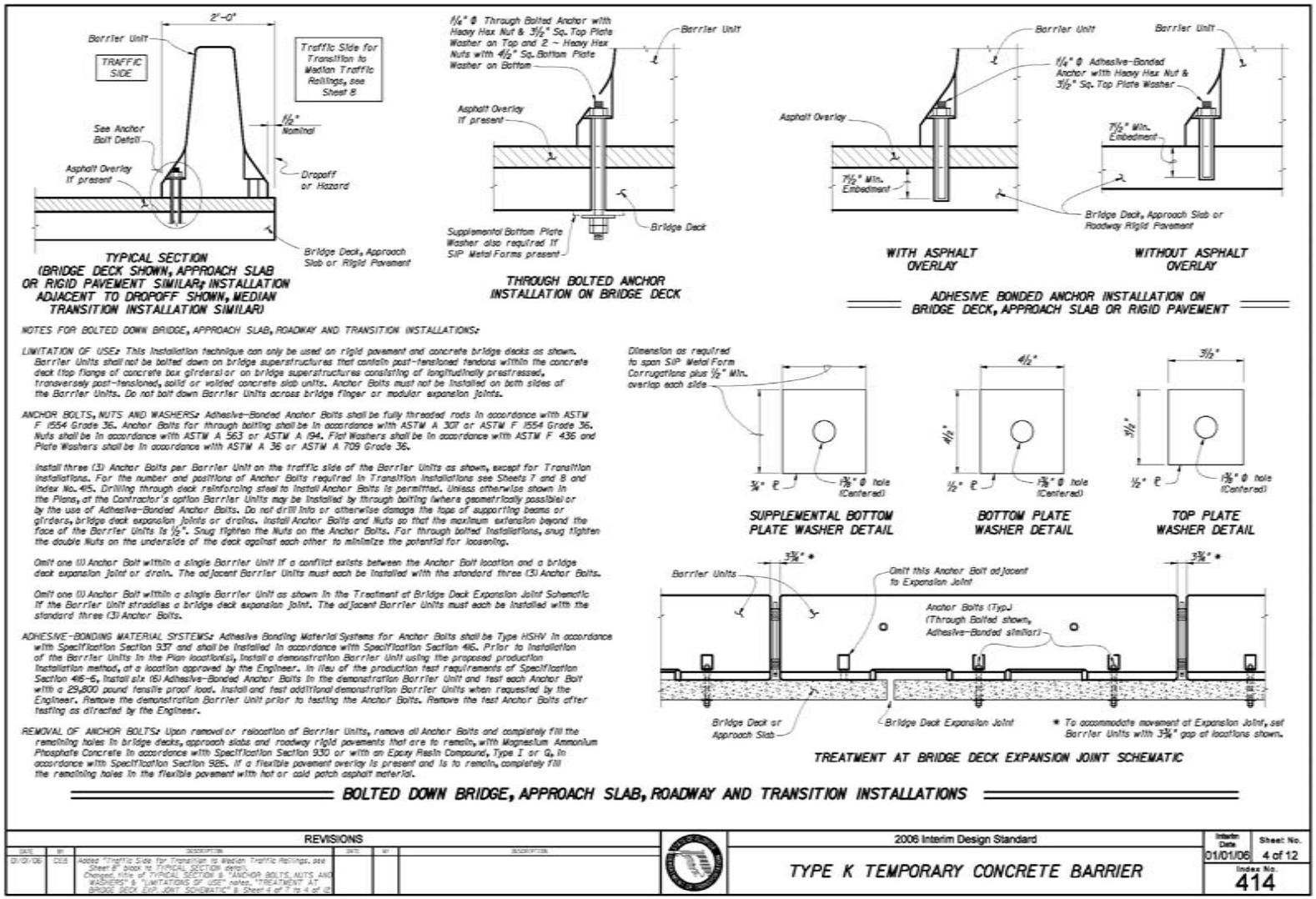

Figure I-4. Florida Department of Transportation – F-shape PCB Standards

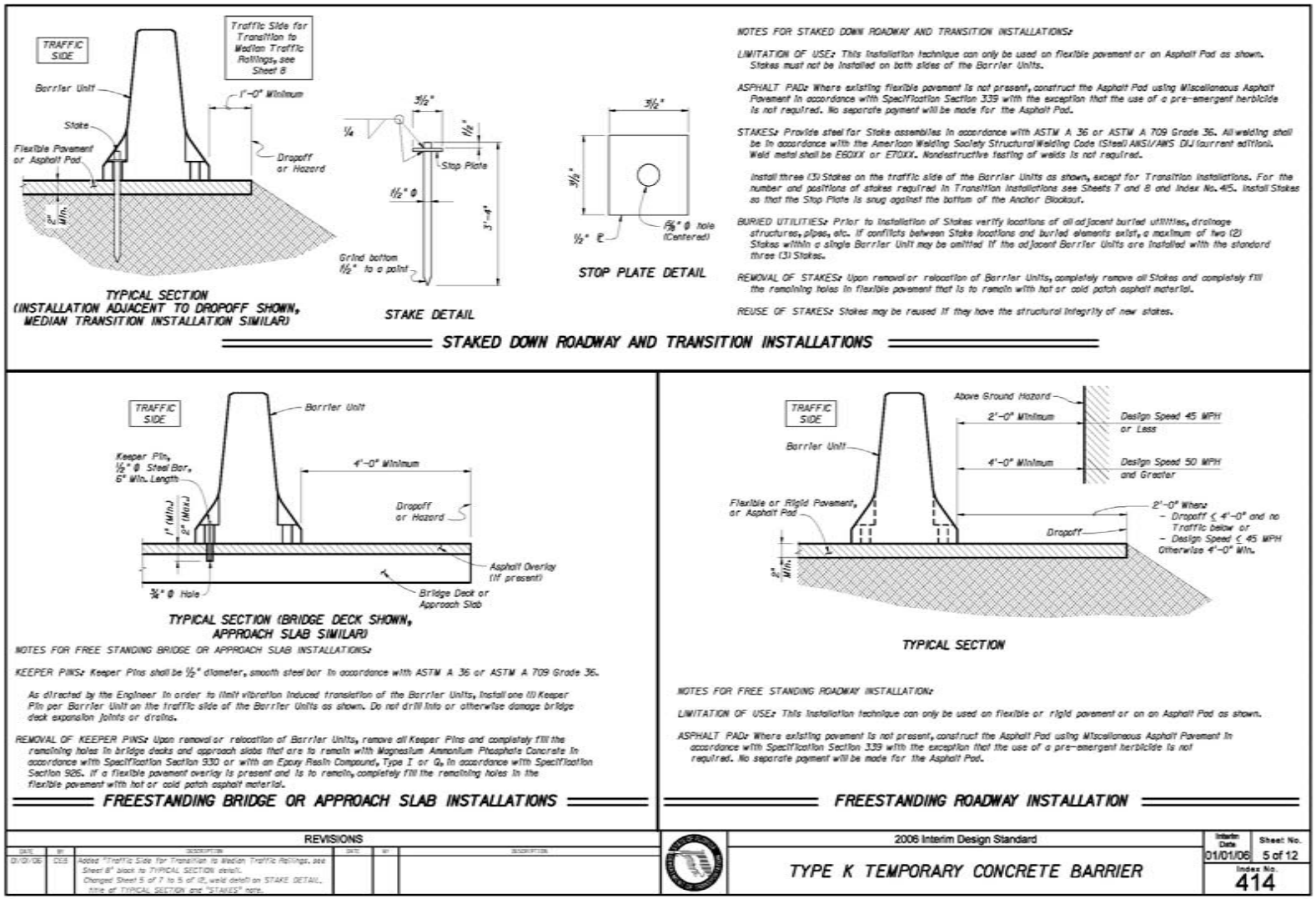

Figure I-5. Florida Department of Transportation – F-shape PCB Standards

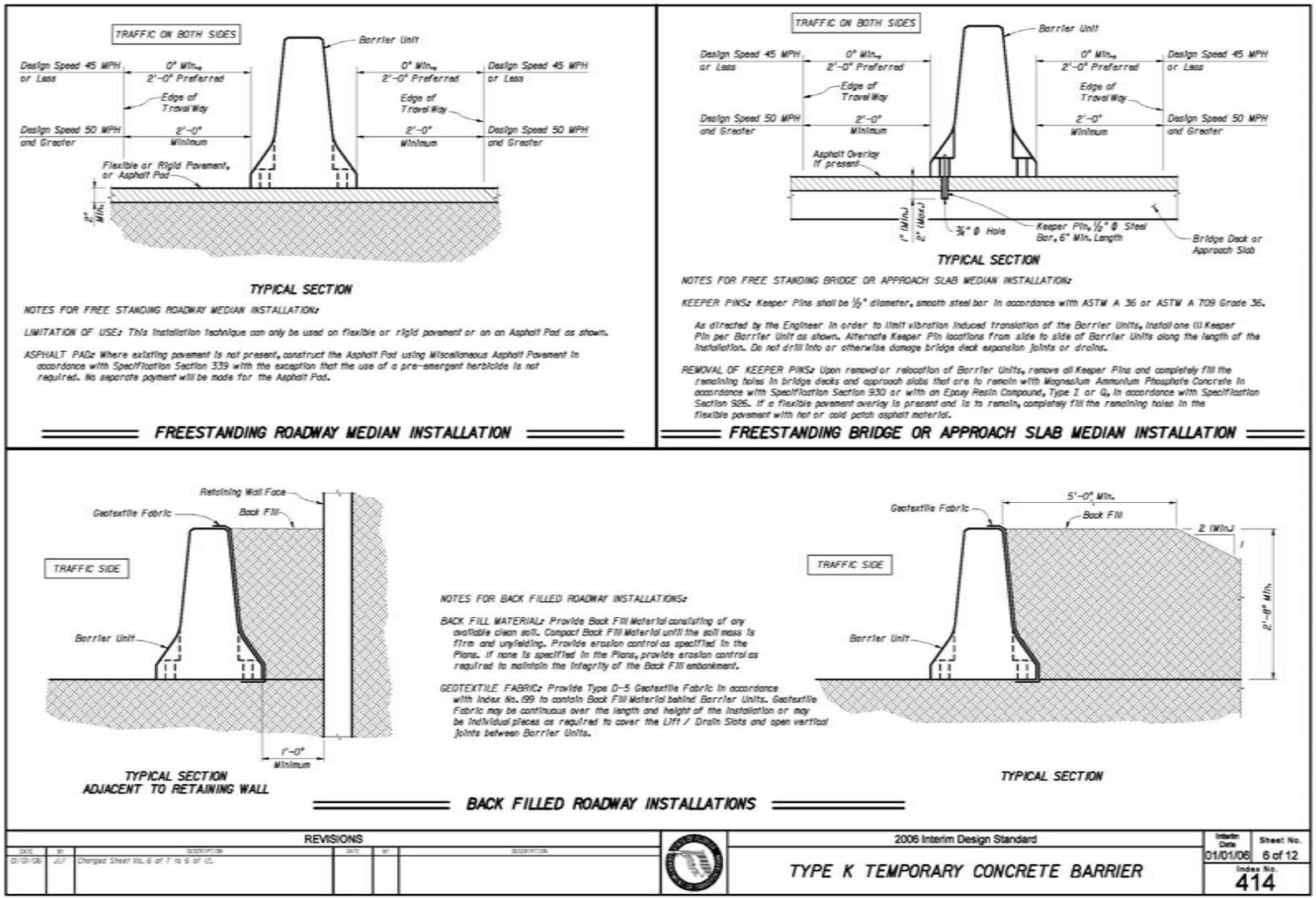

Figure I-6. Florida Department of Transportation – F-shape PCB Standards

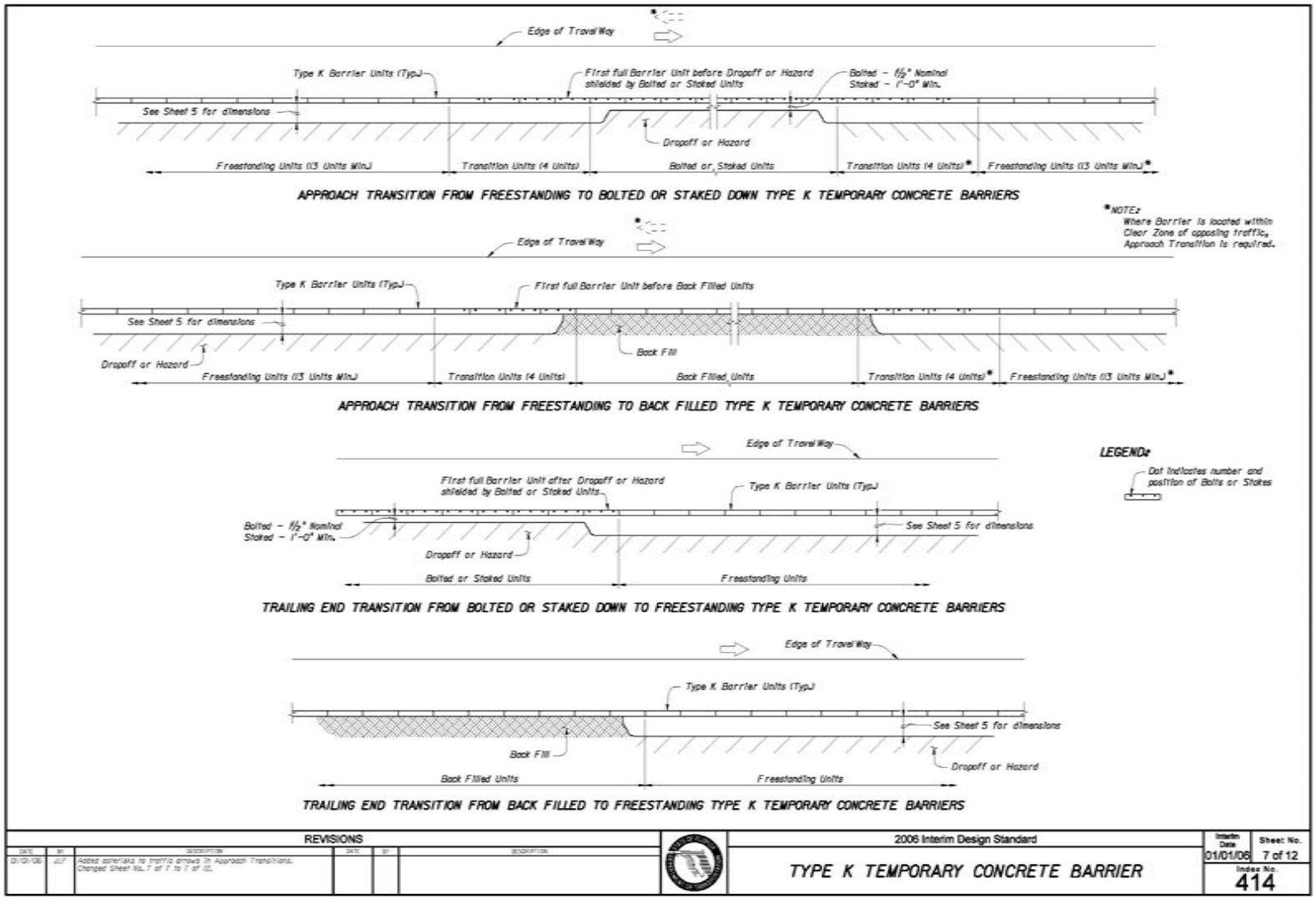

Figure I-7. Florida Department of Transportation – F-shape PCB Standards

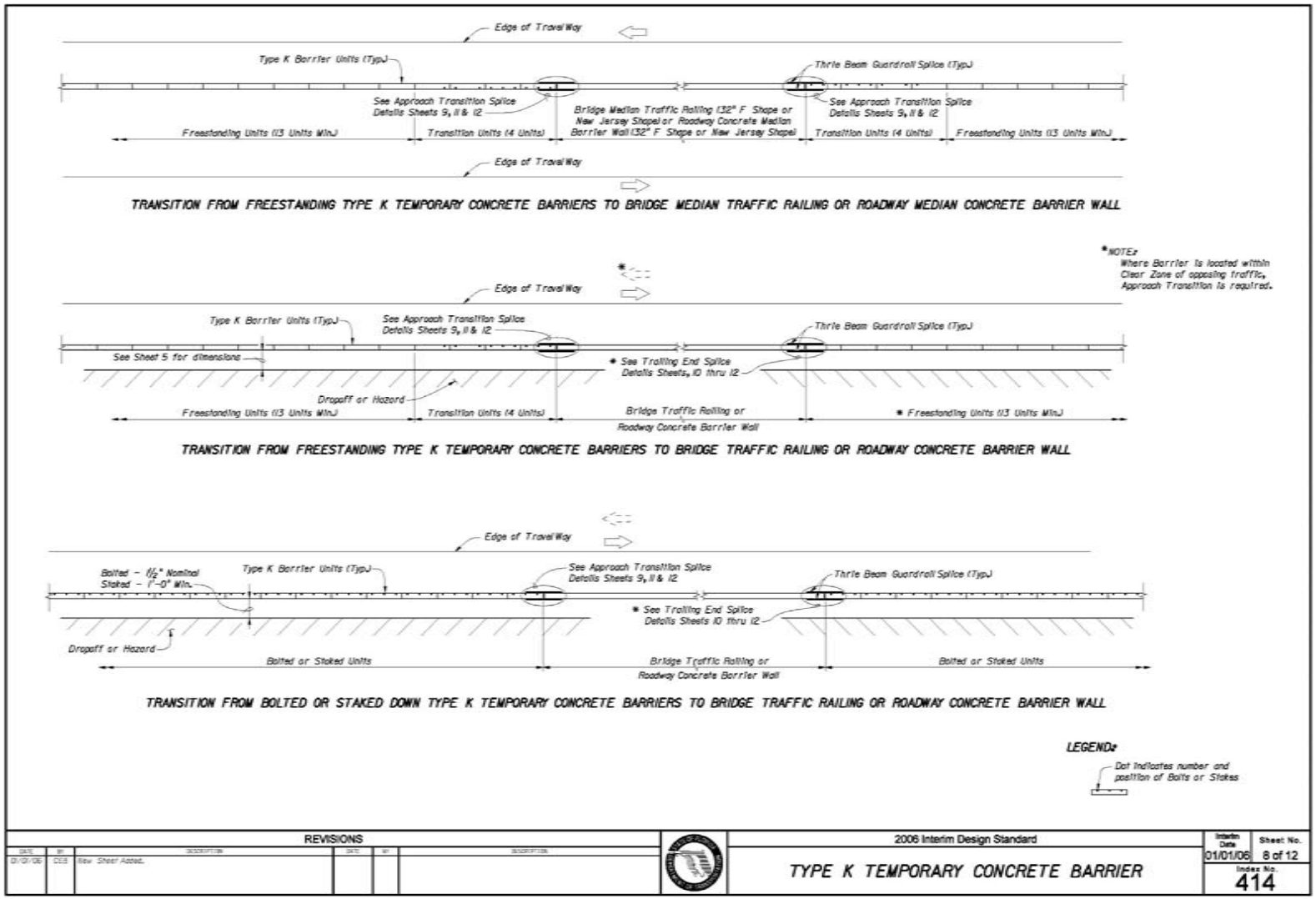

Figure I-8. Florida Department of Transportation – F-shape PCB Standards

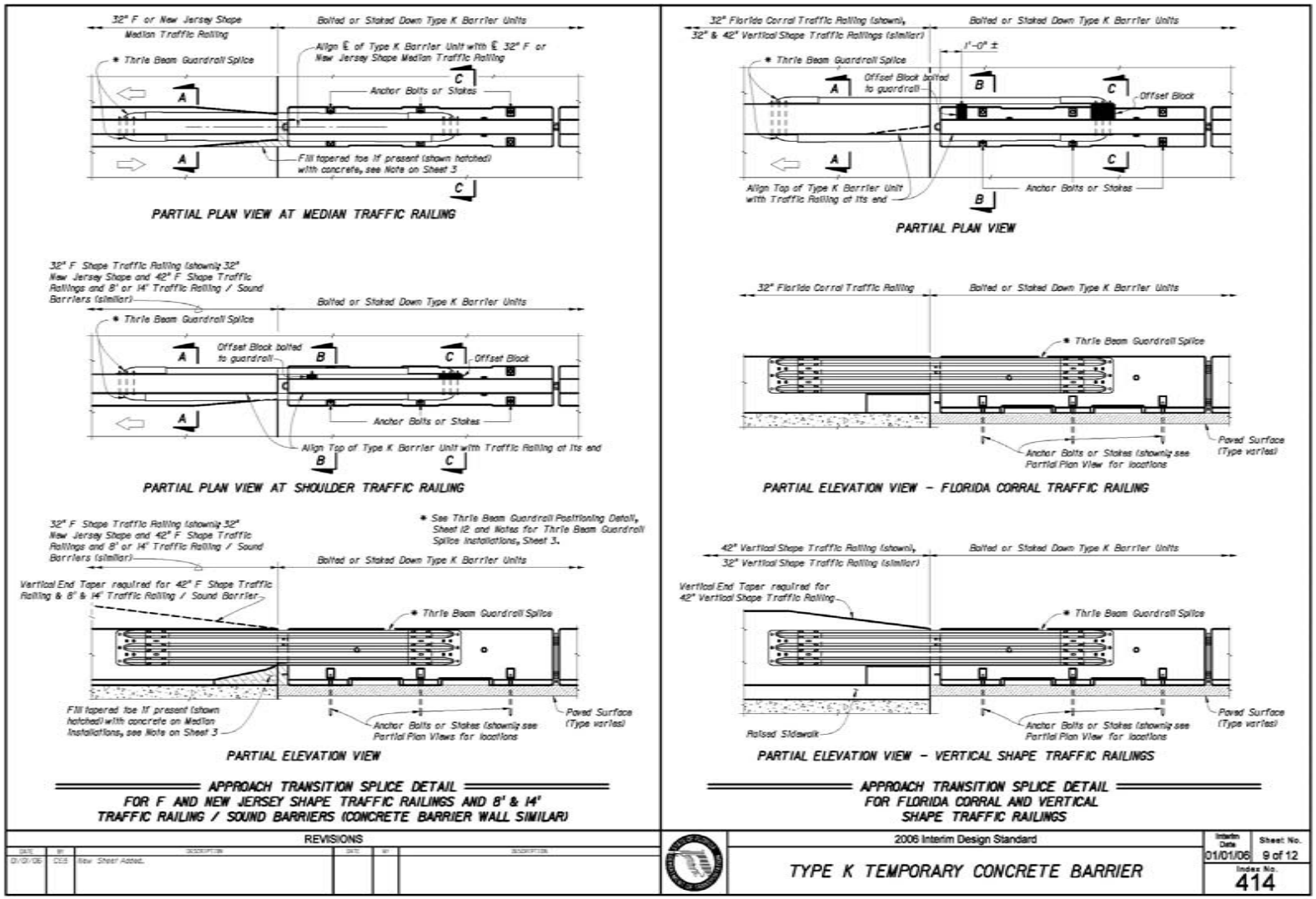

Figure I-9. Florida Department of Transportation – F-shape PCB Standards

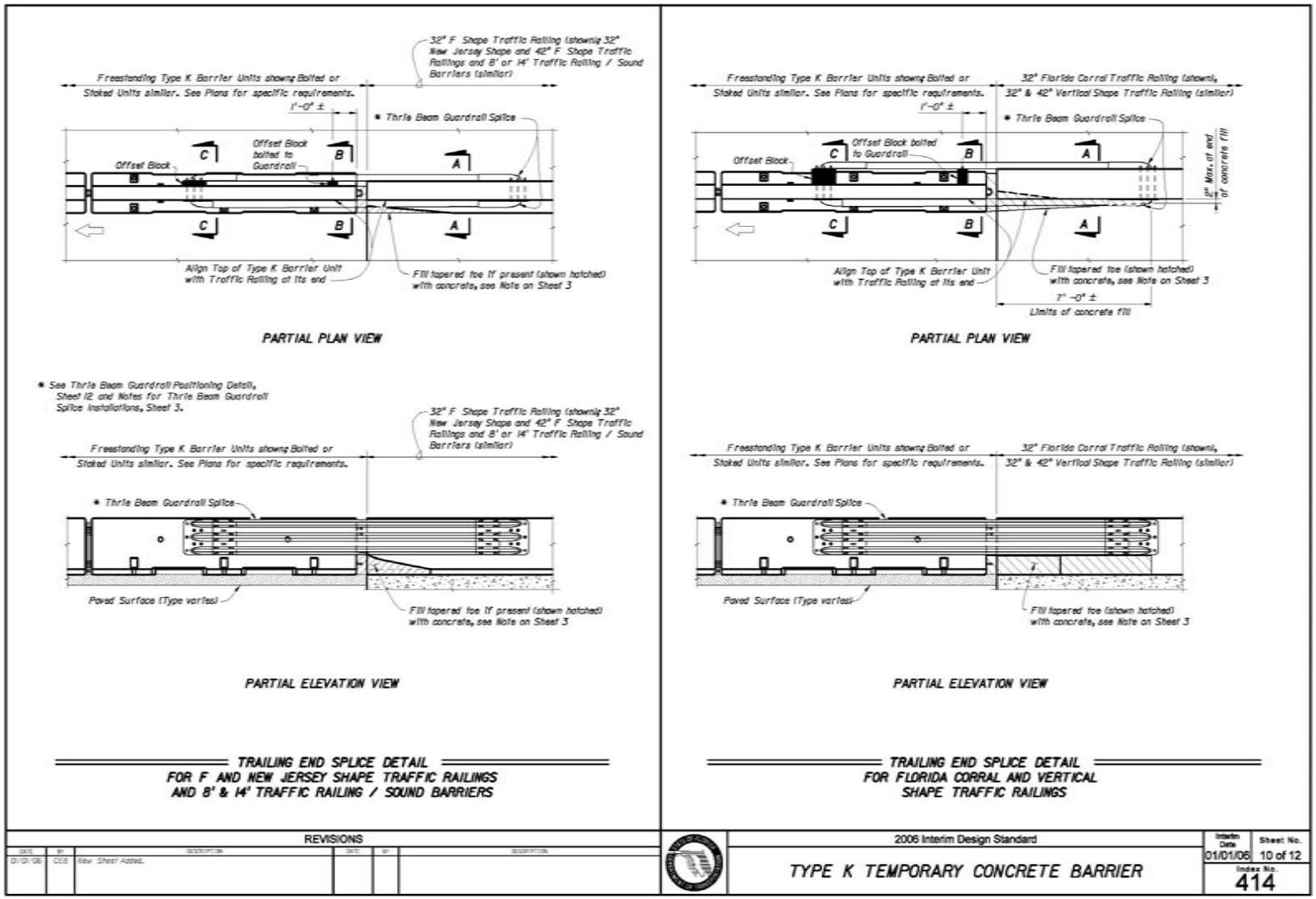

Figure I-10. Florida Department of Transportation – F-shape PCB Standards

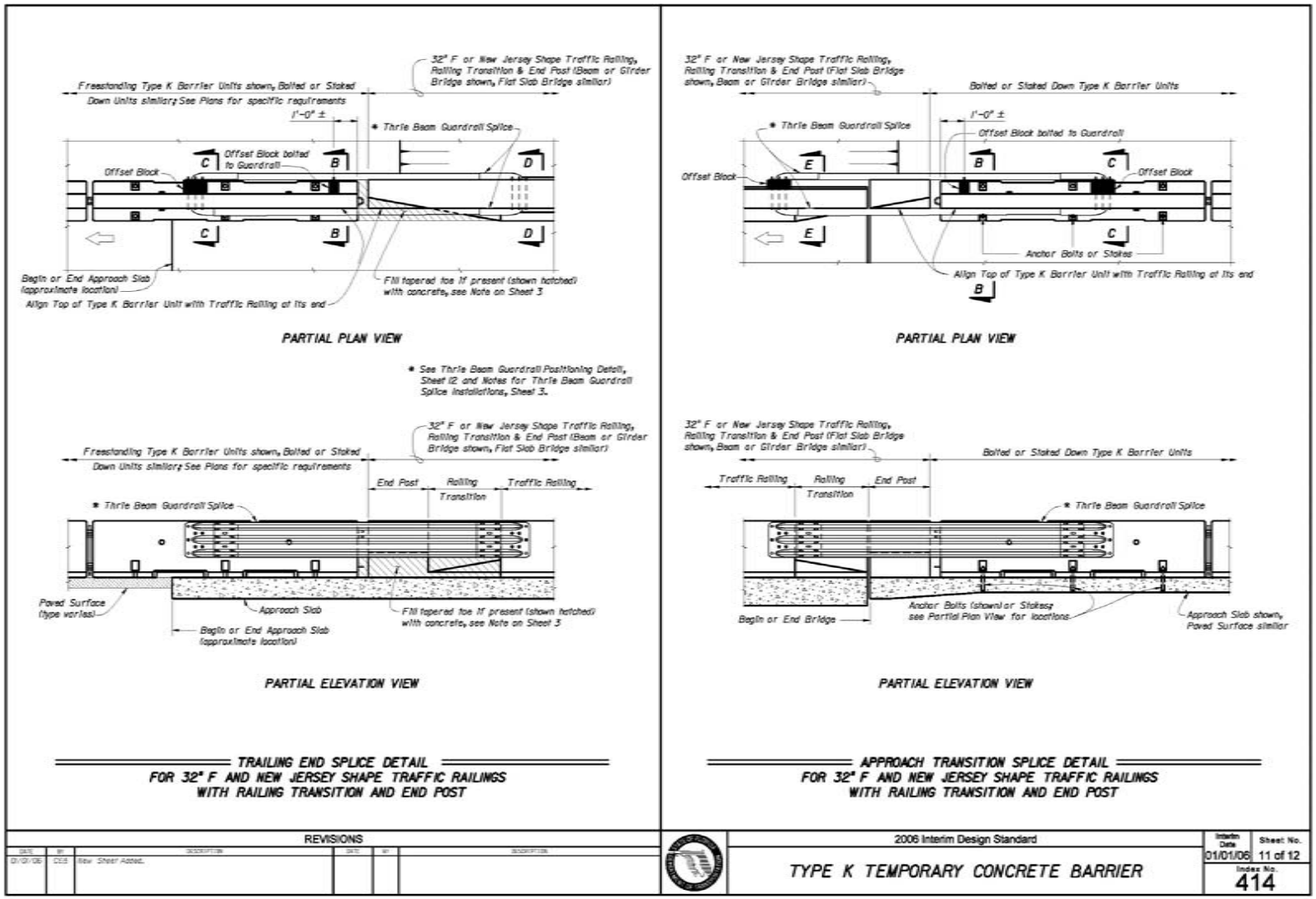

Figure I-11. Florida Department of Transportation – F-shape PCB Standards

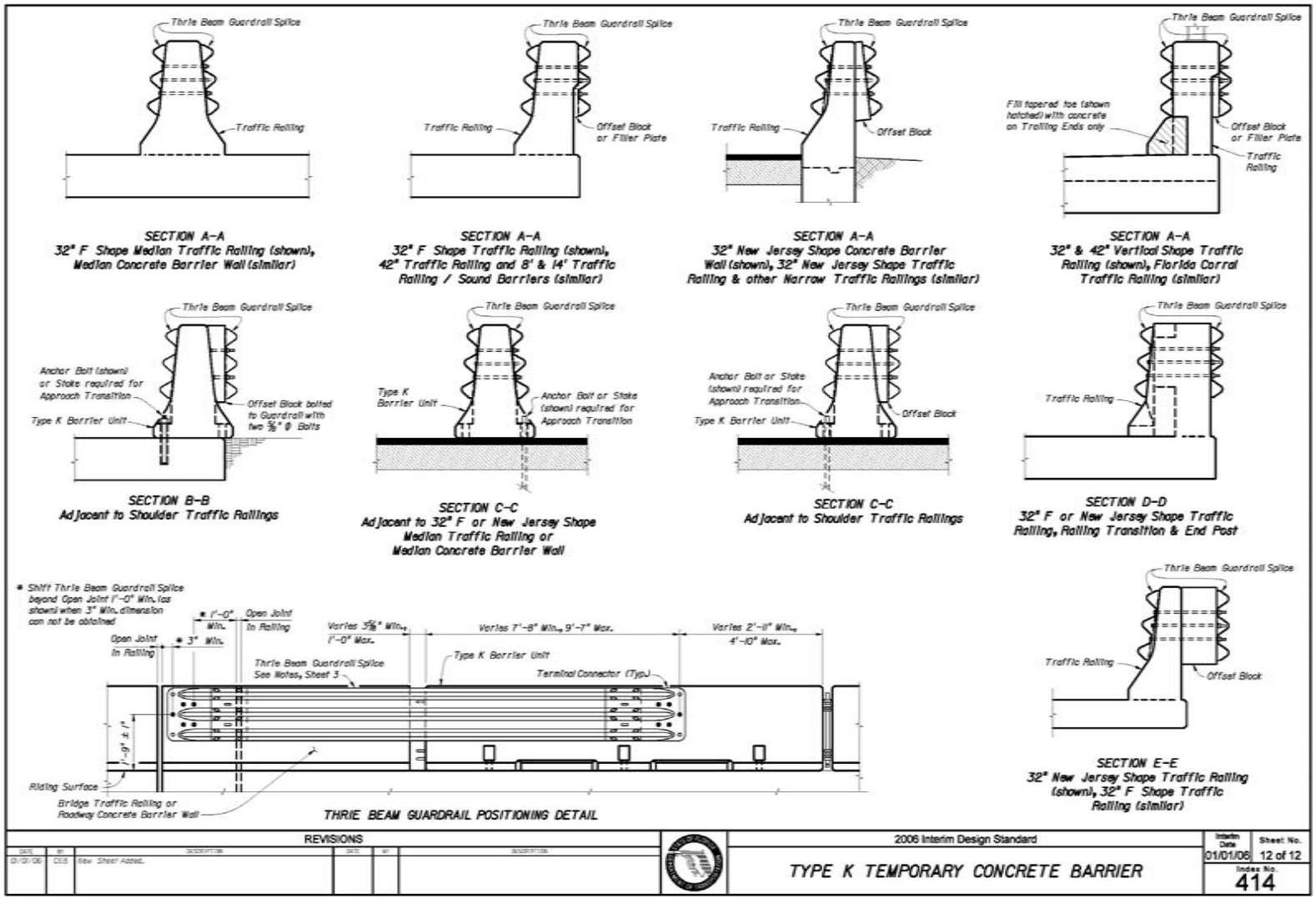

Figure I-12. Florida Department of Transportation – F-shape PCB Standards

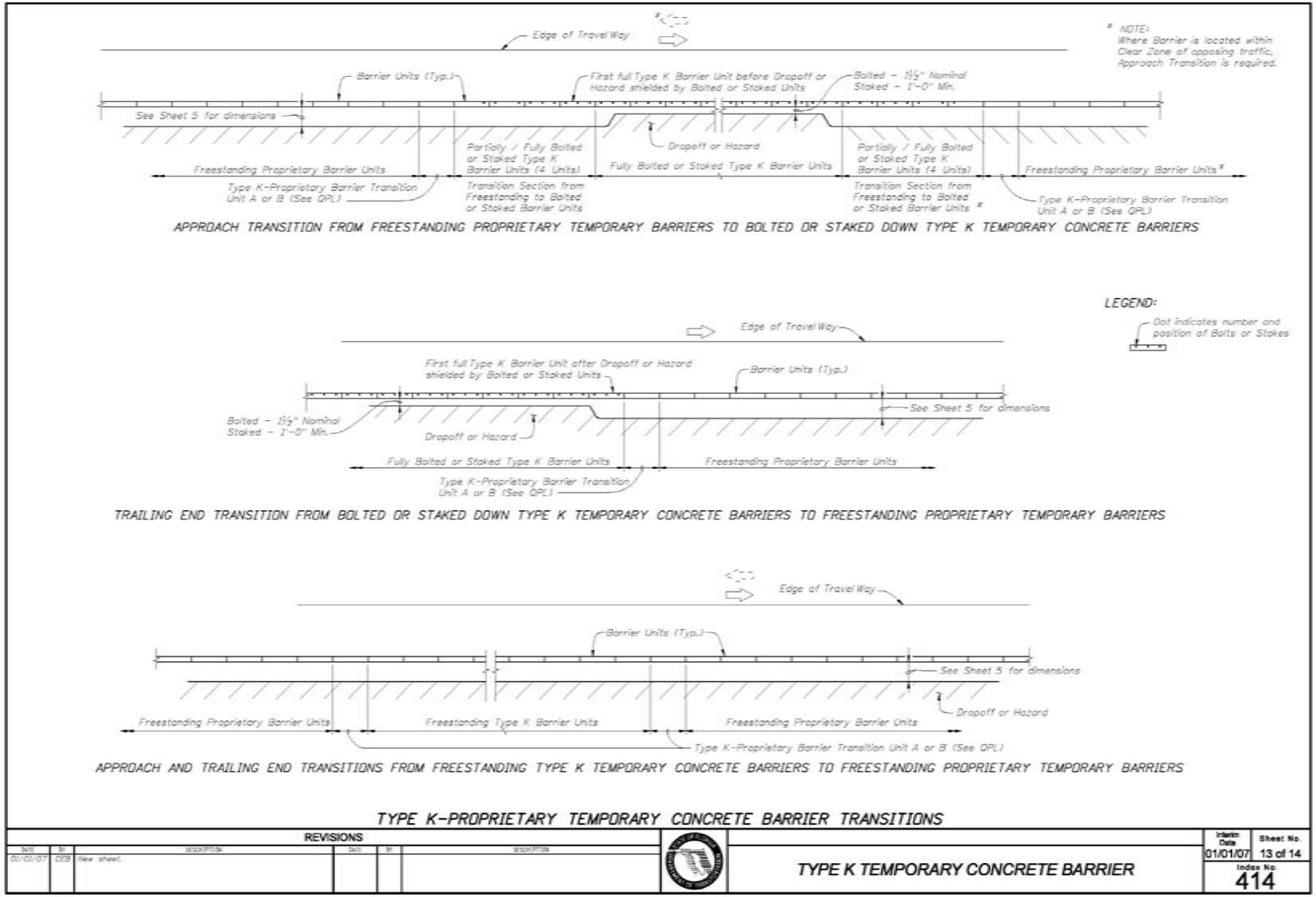

Figure I-13. Florida Department of Transportation – F-shape PCB Standards

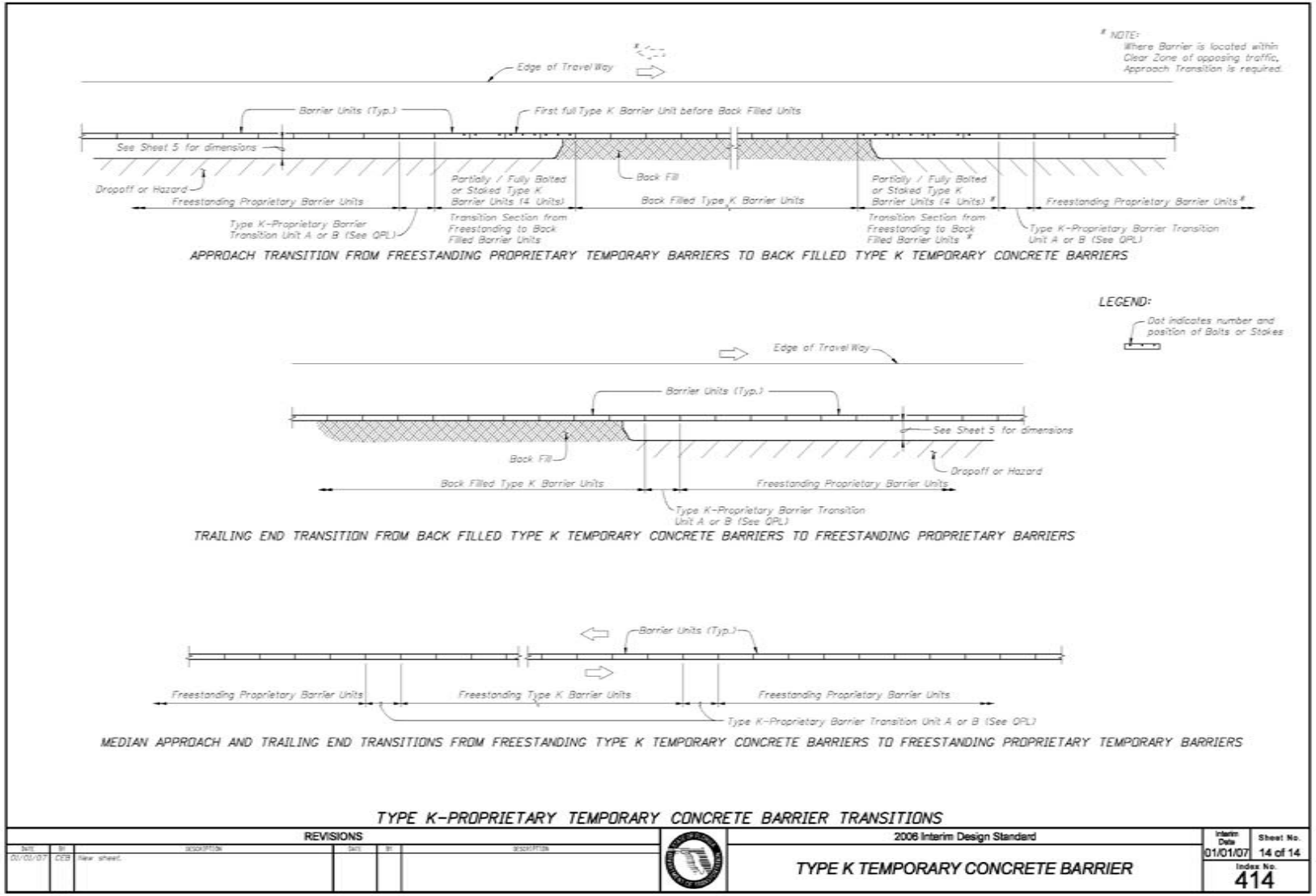

Figure I-14. Florida Department of Transportation – F-shape PCB Standards